Mechanisms of nodule-specific melanization in the hemocoel of the silkworm, *Bombyx mori*

2016. 3

Major of Bio-Applications and Systems Engineering

Graduate School of Bio-Applications and

Systems Engineering

Tokyo University of Agriculture and Technology

Min Shu

Tables of Contents

Abbreviations

AMPs	Antimicrobial peptides
GNBP	Gram-negative bacteria-binding protein
HPs	Serine proteinases
LBP	Lipopolysaccharide binding protein
MBP	Multibinding protein
PAMPs	Pathogen-associated molecular patterns
PAPs	proPO-activating proteinases
PGRP	Peptidoglycan recognition protein
PO	Phenoloxidase
PPAE	proPO activating enzyme
PPAF	proPO-activating factor
proPAP	proPO-activating proteinase precursor
proPO	Prophenoloxidase
proPPAE	proPO-activating enzyme precursor
PRRs	Pattern recognition receptors
ROS	Reactive oxygen species
SPHs	Serine proteinase homologs

Abstract

In the insect immune system, nodules are known to be a product of the cellular response against microorganisms and may be a preferential target for melanization. However, the mechanism of nodule-preferential melanization remains to be explored. In this study, several mechanisms of nodule-preferential melanization were identified by analyzing the process of congregation and the activation of several factors involved in the prophenoloxidase (proPO)-activating system in the silkworm, *Bombyx mori*. Microorganism-binding assays revealed that *B. mori* larval plasma have an effective invading microorganism-surveillance network consisting of at least six pattern-recognition receptors (PRRs). It was also found that a hemolymph serine proteinase, BmHP14, can bind to *Saccharomyces cerevisiae*. Pull-down assays showed that a group of PRR, C-type lectins form protein complexes with serine proteinase homologs, BmSPH1 and BmSPH2 and BmSPH1 and BmSPH2 are gathered on microorganisms by the help of C-type lectins and then activated on them, leading to the result that active forms of BmSPH1 and BmSPH2 with their active forms are trapped into nodules with microorganisms. Immunostaining analysis revealed that most factors in the proPO-activating system and some factors in the triggering system for antimicrobial peptide production exist in the granules of hemocytes which can gather in nodules. Western blot analysis and observation of nodule cryosections showed that factors in the proPO-

activating system are congregated in formed nodules by concentrating them from the plasma owing to the microorganism-binding property and by aggregating hemocytes which produce those factors.

General Introduction

Insects lack adaptive immunity, but they do have a highly efficient innate immune system for fighting off invading pathogens (Vilmos and Kurucz, 1998). This system consists of cellular responses such as phagocytosis, encapsulation, and nodule formation, which are mediated by circulating hemocytes (Eleftherianos et al., 2007; Marmaras and Lampropoulou, 2009; Schmidt et al., 2001). Their immune system also consists of humoral responses, such as the synthesis of antimicrobial peptides (AMPs) and the activation of the prophenoloxidase (proPO) system (Cerenius and Söderhäll, 2004; Fauvarque and Williams, 2011; Hultmark, 2003).

Many previous studies on the humoral response focused on the molecular mechanisms of proPO activation, discovering that the recognition of invading pathogens was a critical step in immune responses (An and Kanost, 2010; Wang et al., 2011). The recognition process is mediated by several groups of proteins known as pattern recognition receptors (PRRs) or pattern recognition proteins (PRPs) (hereafter, referred to as PRRs), which can specifically recognize and bind to highly conserved pathogen-associated molecular patterns (PAMPs) such as peptidoglycan (PGN), lipoteichoic acid (LTA), lipopolysaccharide (LPS), β-1, 3-glucan, and mannan, which is found on the cell walls of bacteria and fungi (Medzhitov and Janeway, 2002; Sumathipala and Jiang, 2010; Yu and Kanost, 2002). Genetic and biochemical studies have revealed more than 10 groups of PRRs in

invertebrates, including β-1, 3-glucan recognition proteins (βGRPs), peptidoglycan recognition proteins (PGRPs), C-type lectins, hemocytins, Hemolin, fibrinogen-related proteins, galectins, Nimrods, thioester-containing proteins (TEPs), scavenger receptors, Down syndrome cell adhesion molecules (Dscams), Eaters, and Drapers (Tanaka et al., 2008; Wang et al., 2011; Yu et al., 2002). Upon binding to the invading microorganisms, a part of PRRs trigger the activation of the proPO cascade, which involves serine proteinases (SPs or hemolymph proteases, HPs; hereafter, referred to as HPs) and serine proteinase homologs (SPHs) (An et al., 2009; Gupta et al., 2005; Lu and Jiang, 2008; Wang and Jiang, 2006). Some activated HPs involved in the proPO cascade, including *Manduca sexta* (tobacco hornworm) HP6, also have ability to activate other HPs, such as MsHP8 for the regulation of the Toll pathway for AMP production (An et al., 2009). More than 20 HPs have been identified in the hemolymph of *M. sexta*, but only partial functions of HP14, HP21, HP6, and HP8 are known (An et al., 2009; Ji et al., 2004; Wang and Jiang, 2006, 2007, 2010).

In terms of cellular responses, hemocytes recognize invading microorganisms by directly interacting with PAMPs located on the surface of invading pathogens or indirectly through interaction with PRRs-PAMPs complexes in the plasma (Au et al., 2004; Eleftherianos et al., 2007; Lavine and Strand, 2002; Ohta et al., 2006; Ribeiro and Brehélin, 2006). Inter- and intra-cellular signaling events then coordinate effector cell responses, such

as phagocytosis and nodule formation (Eleftherianos et al., 2007; Lavine and Strand, 2002; Suzuki et al., 2011). Although insect innate immune system is subdivided into cellular and humoral responses as I have explained above, recent evidences have implied that the proPO-activating system (the melanization responses) is intimately associated with the generation of factors which stimulate cellular responses by aiding phagocytosis, encapsulation and nodulation (Cerenius et al., 2008; Nappi and Vass, 1993; Richman and Kafatos, 1996; Suzuki et al., 2011). In the *Tnebrio molitor* proPO-activating system, melanization reaction was indicated to generate antimicrobial activity which is supposed to depend on the production of microbicidal reactive oxygen species (ROS) (Kan et al., 2008). Although melanization is a highly effective system for killing invading microorganisms, it is also harmful to the insects themselves, because ROS can injure not only invading pathogens but also insect tissues. However, melanization responses are faster and stronger in nodules than in hemolymph (Sakamoto et al., 2011). Therefore, a hypothesis that the melanization of hemolymph is not the main objective but rather a byproduct of nodule melanization cannot be ruled out (Tokura et al., 2014). On the other hand, if the melanization system evolved to enhance the role of nodules, nodules must have many mechanisms to implement the nodule-preferential melanization.

The previous report in our laboratory showed that addition of

melanization substrate l-3, 4-dihydroxyphenylalanine (DOPA) to the freshly-formed nodules promoted nodule melanization drastically, suggesting that melanization-related proteins are involved in the freshly-formed nodules (Sakamoto et al., 2011). Moreover, they confirmed that BmproPO1 is located in nodules and is produced by aggregated hemocytes, and further suggested that *Bombyx mori* lipopolysaccharide binding protein (BmLBP), BmSPH1 and BmSPH2 regulate melanization of *Escherichia coli*-induced nodule through protein complex formation (Tokura et al., 2014). In this study, the mechanism of congregation of melanization-related proteins in *B. mori* larvae nodules was explored. Specifically, the expression patterns of 11 putative melanization-related proteins, including six *B. mori* PRRs (BmPRRs), two *B. mori* SPHs (BmSPHs), and three *B. mori* HPs (BmHPs) were investigated. Moreover, a network of major BmPRRs involved in the surveillance of invading pathogens, C-type lectin-dependent congregation routes to nodules of proPO-controlling factors, *B. mori* serine proteinase homologs BmSPH1 and BmSPH2, stickiness-dependent congregation routes to nodules of BmHP14, and the production of melanization-related factors in hemocytes were also investigated. These investigations revealed two origins of melanization-related factors in nodules and ways by which those factors are transported into nodules.

CHAPTER 1

The effective invading microorganism-surveillance network consisting of BmPRRs and the congregation routes of BmPRRs to *B. mori* larvae nodules

1.1 Introduction

All animals including insects rely on the innate immunity as the first line to combat pathogens (Strand, 2008). A critical step for innate immunity has been known as the recognition of invading pathogens (An and Kanost, 2010; Wang et al., 2011). This process is mediated by several proteins termed as pattern recognition receptors (PRRs), and PRRs can be subdivided into more than 10 groups in invertebrates (Tanaka et al., 2008). However, even if PRRs belong to the same groups, they do not always have the same roles. In *Drosophila*, peptidoglycan recognition protein (PGRP)-LE can activate the prophenoloxidase (proPO) cascade upstream of proPO activating enzyme PPAE (also named PAP) by binding to Gram-negative and -positive bacteria. In contrast, PGRP-SA can activate the Toll pathway cooperating with Gram-negative bacteria-binding protein (GNBP) 1 and binding to Gram-positive bacteria. In addition, GNBP3 alone can mediate Toll pathway by binding to yeast (Kurata, 2010). In *M. sexta*, β-1, 3-glucan recognition protein (βGRP) 1 and multibinding protein (MBP) exhibited a broad binding properties to *Escherichia coli*, *Micrococcus luteus* and *Saccharomyces cerevisiae* cells and were involved in proPO activating system (Ma and Kanost, 2000; Wang et al., 2011). However, little is known about the roles of PRRs in *Bombyx mori*. *B. mori* βGRP1 (BmβGRP1) has been known to bind to component of the yeast cell wall (Ochiai and Ashida, 2000), and BmβGRP2 has been reported to have strong affinity to the cell wall of Gram-negative bacteria

(Lee et al., 1996).

A previous study in our laboratory focused on pathogen recognition by a C-type lectin, *B. mori* lipopolysaccharide binding protein (BmLBP) in order to better understand the process of innate immunity for defense against pathogens, and suggested that BmLBP is involved in cellular responses such as nodule formation by binding to *E. coli* (Koizumi et al., 1999). Furthermore, it was indicated that the progress of melanization of nodule is faster than that of hemolymph, suggesting that the melanization of hemolymph maybe only a byproduct of nodule melanization (Sakamoto et al., 2011). If this hypothesis is true, mechanism of nodule-specific melanization should exist in the hemolymph in *B. mori* larvae, and nodule-specific melanization system should be triggered by PRRs. However, it has to be mentioned that granulocytes and oenocytoids are major constituents of nodules during the early stages of their formation (Arai et al., 2013). Moreover, granulocyte granules and unidentified molecules in the cytoplasm of oenocytoids may be released by degranulation and autolysis, respectively, in response to microorganism recognition (Akai and Sato, 1973; Ashida and Brey, 1998). Furthermore, BmβGRP1 has been found to be located in the cytoplasm and granules of granulocytes and in the cytoplasm and spherules of spherulocytes (Ochiai et al., 1992). This means the mechanism of nodule melanization should be more complicated than that of hemolymph. To explore the mechanism of nodule melanization, the effective invading

microorganism-surveillance network consisting of PRRs in plasma were studied by microorganism-binding assay and using antisera against PRRs, and then the congregation routes of PRRs in *B. mori* larvae nodules were investigated by several examinations.

1.2 Materials and Methods

1.2.1. Collection of plasma, hemocytes fractions and nodules

Silkworms, *B. mori* (hybrid strain, Kinshu × Showa), were reared on an artificial diet (Silkmate 2M; Nihon-Nosanko, Yokohama, Japan) containing chloramphenicol (Wako, Osaka, Japan) at 25 °C. Fifth-instar 3–4 days' larvae after molting were swabbed with 70% ethanol and bled by proleg puncture using a sterile needle. Hemolymph was collected and diluted 3 times with insect physiological saline (IPS; 150 mM NaCl, 5 mM KCl, 0.1 M Tris-HCl, 1 mM $CaCl_2 \cdot 2H_2O$, pH 6.8) mixed with 1× concentration protease inhibitor (EDTA-free; Roche, Mannheim, Germany) and centrifuged at 800 g for 15 min at 4 °C. Cell free supernatant was collected as a plasma fraction. Low concentration of protease inhibitor could prevent autoactivation of several hemolymph proteins during collection and centrifugation of the hemolymph, but did not inhibit completely the protein activations in the microorganism-binding assay. Hemocytes pellet was washed twice with IPS by repeating the centrifugation. As previously reported (Sakamoto et al., 2011), nodules induced to form in the hemocoel of *B. mori* fifth-instar larvae were dissected 30 min after injection of CBB stained *E. coli*, *M. luteus* and *S. cerevisiae* cells (10^6 cells in 10 μl) into the hemocoel using a Microliter Syringe (Hamilton, Reno, NV, USA). In order to remove the surrounding plasma and loosely bound hemocytes, collected nodules were washed twice with IPS containing high concentration of

protease inhibitor. Shapes and purities of nodules collected by this method were previously shown in Sakamoto et al. (2011).

1.2.2. Preparation and cultivation of bacteria and yeast cells

Gram-positive bacteria *M. luteus* (IAM1056) and Gram-negative bacteria *E. coli* (K-12W3110) were cultured in Luria Bertani (LB) medium (peptone 10 g, yeast extract 5 g, NaCl 5 g, distilled water 1 l). *S. cerevisiae* (IAM4125) was cultured in yeast and malt (YM) medium (glucose 10 g, peptone 5 g, yeast extract 3 g, malt extract 5 g, distilled water 1 l). Microorganisms grown in the logarithmic phase were collected by centrifugation at 8000 rpm for 20 min at 4 °C, washed twice with IPS and fixed in 4% paraformaldehyde (Wako, Osaka, Japan) with gentle shaking for 90 min. The fixed cells were collected by centrifugation at 3300 rpm for 20 min at 4 °C, then washed 5 times with IPS and resuspended in IPS to store at 4 °C.

1.2.3. Preparation and specificity analysis of BmPRRs antisera

Antisera against BmPRRs including BmβGRP1 (NP_001036840), BmβGRP2 (NP_001037450), BmβGRP3 (NP_001128672), BmPGRP-S1 (NM_001043371) were prepared by immunization of the mature peptides encoding regions. The cDNA fragments were amplified by PCR using specific primers in table 1.1 and inserted into the GST fusion protein expression vector pGEX-4T-3 (GE Healthcare, Little Chalfont, UK).

Following sequence verification, the resulting plasmids were used for producing recombinant proteins in *E. coli* BL21 competent cells (TaKaRa, Shiga, Japan). Transformed-BL21 cells were picked up from a single colony on the LB plates with 50 μg/ml ampicillin (Wako, Osaka, Japan) and incubated in LB medium containing 50 μg/ml ampicillin at 37 °C for 12–14 h. The cultures were then diluted in 100-fold volume of fresh LB medium and incubated until the OD_{600} became 0.5. Production of the fusion proteins was induced by the addition of isopropyl-b-D- thiogalactoside (IPTG; Wako, Osaka, Japan) at a final concentration of 1 mM. After additional incubation for 8 h, the bacterial cells were harvested by centrifugation and sonicated to release the inclusion bodies. The inclusion bodies were then washed twice using 1% Polyoxyethylene (10) octylphenyl ether (Triton X-100; Wako, Osaka, Japan) for 15 min and twice using purified water. The fusion proteins were prepared by the preparative electrophoresis (422 electro-eluter, Bio-Rad, USA) and dialyzed with phosphate-buffered saline (PBS; 137 mM NaCl, 2.7 mM KCl, 1.8 mM KH_2PO_4, 10 mM $Na_2HPO_4·12H_2O$, pH 7.4) at 4 °C for 16 h. To raise antisera, the fusion proteins were first injected to female mouse with complete Freund's adjuvant (CFA; Wako, Osaka, Japan) and subsequently with incomplete Freund's adjuvant (IFA; Wako, Osaka, Japan). Anti-BmLBP, anti-BmMBP antisera were raised as previously reported (Koizumi et al., 1997; Watanabe et al., 2006). Specificities of all antisera were evaluated using normal *B. mori* plasma by Western blot.

1.2.4. Microorganism-binding assay for the analysis of invading surveillance factors BmPRRs

Paraformaldehyde-fixed *E. coli*, *S. cerevisiae* or *M. luteus* cells (60 μl of precipitate) were mixed with 1 ml of cell free plasma diluted with IPS for 3 times or IPS alone, and incubated for 8 min with mild agitation. The mixtures were separated by centrifugation at 2500 g for 3 min at 4 °C and pellets were washed with IPS twice. Proteins bound to microorganisms were treated with 120 μl of 2×SDS-sample buffer (125 mM Tris-HCl, pH 6.8, 4% SDS, 10% 2-mercaptoethanol, 0.05% bromophenol blue, 20% glycerol) at 98 °C for 5–30 sec. Eluted samples (12–25 μl) were separated by Laemmli-SDS-PAGE (Laemmli, 1970) and bound proteins were detected by immunoblot using the antibodies described in Section 1.2.3.

1.2.5. Expression analysis of BmPRRs by RT-PCR

Fat bodies, hemocytes and nodules which were induced by *E. coli*, *M. luteus* or *S. cerevisiae* cells injection were collected and total RNA were extracted with the RNA extraction reagent, ISOGEN Ⅱ (Nippon Gene, Tokyo, Japan). The first strand cDNA was synthesized from total RNA using oligo(dT)$_{20}$ primers and ReverTra Ace® (TOYOBO, Osaka, Japan). Double-stranded BmPRRs cDNA fragments were amplified by PCR using GoTaq DNA polymerase (TaKaRa, Shiga, Japan) with 35 cycles and the gene-specific primers for individual proteins indicated in table 1.2. The *B. mori β-actin*

was used as an internal standard to normalize the cDNA pools. PCR products were separated by agarose gel electrophoresis and stained by ethidium bromide.

1.2.6. Immunofluorescent staining for the observation of BmPRRs expression and storage in hemocytes

Immunofluorescent staining was carried out essentially according to Tokura et al. (2014) with some modifications (Tokura et al., 2014). Briefly, hemolymph of *B. mori* fifth-instar larvae were collected and mixed with 4 mM dithithreitol (DTT; Wako, Osaka, Japan). The hemolymph were loaded on the glass slides. After loading, cells were smeared, fixed with 4% paraformaldehyde and washed using PBS. Glass slides were then air-dried for 2 h at room temperature and permeabilized with 0.1% Triton X-100. After PBS washing, hemocytes were reacted with mouse antiserum raised against BmβGRP1, BmβGRP2, BmβGRP3, BmLBP, BmPGRP-S1 and rabbit antiserum raised against BmMBP and stained with 1000-fold diluted Alexa Fluor 488® conjugated goat anti-mouse IgG or goat anti-rabbit IgG (Bio-Rad, Hercules, CA, USA). Preimmune mouse and rabbit sera were used as primary antibodies for negative controls to evaluate the staining. Antisera were diluted using 1% BSA solution containing 0.1% Triton X-100. The nuclei of hemocytes were counter stained with 4', 6-diamidine-2'-phenylindole dihydrochloride (DAPI; 1 μg/ml, Sigma Aldrich, Schnelldorf,

Germany). Fluorescence was observed under a microscope, LSM710/LSM710 NLO (CARL ZEISS). Oenocytoids were identified by the existence of big cell bodies, big nuclei and large spindle-shaped granules in the cytoplasm. Granulocytes were identified by the existence of small nucleus and many irregularly shaped granules varied in size inside the cytoplasm. Spherulocytes were identified by the existence of obvious large granules in the cytoplasm. Plasmatocytes were differentiated from granulocytes based on the existence of fairly bigger nucleus and irregularly cell shape. Prohemocytes are identified as round and smooth cells with small cell bodies and bigger nuclei.

1.2.7. Western blot analysis to confirm the concentration of BmPRRs in the nodules

Paraformaldehyde-fixed microorganism cells were adjusted to $OD_{600} = 0.8$. Cells were stained with Coomassie Brilliant Blue R-250 (CBB; Wako, Osaka, Japan) and washed five times with IPS. Precipitates were harvested after centrifugation at 8000 rpm for 10 min at 4 °C. Cells of 1.0×10^7 were suspended in 100 μl of IPS for each microorganism. Nodules induced to form in the hemocoel of *B. mori* fifth-instar larvae were dissected 30 min after injection of CBB stained *E. coli*, *M. luteus* and *S. cerevisiae* cells (10^6 cells in 10 μl) into the hemocoel using a Microliter Syringe (Hamilton, Reno, NV, USA) as indicated in the section 1.2.1. The plasma (10 μl) and

hemocytes (10 µl as a precipitate) prepared previously were mixed with 40 µl 2 × SDS-PAGE sample buffer. Nodules (10 µl as a precipitate) were homogenized and mixed with 40 µl 2 × SDS-PAGE sample buffer. Samples (10 µl of each) were loaded and separated by 12.5% Laemmli-SDS-PAGE. For Western blot analysis, the proteins were transferred onto a polyvinylidene difluoride (PVDF; Bio-Rad, Hercules, CA, USA) membrane. After blocking with 2% BSA, the membrane was incubated with mouse antisera against BmβGRP1, BmβGRP2, BmβGRP3, BmLBP, BmPGRP-S1 or rabbit antiserum against BmMBP for 90 min following the appropriate dilution. After washing, the membrane was incubated with 30,000-fold diluted peroxidase-conjugated goat anti-mouse IgG (Bio-Rad, Hercules, CA, USA) or 30,000-fold diluted peroxidase-conjugated goat anti-rabbit IgG (Bio-Rad, Hercules, CA, USA) for 45 min, and then stained using ECL^{TM} prime Western blotting detection reagent (GE Healthcare, Little Chalfont, UK).

1.2.8. Immunofluorescent staining for the confirmation of BmPRRs in nodules

Nodules formed in the hemocoel of *B. mori* fifth-instar larvae were dissected 30 min after injection of CBB stained *E. coli*, *M. luteus* and *S. cerevisiae* cells (10^6 cells in 10 µl) respectively. Subsequently, washed twice with 5 ml IPS containing 200 µl 1× conc. protease inhibitor, and fixed overnight (12-

24 h) at 4 °C in 4% paraformaldehyde. After fixation, each nodule was embedded in Tissue-Tek O.C.T. compound (Sakura Finetek Japan, Tokyo, Japan) and frozen at -80 °C. For section preparation, the embedded specimens were mounted on an object holder and sectioned using a Tissue-Tek Cryo3® cryostat (Sakura Finetek Japan, Tokyo, Japan). 10 μm thick cryosections of each nodule were placed on MAS-GP type-A coated slide glasses (Matunami glass, Osaka, Japan) and air dried at RT for overnight. The immunofluorescent staining of nodule cryosections were performed and observed as described in section 1.2.6 as hemocytes.

Table 1.1. The specific primers for antisera production

Gene name	Forward primer (5´-3´)	Reverse primer (5´-3´)
BmβGRP1	TAAGGATCCCCGGCCA CGCTCGAAGCA	CCCACGTAGGGGATCC CTGACTACGG
BmβGRP2	GCAGAGGTACTGAATT CAGTCAACGGC	CTTTGACAAAGTCGAC GATTAAAGATGGC
BmβGRP3	ACAGTGCCAGTCGACG GTTTCTCG	AACCCTCATGGCGGCC GCGTACCACGT
BmPGRP-S1	ACTGAATTCGCAATGG GACGGTTTGAT	AATGTCGACCACGTTC TCCAGCCACTCA

Table 1.2. Primers for individual proteins used in RT-PCR

Gene name	Forward primer (5´-3´)	Reverse primer (5´-3´)
BmβGRP1	TAAGGATCCCCGGCCACGCTCGAAGCA	CCCACGTAGGGGATCCCTGACTACGG
BmβGRP2	TCCGAATTCAGTATCCGTTCAAGATGTCC	CAGGTCGACTTTGGCGTTAATATGTAGGT
BmβGRP3	GATGAATTCTCCTCAACAAGCCAGCACTC	TCCGTCGACATTCGTTAAATCAAGGTC
BmLBP	GGGACATAAATGGGTGGTTG	GAGCCGAGCGGTAGATAGAG
BmMBP	ATTACCTTCGGAACTCA	TGTATGCTTCGGACCAG
BmPGRP-S1	ACTGAATTCGCAATGGGACGGTTTGATC	AATGTCGACCACGTTCTCCAGCCACTCA
β-actin	AACTGGGATGACATGGAGAAGATCTGGC	GAGATCCACATCTGCTGGAAGGTGGA

1.3 Results

1.3.1. Specificity analysis of BmPRRs antisera

Mouse or rabbit polyclonal antisera were prepared against 6 representative BmPRRs and their specificities were confirmed. Mouse antisera raised against BmβGRP1, BmβGRP2, BmβGRP3 and BmPGRP-S1 recognized single bands at 62, 50, 62 and 19 kDa, respectively, in normal plasma (Fig. 1.1). Mouse anti-BmLBP antiserum recognized two bands at 43 and 40 kDa, and rabbit anti-BmMBP antiserum recognized a single band at 43 kDa (Fig. 1.1). Apart from BmβGRP3, which has not been studied, all these results corresponded well to previous reports (Koizumi et al., 1997; Lee et al., 1996; Ochiai and Ashida, 2000; Tokura et al., 2014; Watanabe et al., 2006; Yoshida et al., 1996), indicating that all prepared antisera were specific and could therefore be used in other experiments.

1.3.2. Microorganism-binding assay of BmPRRs

In hemolymph, the proPO-activating cascade can be triggered by PRRs through specific interactions with molecules on the surface of invading pathogens (An et al., 2009; Wang et al., 2011). Furthermore, binding to microorganisms may help to protein concentration in the nodules (Tokura et al., 2014). To explore the role of PRRs by examining their specific binding properties to different microorganisms, a microorganism-binding assay was performed. In this study, cell-free plasma from *B. mori* larvae was incubated
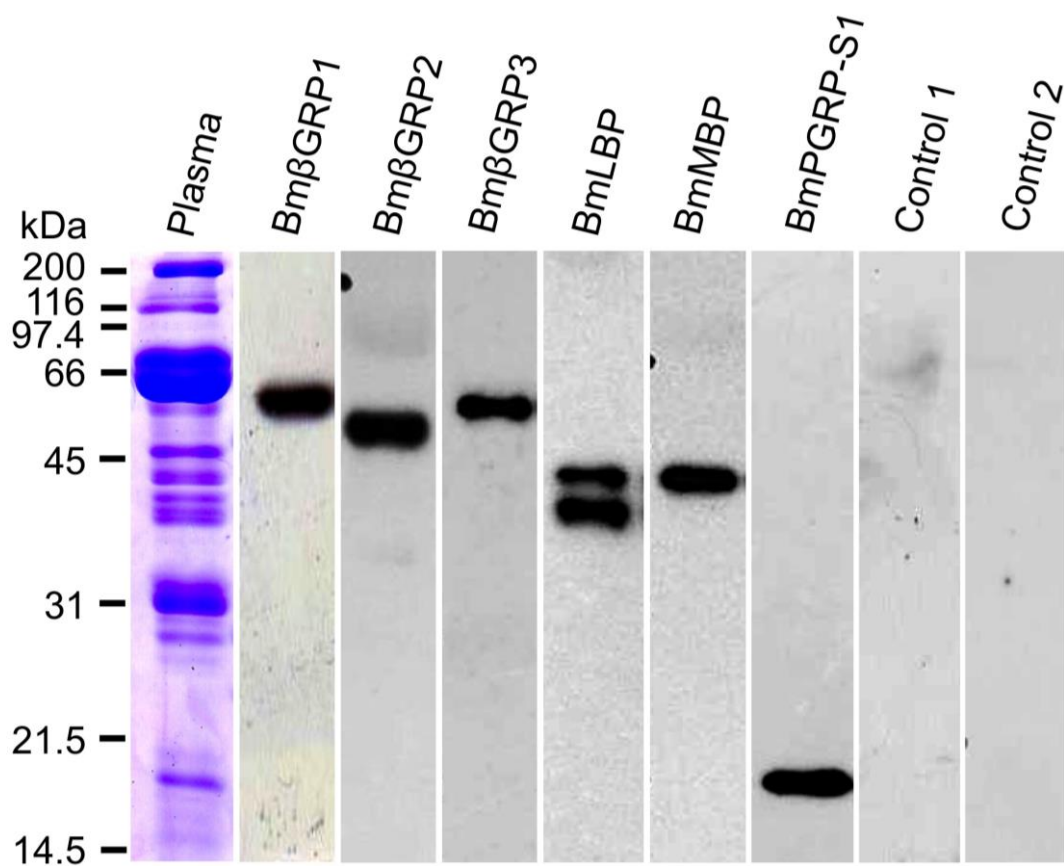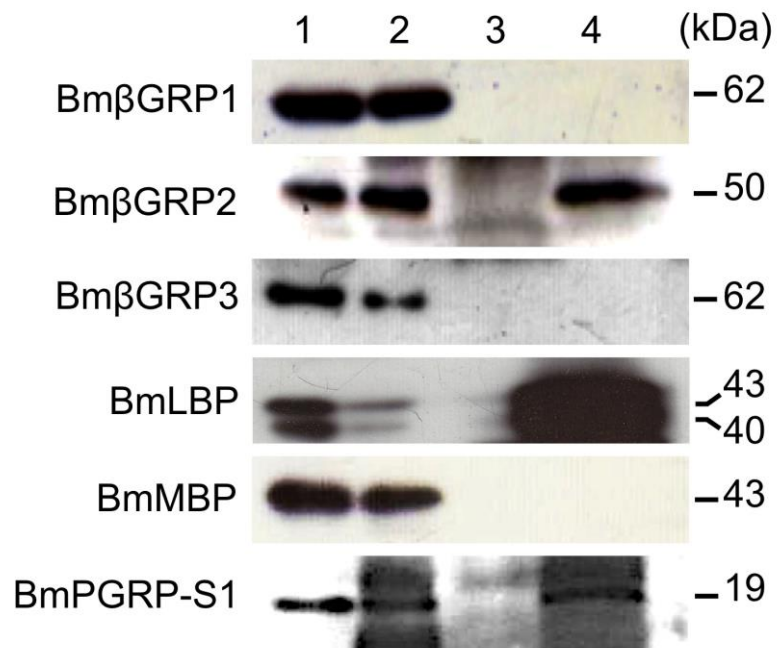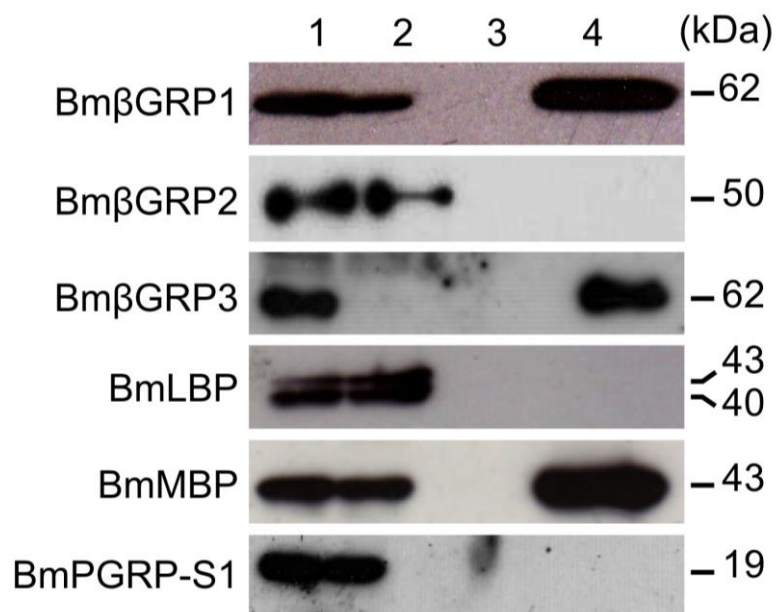
Fig. 1.1. Western blot analysis for confirmation of BmPRRs antisera specificity. The specificity of 5 mouse antisera against BmβGRP1, BmβGRP2, BmβGRP3, BmLBP and BmPGRP-S1 and a rabbit antiserum against BmMBP were confirmed using the plasma of *B. mori* larvae. Preimmune mouse (control 1) and rabbit (control 2) sera were used as primary antibodies for negative controls.

separately with three representative microorganisms, *E. coli*, *S. cerevisiae*, and *M. luteus* of the Gram-negative bacterium, fungus, and Gram-positive bacterium, respectively. Proteins that bound to these microorganisms were eluted and then detected by Western blot. In the *E. coli*-binding assay, BmβGRP2, BmLBP and BmPGRP-S1 were detected, whereas BmβGRP1, BmβGRP3 and BmMBP were not (Fig. 1.2A). In the *S. cerevisiae*-binding assay, BmβGRP1, BmβGRP3 and BmMBP were detected, whereas BmβGRP2, BmLBP and BmPGRP-S1 were not (Fig. 1.2B). In the *M. luteus*-binding assay, BmβGRP2, BmβGRP3, BmMBP and BmPGRP-S1 were detected, whereas BmβGRP1 and BmLBP were not (Fig. 1.2C). These results suggest that PRRs belonging to the same protein group can recognize different microorganisms. On the other hand, PRRs belonging to different protein groups can recognize the same microorganisms. Taken together, these results suggest that *B. mori* larvae have an effective microorganism-detection network in which at least one C-type lectin and more than one BmβGRP and BmPGRP are involved in the recognition of one microorganism.

Specific binding of proteins was further confirmed by CBB-staining after SDS-PAGE. As shown in Fig. 1.3, five specifically bound bands at 43, 40, 36, 29, and 27 kDa were found with *E. coli* cells, two specifically bound bands at 62 and 43 kDa were found with *S. cerevisiae* cells, but no distinguishable bands could be observed with *M. luteus* cells. The bands in
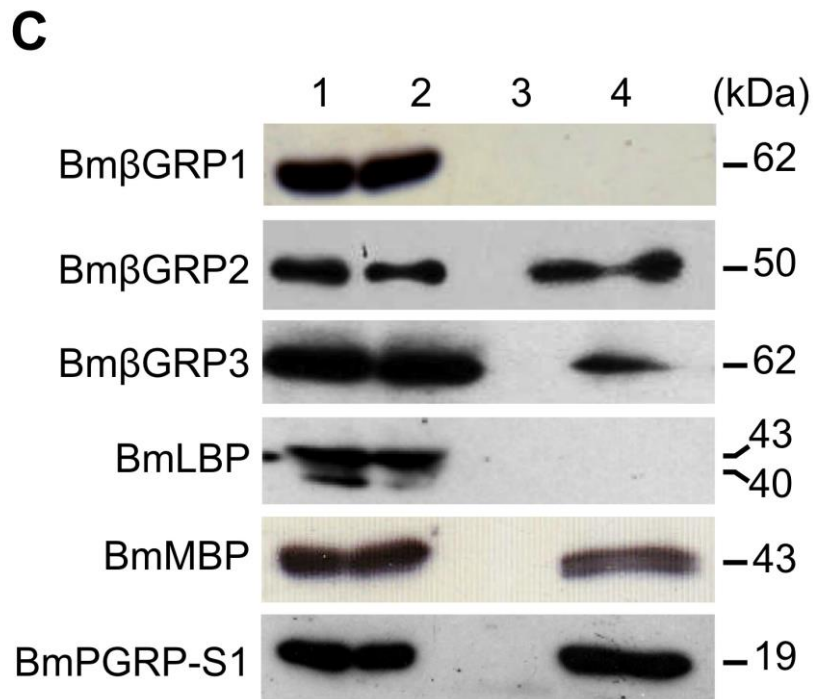
Fig. 1.2. Confirmation of specific binding of BmPRRs in plasma to microorganisms by Western blot. The specific binding of BmβGRP1, BmβGRP2, BmβGRP3, BmLBP, BmMBP and BmPGRP-S1 to microorganisms were detected by immunoblot analyses after plasma (cell-free hemolymph) was incubated with paraformaldehyde-fixed *E. coli* (A), *S. cerevisiae* (B), and *M. luteus* (C) cells. Preimmune mouse and rabbit sera were used as primary antibodies for negative controls and no signals were observed (data not shown). Lane 1, cell-free plasma; lane 2, cell-free plasma after absorption to microorganisms; lane 3, eluate from microorganisms reacted with IPS; lane 4, eluate from microorganisms reacted with cell-free plasma.
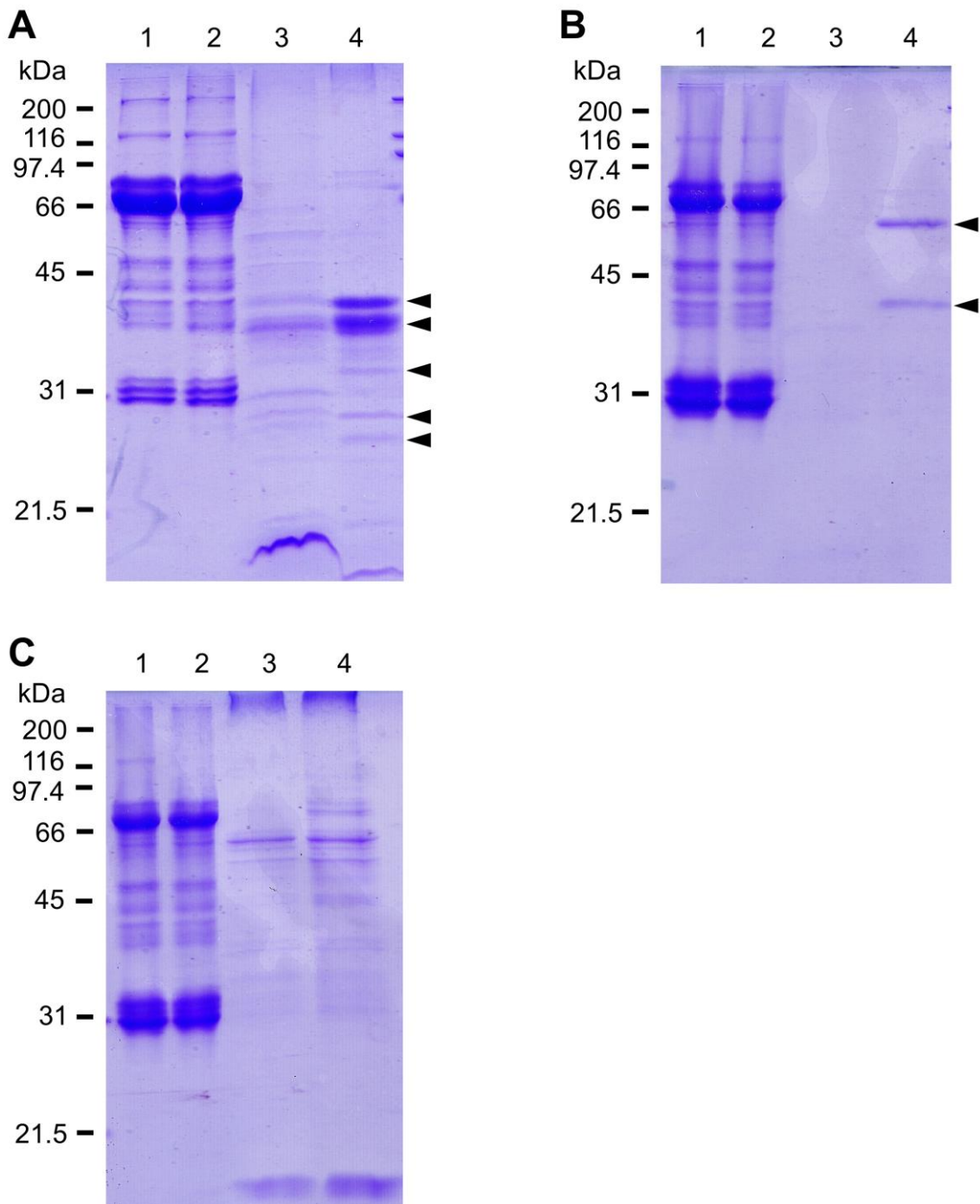
Fig. 1.3. Confirmation of specific binding of BmPRRs in plasma to microorganisms by CBB-staining. Specific binding of *B. mori* plasma proteins to paraformaldehyde-fixed *E. coli* (A), *S. cerevisiae* (B), and *M. luteus* (C) cells were confirmed with CBB-staining of SDS-PAGE. Lane 1,

cell-free plasma; lane 2, cell-free plasma after absorption to microorganisms; lane 3, eluate from microorganisms reacted with IPS; lane 4, eluate from microorganisms reacted with cell-free plasma.

E. coli at 43 and 40 kDa have the same molecular masses as BmLBP. The bands in *S. cerevisiae* at 62 and 43 kDa have the same molecular masses as BmβGRPs (1 and 3) and BmMBP, respectively. All four of these bands were also detected by Western blot. However, other proteins detected in the Western blotting were not observable in CBB-staining (Fig. 1.2 and 1.3).

1.3.3. Tissue-specific expression of BmPRRs

In insects, fat bodies and hemocytes have important roles in innate immunity (Krautz et al., 2014). Fat bodies secrete immune humoral factors, including PRRs, for recognition of invading pathogens, and serine proteinases (HPs) and serine proteinase homologs (SPHs) for proPO activation in the hemolymph. Hemocytes are known to play important roles in nodule formation (Arai et al., 2013) and the production of humoral factors, including proPO (Cerenius et al., 2008). To investigate factors involved in nodule melanization in *B. mori* larvae, the expression patterns of 7 genes encoding BmPRRs in fat bodies, hemocytes (the major nodule constituents), and nodules were preferentially examined using RT-PCR. Nodule formation was induced by injecting with *E. coli* (EN), *S. cerevisiae* (SN), or *M. luteus* (MN). DNA sequencing was used to confirm the identity of PCR products. As shown in Fig. 1.4, cDNAs derived from mRNAs encoding three βGRPs (*BmβGRP1*, *BmβGRP2* and *BmβGRP3*), two C-type lectins (*BmLBP* and *BmMBP*), and one PGRP (*BmPGRPS1*) were found in all of fat bodies,
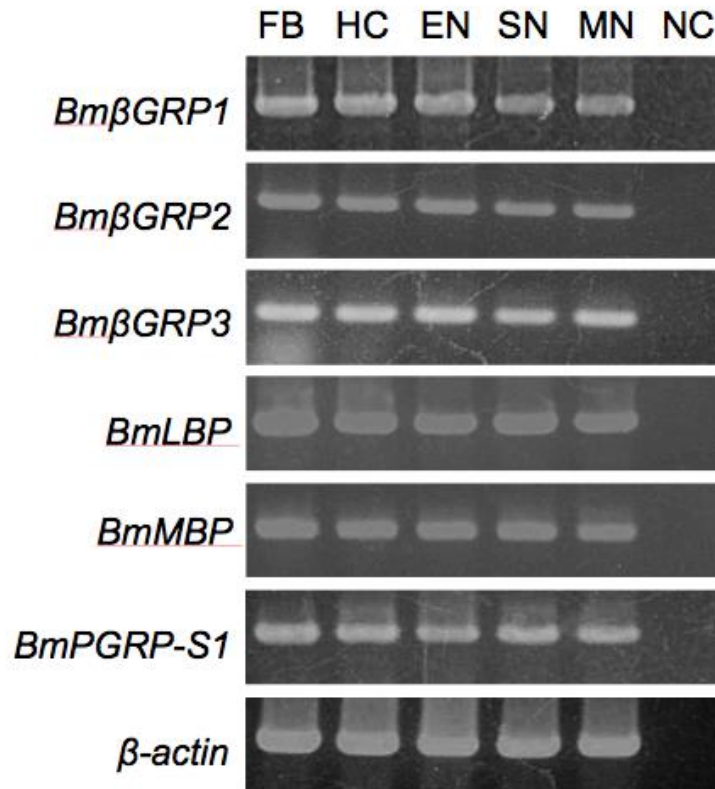
hemocytes, and three types of induced nodules.

Fig. 1.4. RT-PCR analysis of genes encoding BmPRRs. Gene expression of BmPRRs including *BmβGRP1*, *BmβGRP2*, *BmβGRP3*, *BmLBP*, *BmMBP* and *BmPGRP-S1* were analyzed in normal fat bodies (FB), normal hemocytes (HC), and nodules induced by injection with *E. coli* (EN), *S. cerevisiae* (SN), or *M. luteus* cells (MN). *β-actin* was used as an internal standard to normalize the cDNA pools. For the negative controls (NC), cDNA was replaced by an equal amount of pure water.

1.3.4. Immunocytochemical localization of BmPRRs in hemocytes

In previous study, BmβGRP1 was found to be located in the cytoplasm and granules of granulocytes and in the cytoplasm and spherules of spherulocytes (Ochiai et al., 1992). In this study, RT-PCR showed that 6 BmPRRs genes are expressed by *B. mori* hemocytes (Fig. 1.4). Thus, immunofluorescent staining of smeared hemocytes were performed to examine the localization and accumulation of BmPRRs. As a control, it was first confirmed that fig was not observed when hemocytes were incubated with preimmune mouse and rabbit sera (Fig. 1.7).

The localizations of six PRRs (BmβGRP1, BmβGRP2, BmβGRP3, BmLBP, BmMBP, and BmPGRP-S1) were investigated. As shown in Figs. 1.5 and 1.6, the fluorescence in granules was higher in granulocytes than in the cytoplasm for all antisera used; this suggested that humoral factors are possible to be secreted by degranulation in response to immune activation through an undefined mechanism. The cytoplasm of plasmatocytes and oenocytoids was well stained by all antisera (Fig. 1.5A–F), even though only weak fluorescence was observed in oenocytoids when anti-BmMBP antiserum was used (Fig. 1.5E). When spherulocytes were stained with each of the antisera, almost no fluorescence or very weak fluorescence was observed (Fig. 1.5A–F, arrows). As there was only a small population of prohemocytes, immunostaining of this cell type could only be done using anti-BmLBP and -BmMBP antisera (Fig. 1.5D and E).
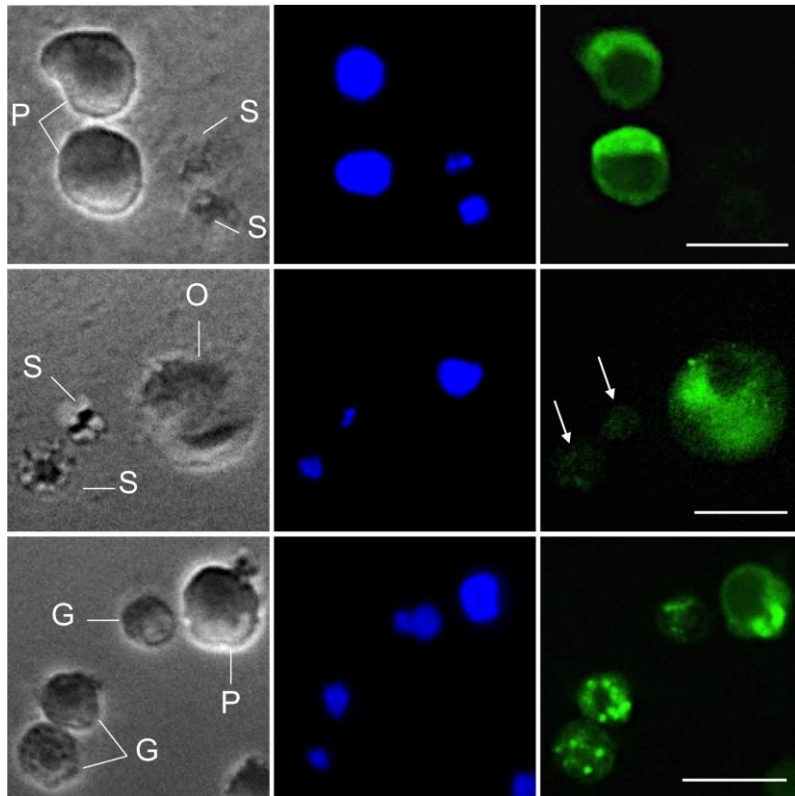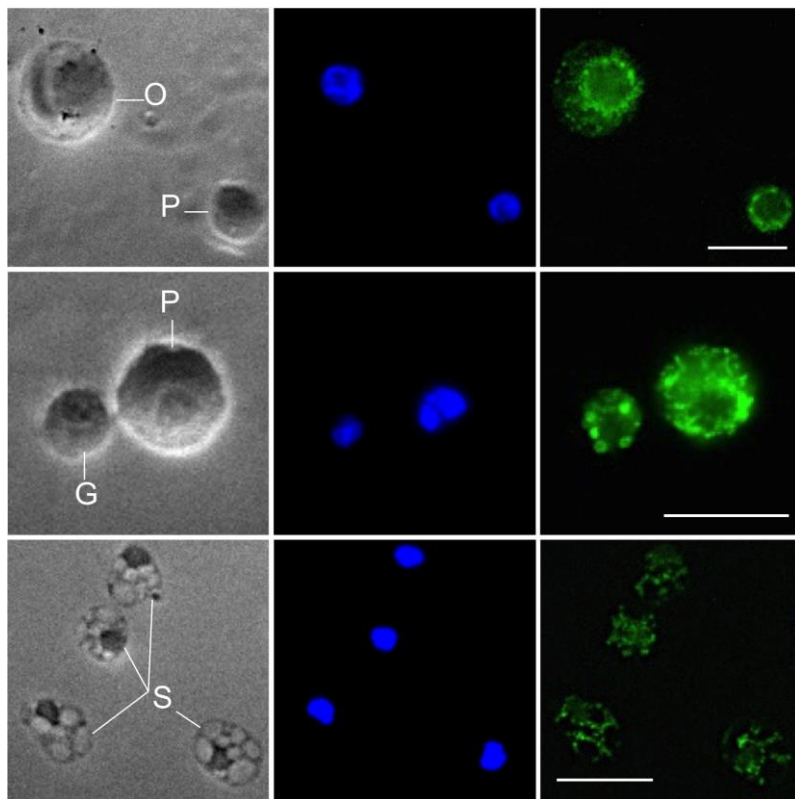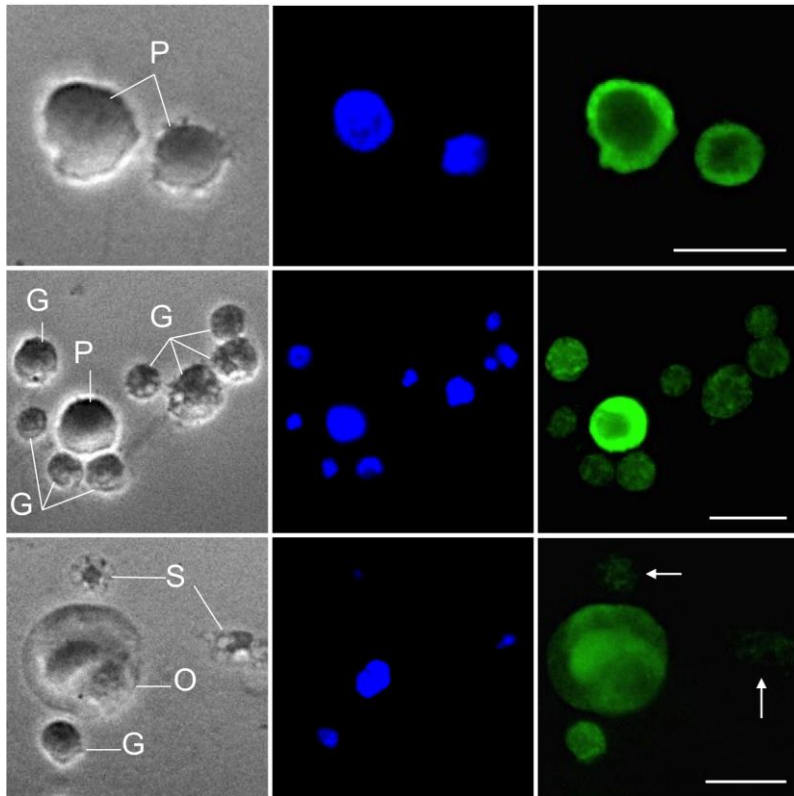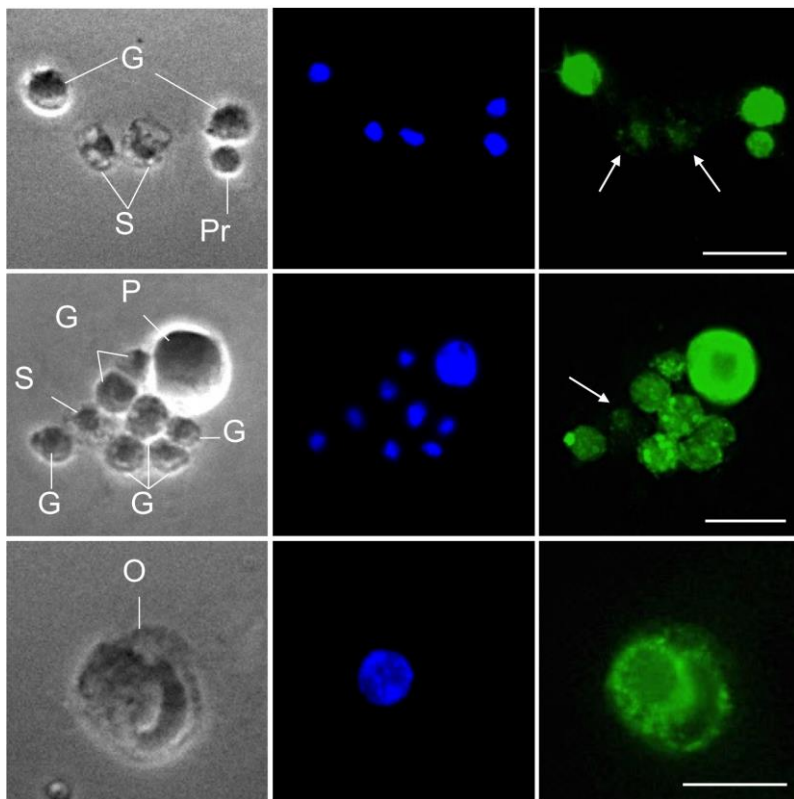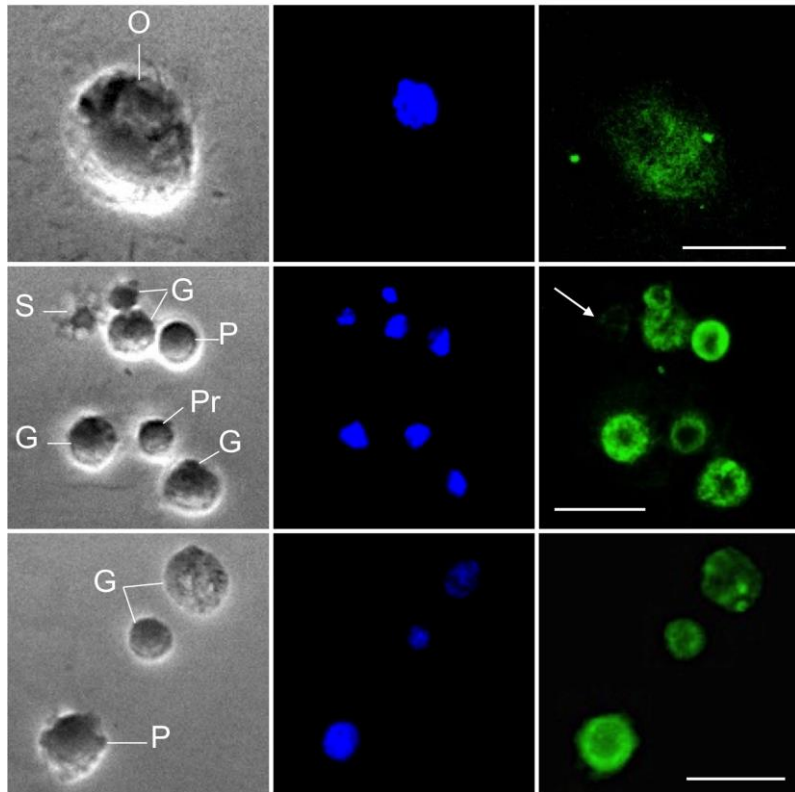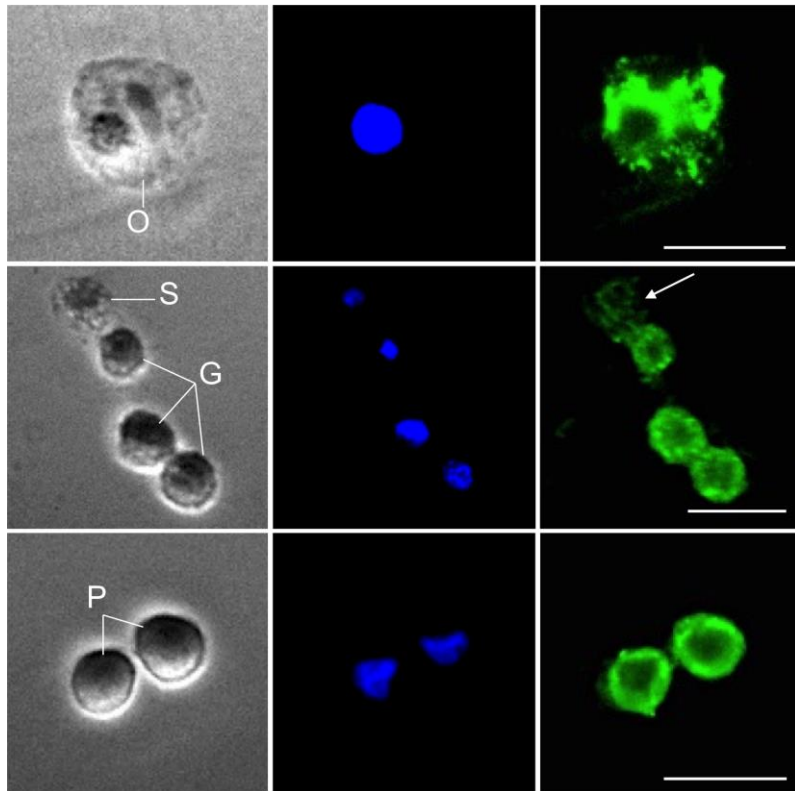
E

F

Fig. 1.5. Immunofluorescent detection of BmβGRP1, BmβGRP2, BmβGRP3, BmLBP, BmMBP, and BmPGRP-S1 in smeared hemocytes from *B. mori* larvae. Hemocytes were smeared on glass slides and fixed. Left panels show transmitted light pictures. Middle panels show DAPI-stained nuclei of hemocytes. Right panels show hemocytes stained with mouse anti-BmβGRP1 (A), anti-BmβGRP2 (B), anti-BmβGRP3 (C), anti-BmLBP (D), and anti-BmPGRP-S1 (F) in combination with anti-mouse IgG conjugated to Alexa Fluor 488® or rabbit anti-BmMBP (E) in combination with anti-rabbit IgG conjugated to Alexa Fluor 488®. P, plasmatocyte; G, granulocyte; O, oenocytoid; S, spherulocyte; Pr, prohemocyte. Arrows indicate weakly immunostained spherulocytes. Scale bars represent 10 µm.
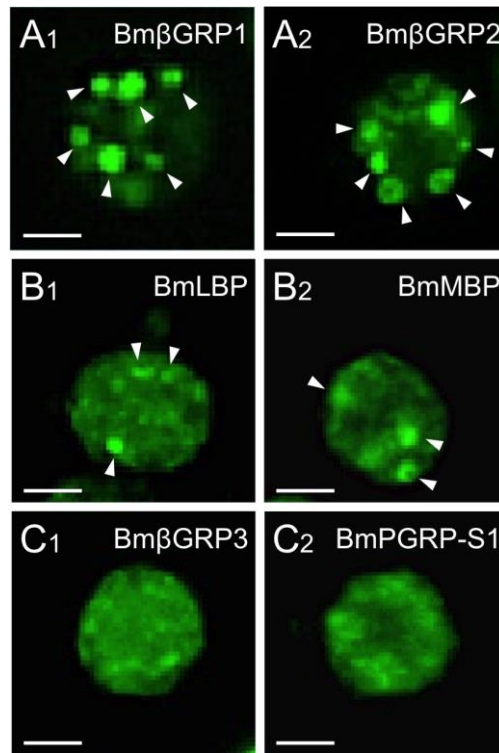
Fig. 1.6. Comparative intense staining of BmPRRs in granulocyte granules in *B. mori* larvae. Granulocytes smeared on the glass slides were stained with six anti-BmPRR antisera in combination with anti-mouse IgG conjugated to Alexa Fluor 488® and observed at high magnification. Intensely stained granules are indicated by arrowheads. Scale bars represent 2 μm.
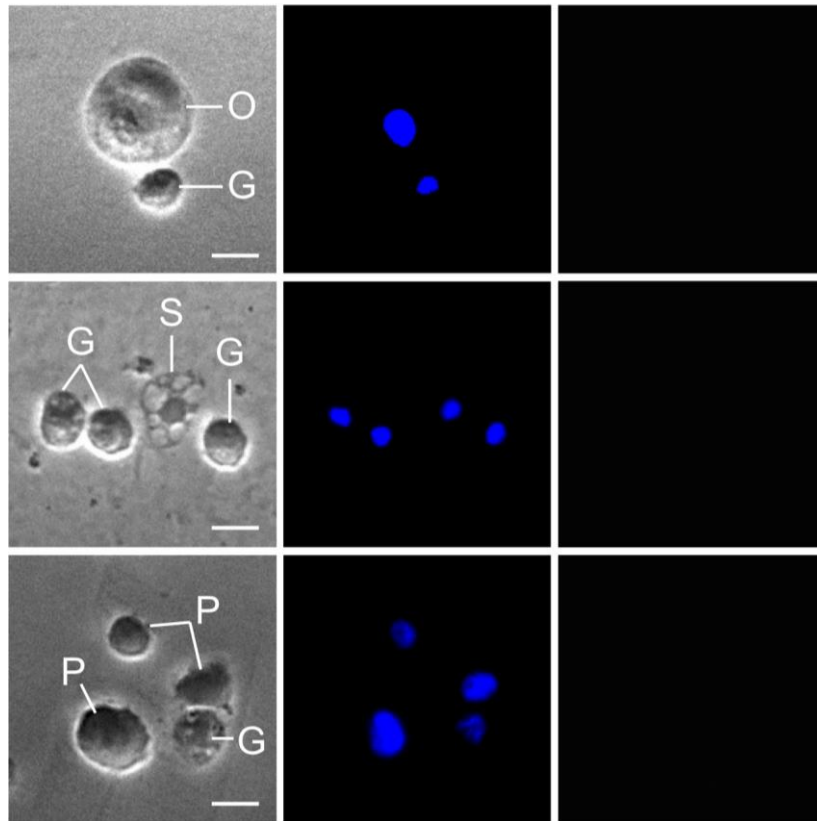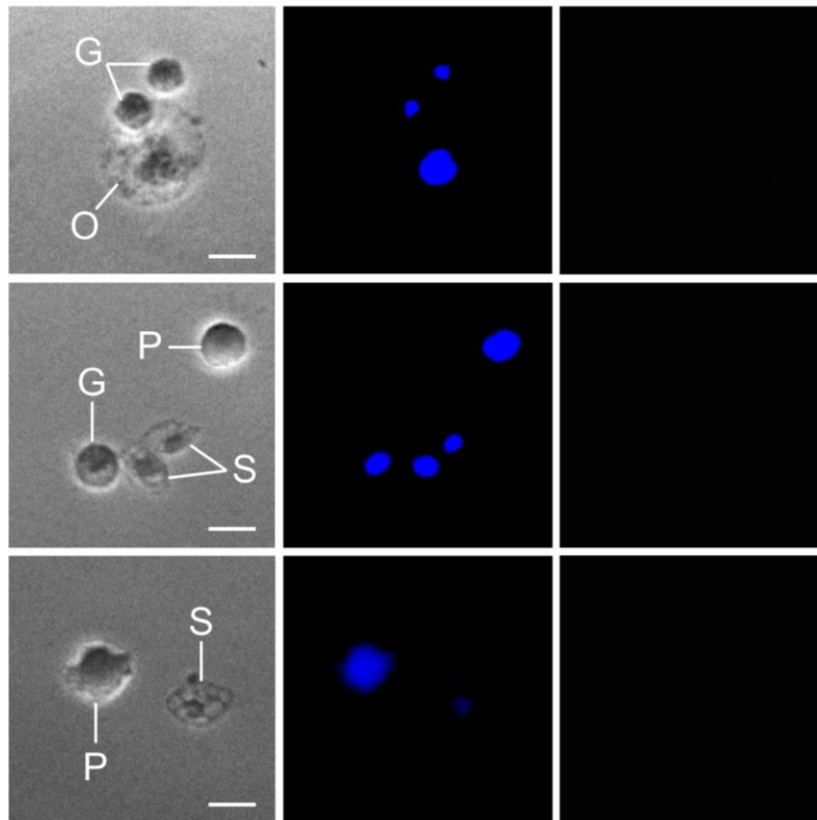
Fig. 1.7. Negative controls for immunostaining of smeared hemocytes.

Left panels show transmitted-light pictures. Middle panels show DAPI-stained nuclei of hemocytes. Right panels show hemocytes stained with preimmune mouse (A) and rabbit (B) sera in combination with anti-mouse IgG conjugated to Alexa Fluor 488®. As expected, no immunoreactive hemocytes were observed. P, plasmatocyte; G, granulocyte; O, oenocytoid; S, spherulocyte. Scale bars represent 5 μm.

1.3.5. Western blot analysis to deduce the origin of BmPRRs and the way to transport them into the nodules

In this study, both RT-PCR and immunostaining showed that all six of BmPRRs in the proPO-activating system can be expressed and stored in hemocytes (Figs. 1.4–1.6). Moreover, previous studies suggested that granulocyte granules and unidentified molecules in the cytoplasm of oenocytoids may be released by degranulation and autolysis, respectively, in response to microorganism recognition (Akai and Sato, 1973; Ashida and Brey, 1998). As the origin of BmPRRs in the nodule and the way to transport them into the nodule was unknown, Western blot analysis using cell-free plasma and, lysates of hemocytes and nodules were performed.

As shown in Fig. 1.8, thick bands were observed when plasma was probed with antibodies against six of the aforementioned PRRs, indicating that these six PRRs were highly abundant in normal plasma. BmβGRP1 and BmβGRP3, which were previously showed could bind well to *S. cerevisiae* (Fig. 1.2), were detected in *S. cerevisiae*-induced nodules, even though hemocytes did not have detectable levels of these proteins, indicating that BmβGRP1 and BmβGRP3 in the induced nodules came from the plasma (Fig. 1.8). A significant quantity of BmβGRP2, which was previously showed could bind well to *M. luteus*, was detected in *M. luteus*-induced nodules, and a smaller amount was detected in *E. coli*-induced nodules, even though hemocytes did not have a detectable level of this protein. Again, this

indicated that BmβGRP2 in the induced nodules also came from the plasma (Fig. 1.8). BmLBP, which was previously showed could bind well to *E. coli* (Fig. 1.2), was detected in hemocytes. However, this protein was more abundant in *E. coli*-induced nodules than in hemocytes, indicating that most of the protein in the nodules came from the plasma (Fig. 1.8). In the case of *E. coli*-induced nodules, BmMBP, which was previously showed could bind well to both *M. luteus* and *S. cerevisiae* but not to *E. coli* cells, appeared to be derived from hemocytes. However, bands of BmMBP, which were slightly or much thicker than those seen in hemocytes, were detected in *M. luteus*- and *S. cerevisiae*-induced nodules, respectively, indicating that this protein came from the plasma (Fig. 1.8). Although little BmPGRP-S1 was detected in hemocytes and no visible band was detected from *E. coli*-induced nodules, this protein was abundant in *M. luteus*-induced nodules, indicating that the BmPGRP-S1 in these nodules came from the plasma (Fig. 1.8). As expected, the PRRs that were detected in each of the three microorganism-induced nodules were the same PRRs that bound to corresponding microorganisms in the microorganism-binding assays (Fig. 1.2). These results suggested that the six PRRs detected in the nodules were congregated with microorganisms from plasma (in normal conditions) due to the microorganism-aggregating ability of nodules and the microorganism-binding ability of PRRs.
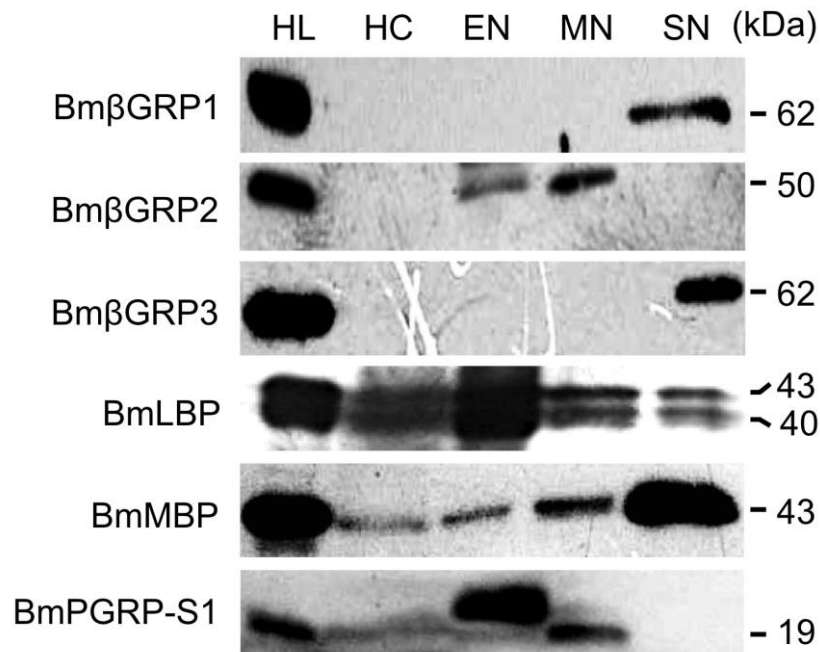
Fig. 1.8. Western blot analysis to deduce the origin and the way to transport into the nodules of BmPRRs. The protein samples come from hemolymph (HL), hemocytes (HC), and nodules induced by injection with *E. coli* (EN), *M. luteus* (MN), and *S. cerevisiae* cells (SN) respectively, were transferred onto a PVDF membrane. Western blot experiments were performed using antisera against BmβGRP1, BmβGRP2, BmβGRP3, BmLBP, BmMBP, and BmPGRP-S1 as the primary antibodies. An intense 21-kDa band was observed in *E. coli*-induced nodules using anti-BmPGRP-S1; it was hypothesized that this was an *E. coli* cell-derived protein. Because anti-BmPGRP-S1 antiserum was raised against an *E. coli*-produced recombinant protein, as described in Materials and Methods, the anti-BmPGRP-S1 antiserum likely includes antibodies raised against *E. coli* cell-derived proteins.

1.3.6. Immunocytochemical localization of BmPRRs in nodules

It is likely that PRRs in plasma well contribute to nodule melanization through specific binding to microorganisms, and then was trapped into nodules (Fig. 1.8). Therefore, a speculation that PRRs should be found mainly around the microorganisms in nodules is reasonable. To validate this, immunostaining of nodule cryosections was observed. As shown in Figs. 1.9–1.14, all six BmPRRs (green fluorescence) were found only in nodules induced by microoganisms which they could recognize (Fig. 1.2). Furthermore, green fluorescence were observed to be scattered all around inside the nodule (Figs. 1.9–1.14). In *E. coli*- or *M. luteus*-induced nodules, at a higher magnification, green fluorescence was mostly observed that located in the area where could not be covered by the nuclei of hemocytes; besides, the shape and scale fit the *E. coli* and *M. luteus* cells (Figs. 1.9–1.14 A and B, arrowheads). The nuclei of hemocytes are bigger, and could be densely stained by DAPI with blue fluorescence. In the case of *S. cerevisiae*-induced nodules, at a higher magnification, green fluorescence was observed that fit the shape and scale of *S. cerevisiae* cells; sometimes, the fluorescence around the nuclei of *S. cerevisiae* cells were observed (Figs. 1.9–1.14 C, arrowheads). The nuclei of *S. cerevisiae* cells are very smaller, and merely weakly stained by DAPI. These results further conformed that BmPRRs have specific binding properties to different microorganisms, and plasma is the main origin route of nodule BmPRRs.
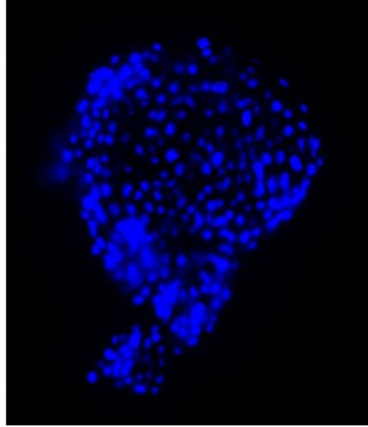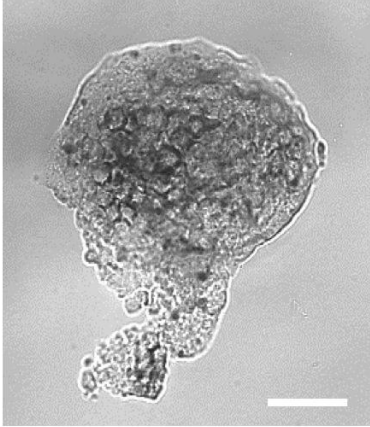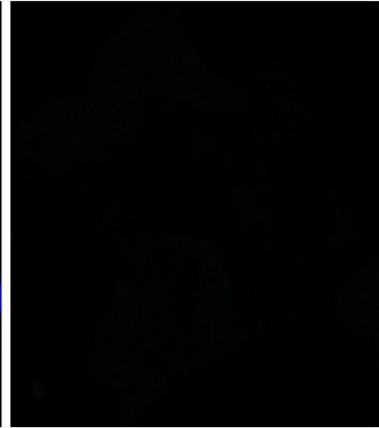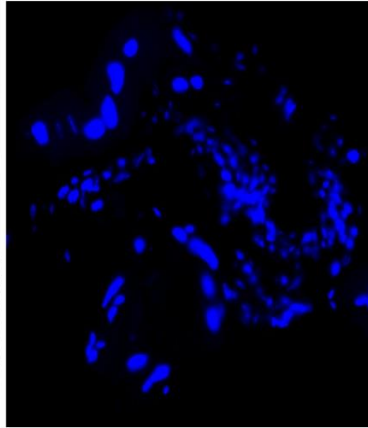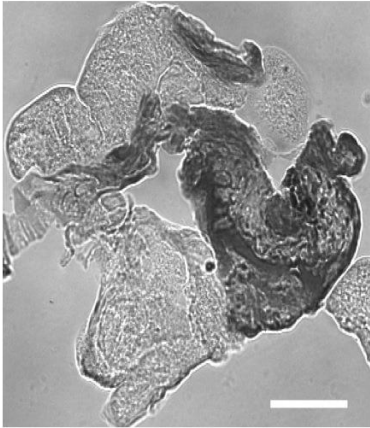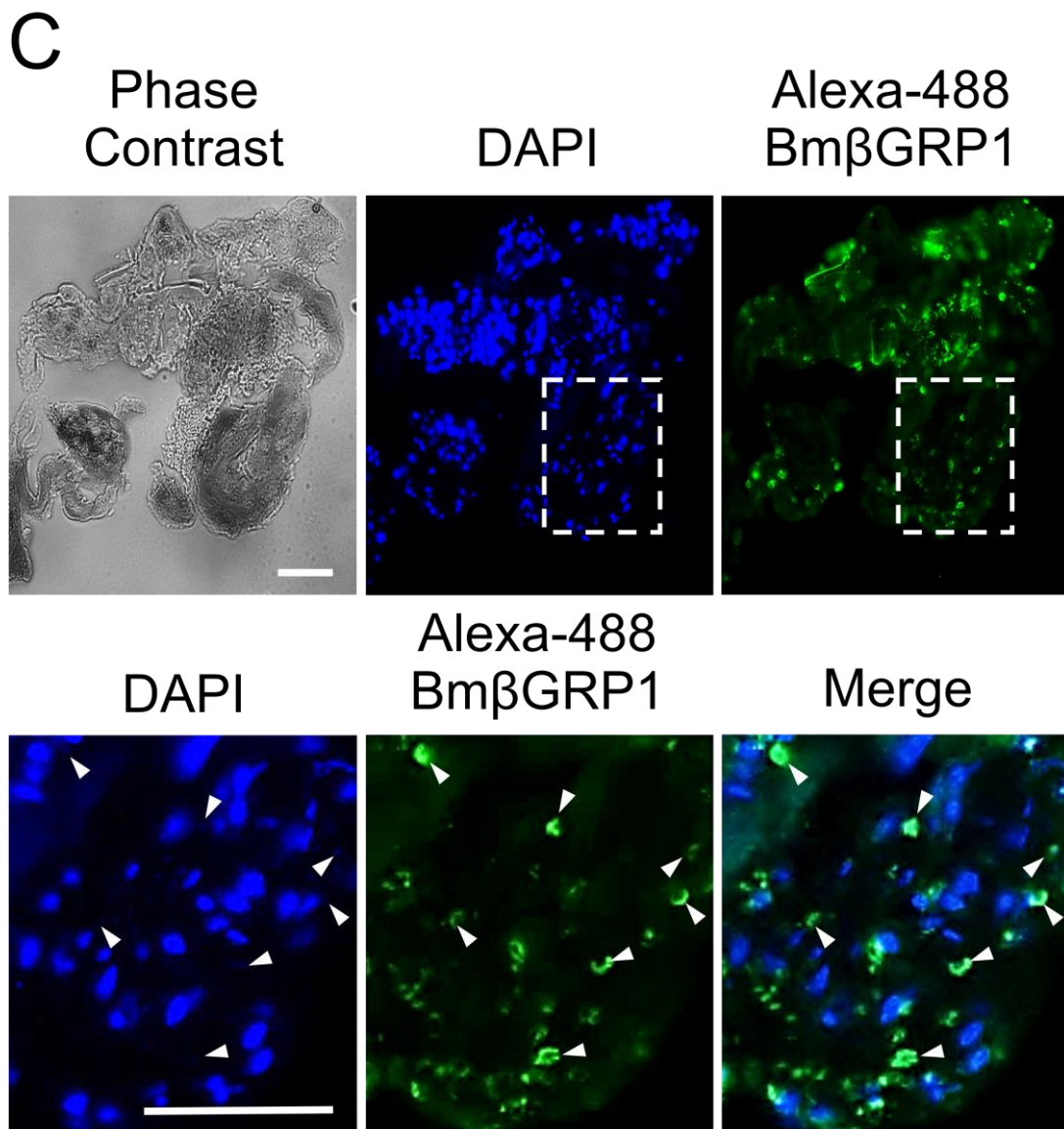
Fig. 1.9. Immunofluorescent detection of BmβGRP1 in cryosections of nodule. A, crysection from *E. coli*-induced nodule; B, crysection from *M. luteus*-induced nodule; C, crysection from *S. cerevisiae*-induced nodule. The nuclei of hemocytes in nodule crysections were densely stained by DAPI with blue fluorescence. BmβGRP1 was stained with mouse anti-BmβGRP1 antiserum in combination with anti-mouse IgG conjugated to Alexa Fluor

488®. Images indicated below in C are higher magnification of the area outlined in the dashed rectangle in the above images; green fluorescence which fit the shape and scale of *S. cerevisiae* cells in nodule, and not merged by blue fluorescence (hemocytes nuclei), are indicated by arrowheads (the middle and right panels); the same regions in DAPI-stained image (left panel) are also indicated by arrowheads. Scale bars represent 20 μm.

A

Phase
Contrast

DAPI

Alexa-488
BmβGRP2

DAPI

Alexa-488
BmβGRP2

Merge

B

Phase Contrast

DAPI

Alexa-488 BmβGRP2

DAPI

Alexa-488 BmβGRP2

Merge

C

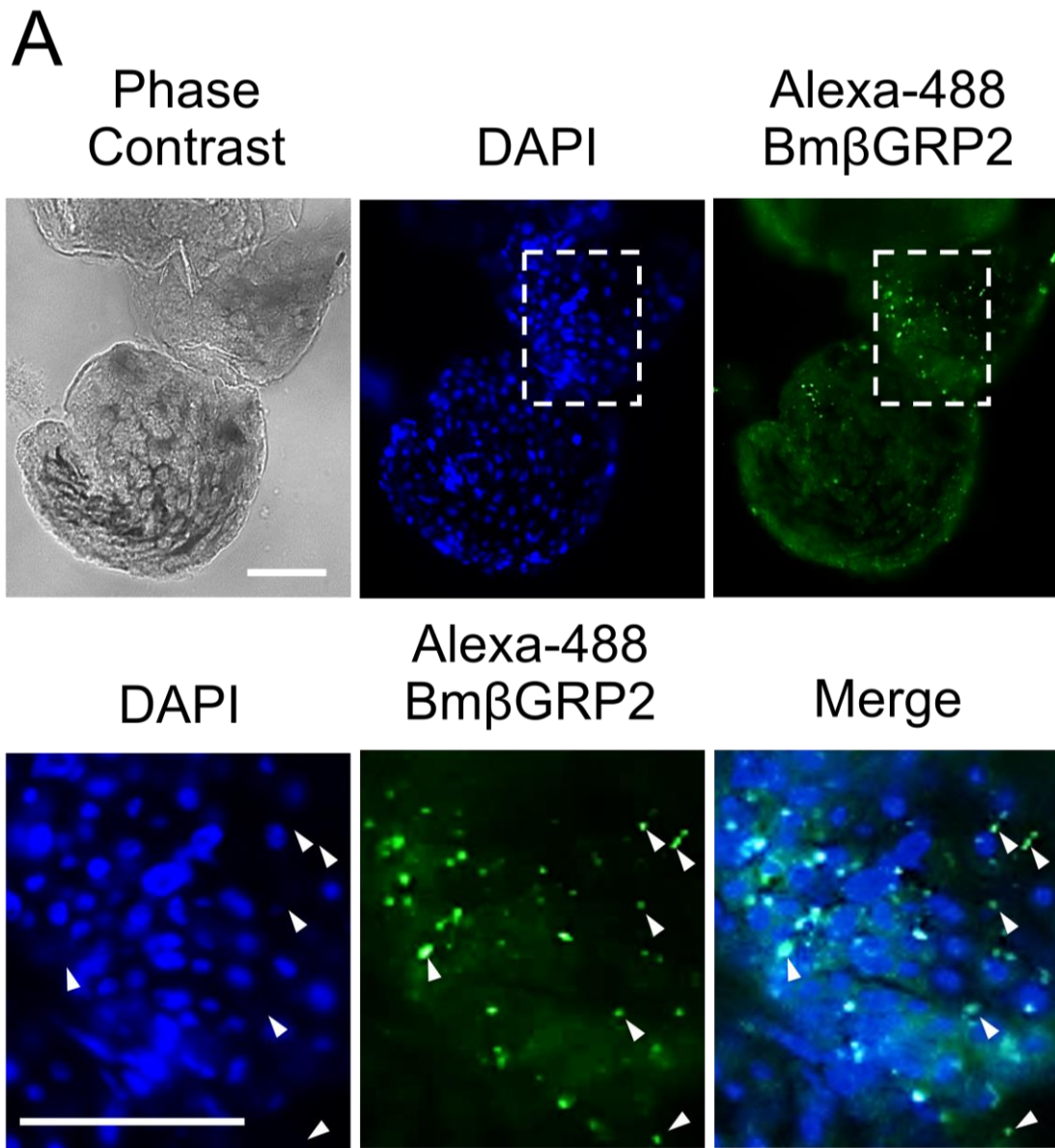Phase Contrast   DAPI   Alexa-488 BmβGRP2

Fig. 1.10. Immunofluorescent detection of BmβGRP2 in cryosections of nodule. A, crysection from *E. coli*-induced nodule; B, crysection from *M. luteus*-induced nodule; C, crysection from *S. cerevisiae*-induced nodule. The nuclei of hemocytes in nodule crysections were densely stained by DAPI with blue fluorescence. BmβGRP2 was stained with mouse anti-BmβGRP2 antiserum in combination with anti-mouse IgG conjugated to Alexa Fluor 488®. Images indicated below in A and B are higher magnification of the area outlined in the dashed rectangle in the above images; green fluorescence which fit the shape and scale of *E. coli*, *M. luteus* cells in nodules, and not merged by blue fluorescence (hemocytes nuclei), are indicated by arrowheads (the middle and right panels); the same regions in DAPI-stained images (left panel) are also indicated by arrowheads. Scale bars represent 20 μm.
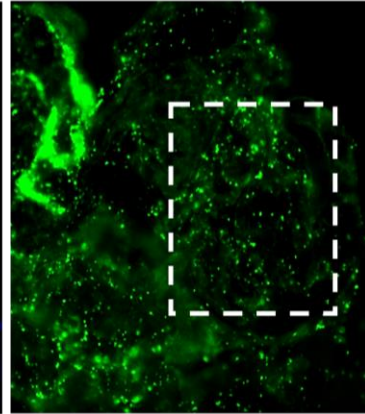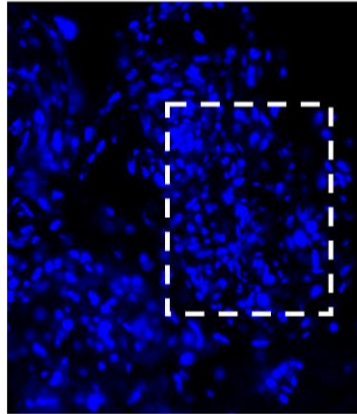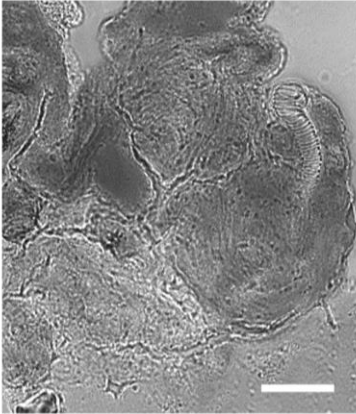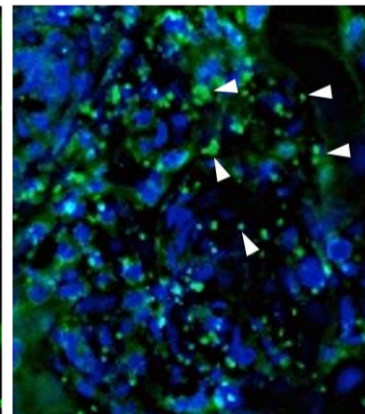
Fig. 1.11. Immunofluorescent detection of BmβGRP3 in cryosections of nodule. A, crysection from *E. coli*-induced nodule; B, crysection from *M. luteus*-induced nodule; C, crysection from *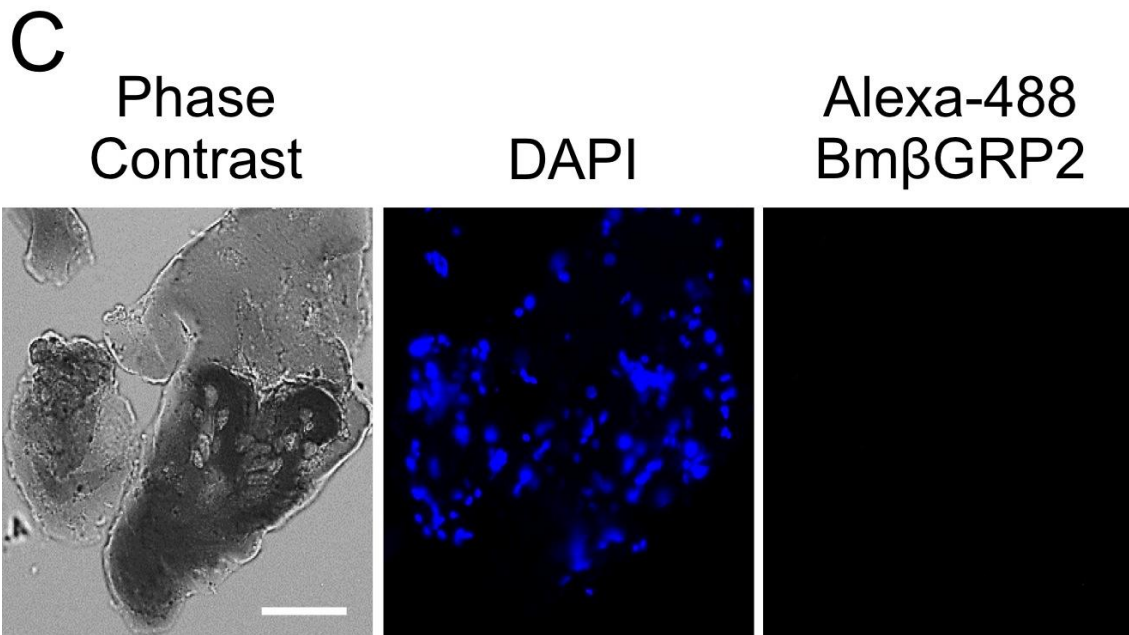S. cerevisiae*-induced nodule. The nuclei of hemocytes in nodule crysections were densely stained by DAPI with blue fluorescence. BmβGRP1 was stained with mouse anti-BmβGRP3 antiserum in combination with anti-mouse IgG conjugated to Alexa Fluor

488[®]. Images indicated below in B and C are higher magnification of the area outlined in the dashed rectangle in the above images; green fluorescence which fit the shape and scale of *M. luteus*, *S. cerevisiae* cells in nodules, and not merged by blue fluorescence (hemocytes nuclei), are indicated by arrowheads (the middle and right panels); the same regions in DAPI-stained images (left panel) are also indicated by arrowheads. Scale bars represent 20 μm.

A

Phase Contrast	DAPI	Alexa-488 BmLBP

DAPI	Alexa-488 BmLBP	Merge

B

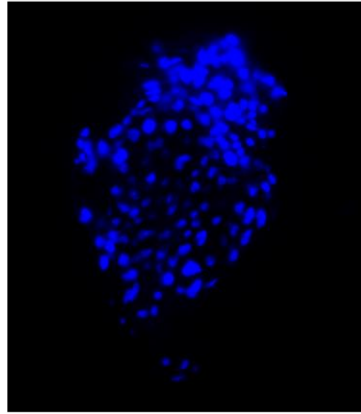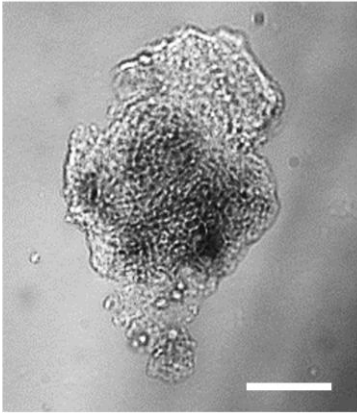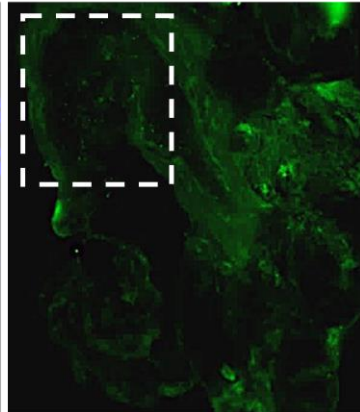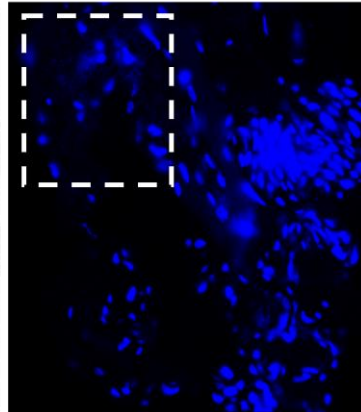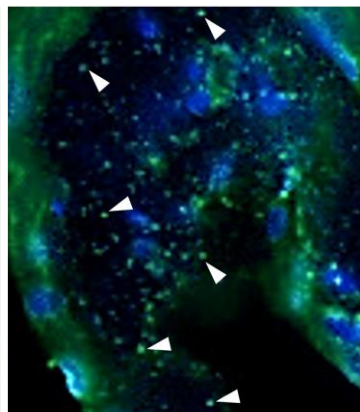| Phase Contrast	DAPI	Alexa-488 BmLBP

C

Phase Contrast | DAPI | Alexa-488 BmLBP

Fig. 1.12. Immunofluorescent detection of BmLBP in cryosections of nodule. A, crysection from *E. coli*-induced nodule; B, crysection from *M. luteus*-induced nodule; C, crysection from *S. cerevisiae*-induced nodule. The nuclei of hemocytes in nodule crysections were densely stained by DAPI with blue fluorescence. BmLBP was stained with mouse anti-BmLBP antiserum in combination with anti-mouse IgG conjugated to Alexa Fluor 488®. Images indicated below in A are higher magnification of the area outlined in the dashed rectangle in the above images; green fluorescence which fit the shape and scale of *E. coli* cells in nodule, and not merged by blue fluorescence (hemocytes nuclei), are indicated by arrowheads (the middle and right panels); the same regions in DAPI-stained image (left panel) are also indicated by arrowheads. Scale bars represent 20 μm.
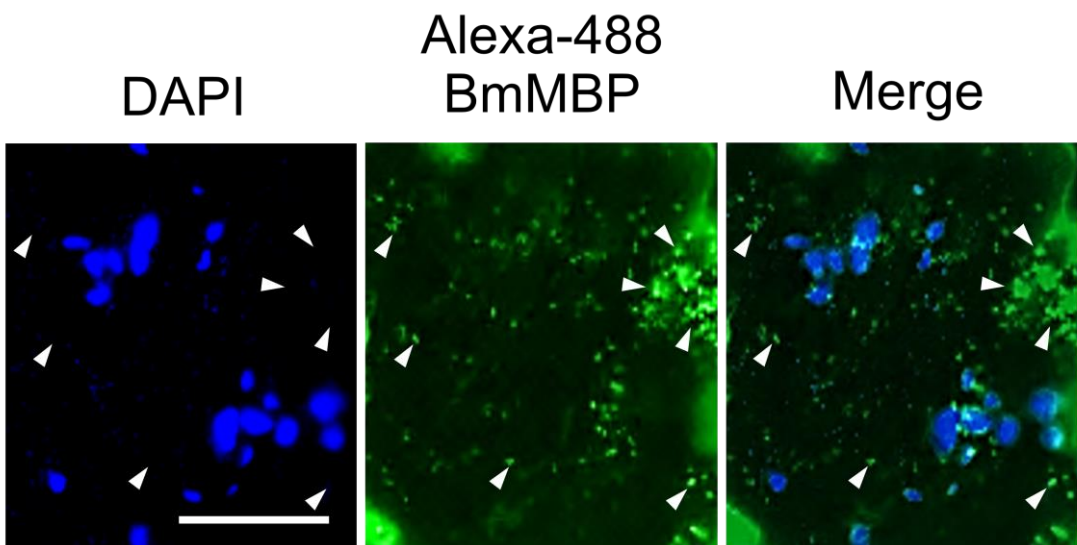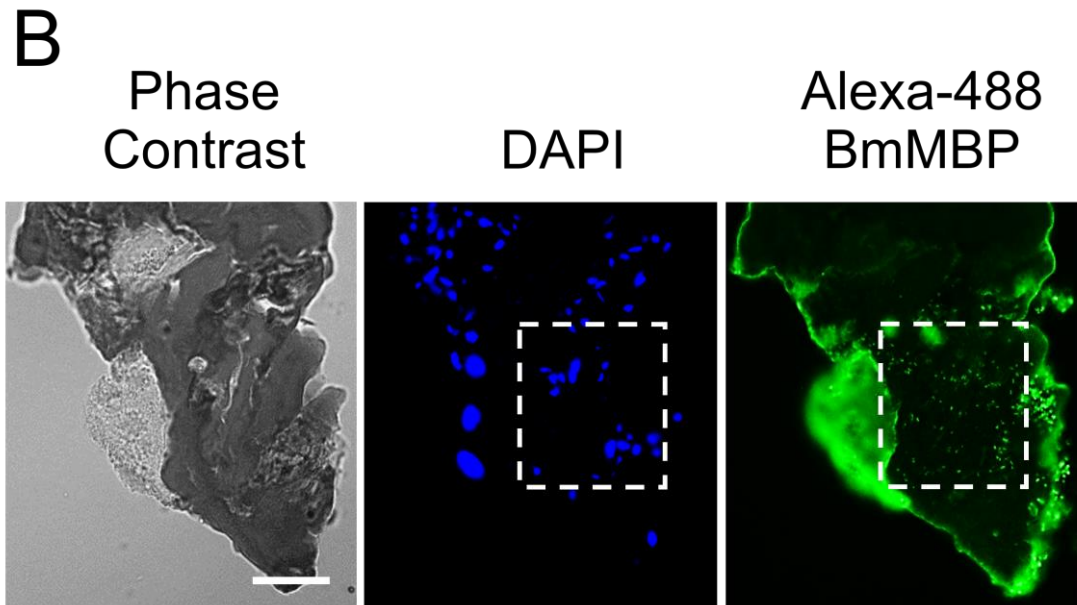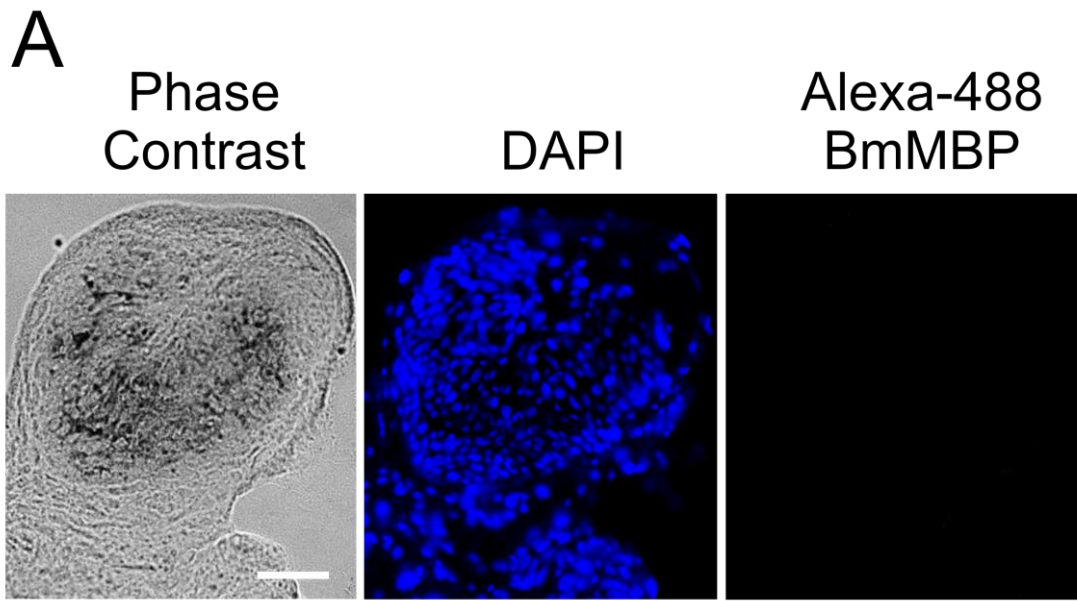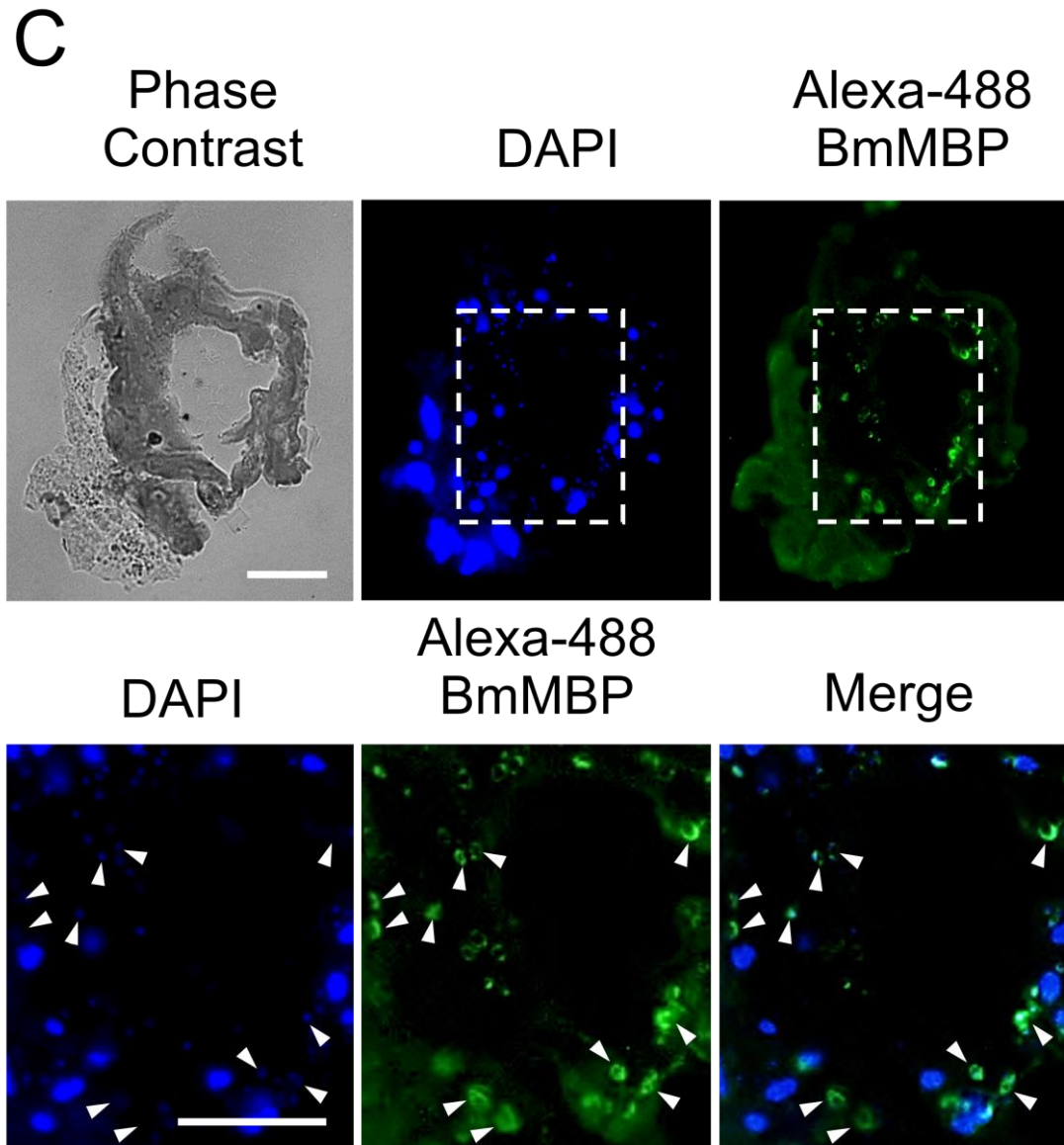
Fig. 1.13. Immunofluorescent detection of BmMBP in cryosections of nodule. A, crysection from *E. coli*-induced nodule; B, crysection from *M. luteus*-induced nodule; C, crysection from *S. cerevisiae*-induced nodule. The nuclei of hemocytes in nodule crysections were densely stained by DAPI with blue fluorescence. BmMBP was stained with mouse anti-BmMBP antiserum in combination with anti-mouse IgG conjugated to Alexa Fluor 488[®]. Images indicated below in B and C are higher magnification of the

area outlined in the dashed rectangle in the above images; green fluorescence which fit the shape and scale of *M. luteus*, *S. cerevisiae* cells in nodules, and not merged by blue fluorescence (hemocytes nuclei), are indicated by arrowheads (the middle and right panels); the same regions in DAPI-stained images (left panel) are also indicated by arrowheads. Scale bars represent 20 μm.
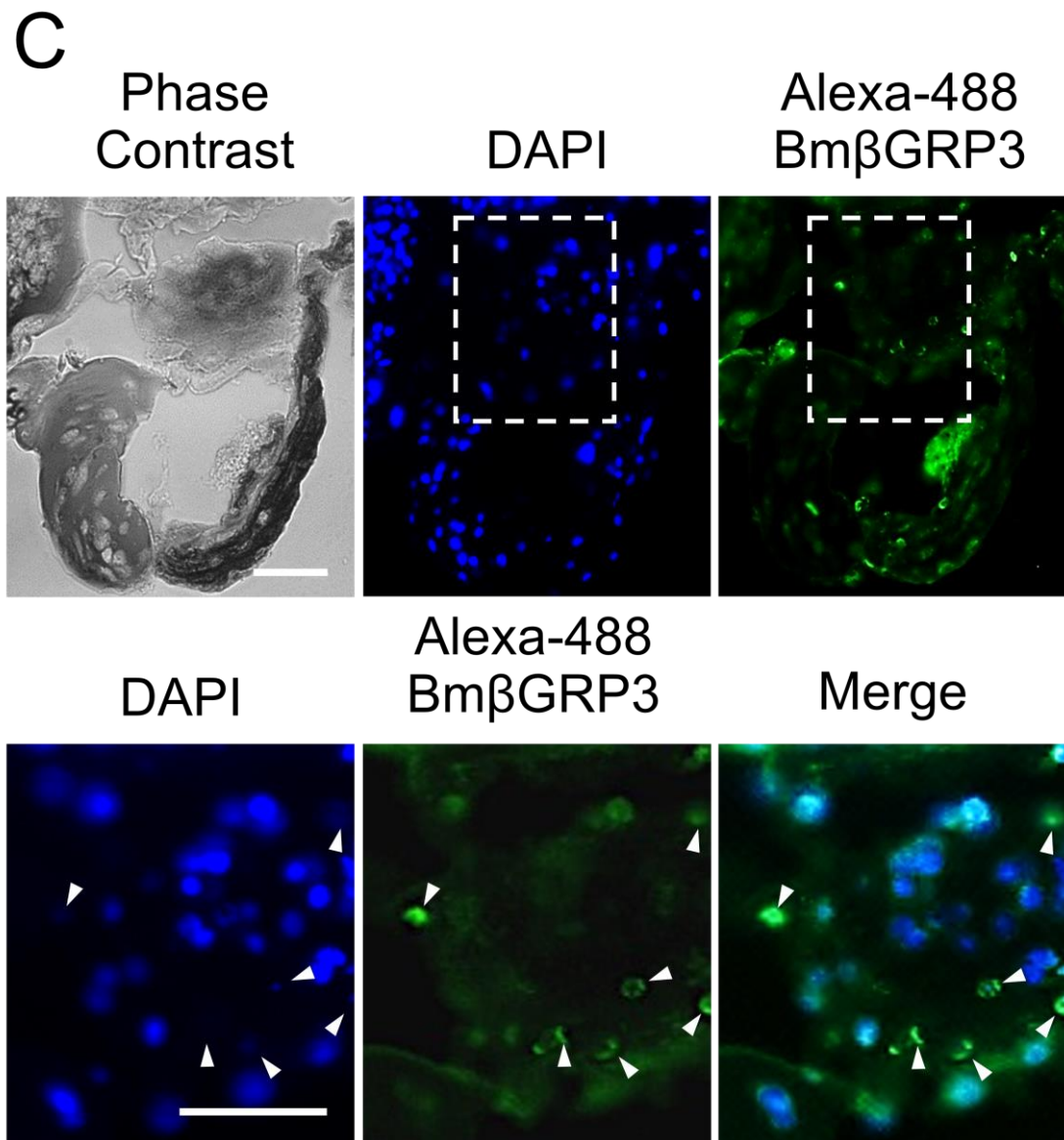
A

Phase Contrast	DAPI	Alexa-488 BmPGRP-S1

DAPI	Alexa-488 BmPGRP-S1	Merge

B

Phase Contrast | DAPI | Alexa-488 BmPGRP-S1

DAPI | Alexa-488 BmPGRP-S1 | Merge

C

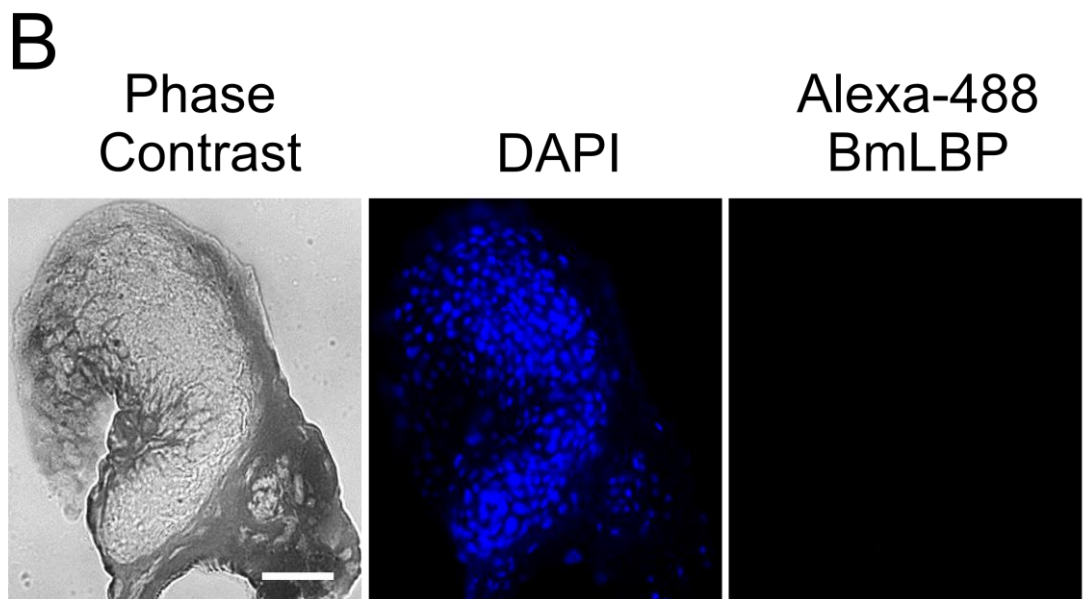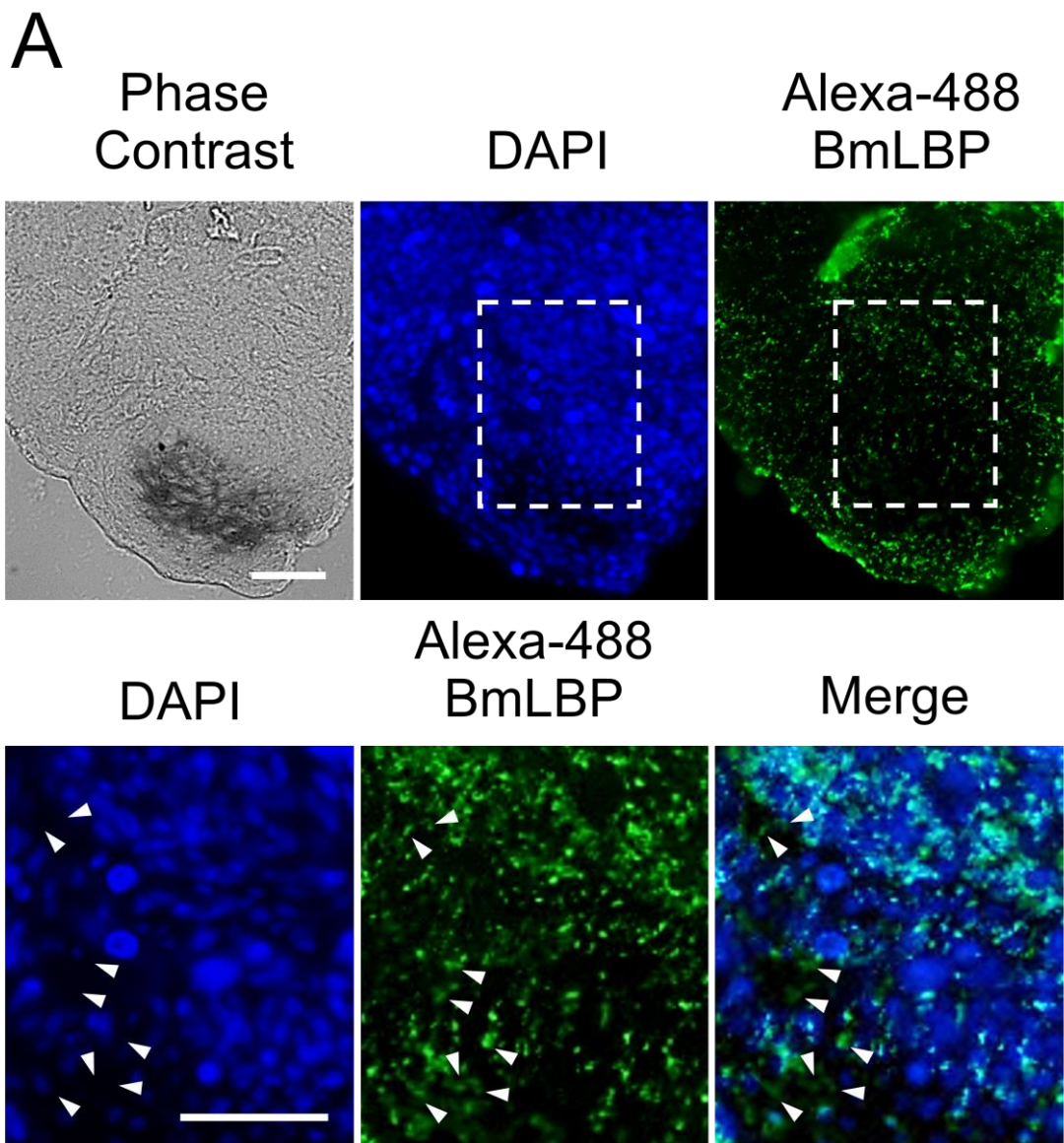| Phase Contrast | DAPI | Alexa-488 BmPGRP-S1 |
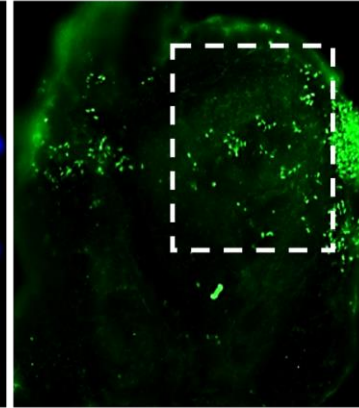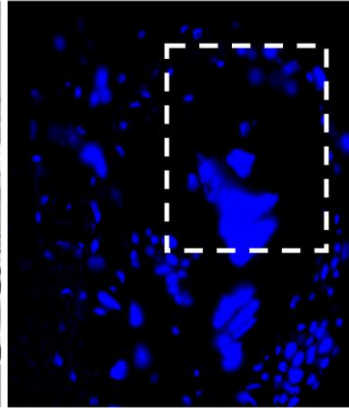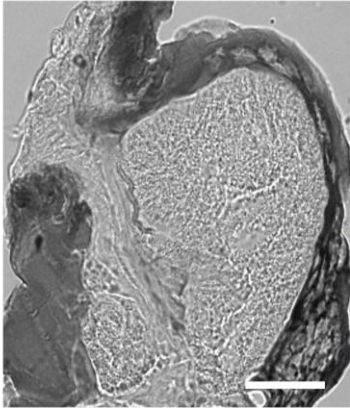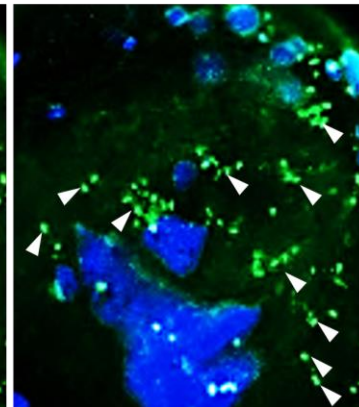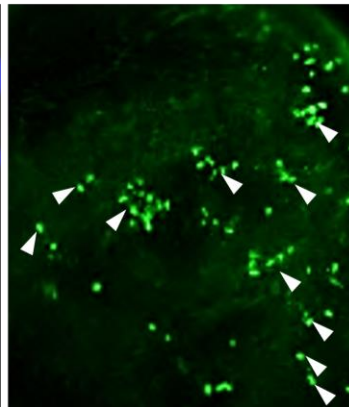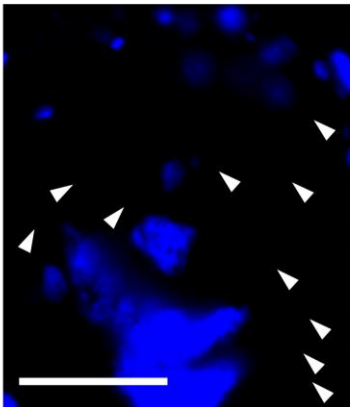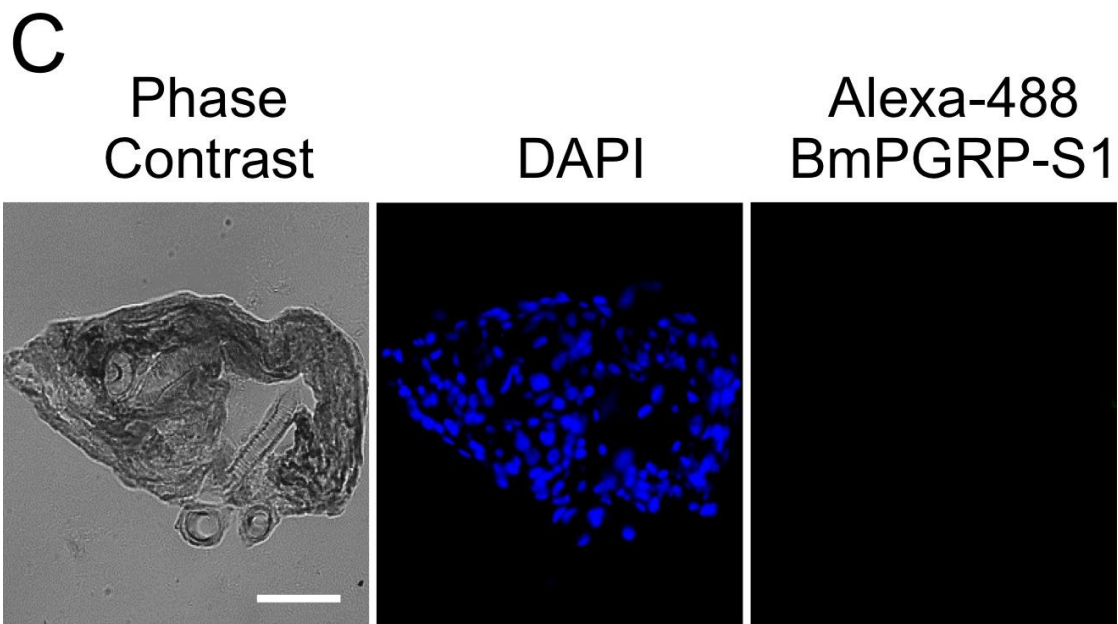
Fig. 1.14. Immunofluorescent detection of BmPGRP-S1 in cryosections of nodule. A, crysection from *E. coli*-induced nodule; B, crysection from *M. luteus*-induced nodule; C, crysection from *S. cerevisiae*-induced nodule. The nuclei of hemocytes in nodule crysections were densely stained by DAPI with blue fluorescence. BmPGRP-S1 was stained with mouse anti-BmPGRP-S1 antiserum in combination with anti-mouse IgG conjugated to Alexa Fluor 488®. Images indicated below in A and B are higher magnification of the area outlined in the dashed rectangle in the above images; green fluorescence which fit the shape and scale of *E. coli*, *M. luteus* cells in nodules, and not merged by blue fluorescence (hemocytes nuclei), are indicated by arrowheads (the middle and right panels); the same regions in DAPI-stained images (left panel) are also indicated by arrowheads. Scale bars represent 20 μm.
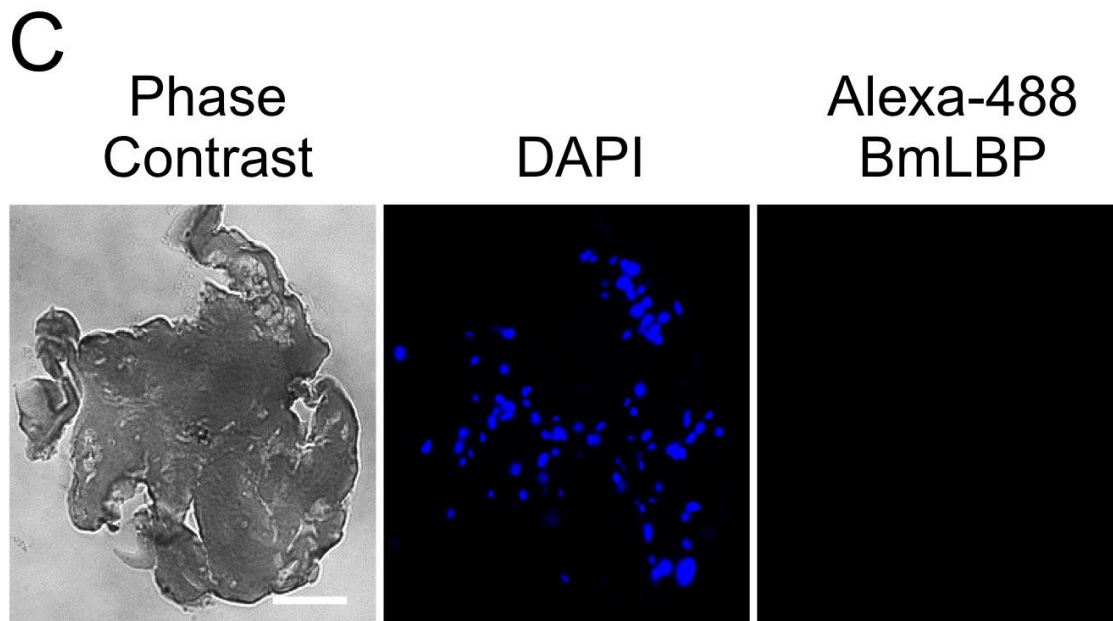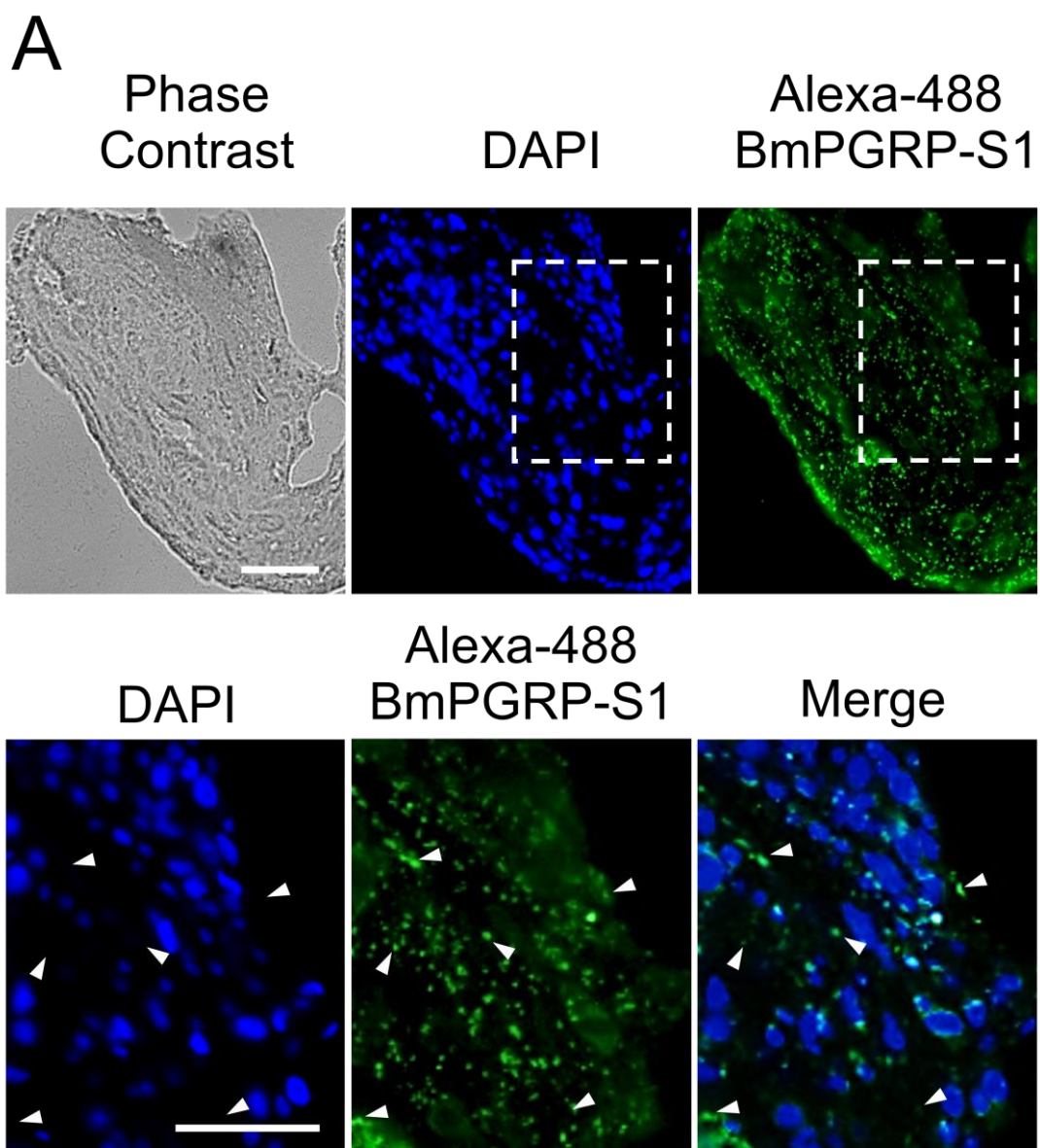
1.4 Discussion

The recognition of pathogens invading the hemocoel is thought to be dependent on the binding of PRRs to molecules on the surface of these pathogens. However, PRRs have restricted binding specificities and therefore do not bind to all microorganisms. In this study, results from microorganism-binding assays showed that BmβGRP1 could bind to *S. cerevisiae* (Fig. 1.2B), and BmMBP could bind to *S. cerevisiae* and *M. luteus* (Fig. 1.2B and C), which are consistent with results of previous studies (Ochiai and Ashida, 1988, 2000; Tokura et al., 2014; Watanabe et al., 2006). Moreover, it was found that BmLBP had an affinity to *E. coli* cells, which is also consistent with previous reports (Koizumi et al., 1997; Tokura et al., 2014). Although a previous study showed that BmβGRP2 (previously called GNBP) had a strong affinity to the cell walls of Gram-negative bacteria (Lee et al., 1996), this study shows that BmβGRP2 had a strong affinity to not only *E. coli* (Gram-negative) but also to *M. luteus* (Gram-positive) (Fig. 1.2A and C), suggesting that BmβGRP2 could be a recognition receptor for a wide range of bacteria. In addition, it was showed that BmβGRP3 (a new BmβGRP) could bind to *S. cerevisiae* and *M. luteus* (Fig. 1.2B and C). However, Yoshida et al. (1996) reported that BmPGRP-S1 (a peptidoglycan recognition protein) had an affinity for peptidoglycan prepared from the cell wall of *M. luteus* (Yoshida et al., 1996). The microorganism-binding assays revealed that BmPGRP-S1 could bind not only to *M. luteus* but also to *E.*

coli, indicating that BmPGRP-S1 may also be a receptor for a wide range of bacteria (Fig. 1.2A and C). Based on the systematic analysis of the specificities of various BmPRRs, it was showed that PRRs have far greater roles than expected and likely form intricate network to supervise invading pathogens.

RT-PCR showed that genes encoding BmPRRs were expressed in fat bodies and hemocytes as well as in *E. coli*-, *S. cerevisiae*-, and *M. luteus*-induced nodules (Fig. 1.4). Furthermore, immunostaining experiments showed that BmβGRP1 and five BmPRRs (BmβGRP2, BmβGRP3, BmLBP, BmMBP, and BmPGRP-S1) were expressed mainly in granulocyte granules and in the cytoplasm of plasmatocytes, oenocytoids, and prohemocytes (Fig. 1.5A–F). Granulocytes from lepidoptera insects are known to have a secretory function (Ochiai et al., 1992). Moreover, it is possible that granulocyte granules and oenocytoid cytoplasm molecules (Fig. 1.5) are released by degranulation and autolysis, respectively, in response to the recognition of microorganisms (Akai and Sato, 1973; Ashida and Brey, 1998). Granulocytes and oenocytoids are major components of nodules during an early stage of their formation (Arai et al., 2013). In this study, 30 minutes after triggering nodule formation, nodules were composed mainly of central granulocyte aggregates and only a thin outer layer of plasmatocytes (seen in Figs. 2.7 and 2.9, Chapter 2). Thus, granulocyte granules and oenocytoid contents may have been discharged in the nodule

after nodule formation. However, assuming BmPRRs were discharged, the function of this discharge is unclear, as the most important function of PRRs is the supervision of invading microorganisms in the hemolymph. Actually, microorganism-binding assay results indicated that BmPRRs in the plasma could recognize and bind to microorganisms (Fig. 1.2). Otherwise, degranulation may function in circumstances in which hemocytes need to reinforce defenses in the hemocoel in response to microorganism invasion. A previous study showed that hemocytes from *B. mori* larvae could bind lipopolysaccharide (LPS), lipoteichoic acid (LTA), and β-1, 3-glucan (Ohta et al., 2006), suggesting that hemocytes can respond to microorganism invasion.

Although both RT-PCR and hemocytes-immunostaining showed that BmPRRs could be expressed and stored in hemocytes, the Western blotting and nodule-immunostaining suggested that hemocytes may be just an auxiliary origin route for concentration increasing of BmPRRs in nodules (Figs. 1.4–1.5 and 1.8–1.14). On the contrary, plasma was considered as the main origin route of BmPRRs in nodules. Microorganism-binding assays suggested that BmPRRs in plasma bind to microorganisms specifically (Fig. 1.2), the Western blotting and nodule-immunostaining confirmed that the BmPRRs in plasma binding to microorganisms can be aggregated and trapped into nodules (Figs. 1.8–1.14). Together, these results suggested that the double origin routes of BmPRRs lead to BmPRRs abundance in nodules,

which may quickly initiate proPO-activating cascade of nodules.

CHAPTER 2

The stickiness-dependent congregation route of BmHP14 and the accumulation mechanisms of other BmHPs to *B. mori* larvae nodules

2.1 Introduction

It is known that by binding to the invading microorganisms, a part of Pattern recognition receptors (PRRs) subsequently trigger the activation of the Prophenoloxidase (proPO) cascade consisting of serine proteinases (HPs) and serine proteinase homologs (SPHs) (An et al., 2009; Gupta et al., 2005; Lu and Jiang, 2008; Wang and Jiang, 2006). For instance, through interaction with molecules of fungal cell wall, *Manduca sexta* β-1, 3-glucan recognition protein (βGRP (1 and 2)) activate *M. sexta* HP14 (MsHP14) which have been suggested as an initiation enzyme of the proPO activation (Wang and Jiang, 2006, 2010). Next, the MsHP14 cleaves MsHP21 which later activates proPO-activating proteinase-2 precursor (proPAP-2), and then, proPO is converted to phenoloxidase (PO) by active form of proPAP-2 (Wang and Jiang, 2007). Whereas, there is inconsistencies with the activation process by *Micrococcus luteus*, in which MsHP14 triggers proPO cascade through its auto-activation by interaction with molecules of *M. luteus* (Ji et al., 2004; Wang and Jiang, 2006). In addition, the MsHP6 is not only involved in proPO-activating system, but also activates MsHP8 to regulate the Toll pathway for antimicrobial peptides (AMP) production (An et al., 2009). However, the roles of most *M. sexta* HPs (MsHPs) are still unclear. Actually, PO exists as a zymogen, proPO in the normal hemolymph, was first reported in the *Bombyx mori* larvae (Ashida and Ohnishi, 1967), and then it was found that pathogen invading triggers proPO proteolytic

activation by means of proPO cascade consisting of several serine proteases in the silkworm (Ashida et al., 1974; Johansson and Söderhäll, 1996; Katsumi et al., 1995; Satoh et al., 1999). Up to present, however, except for a serine protease which was referred to as proPO-activating enzyme precursor (proPPAE), has been found that is required after being cleaved, to convert proPO to active PO (Satoh et al., 1999). Little is known about serine protease members at the upstream part of proPO cascade, and the physiological function of any other serine proteases in *B. mori* larvae. On the other hand, previous reports on *B. mori* in our laboratory have suggested that the melanization of hemolymph maybe only a byproduct of nodule melanization, since it was indicated that the progress of melanization of nodule is faster than that of hemolymph (Sakamoto et al., 2011; Tokura et al., 2014). This means that nodule maybe the preferential target for melanization, and its melanization mechanism should exist in the hemolymph. In this study, it was demonstrated that six of PRRs in *B. mori* hemolymph bound specific to microorganisms and were trapped into nodules for melanization of nodules. This is better evidence supporting the speculation that melanization mechanism of nodule should exist in the hemolymph. Subsequently, to best understand the essence and mechanisms of melanization, the roles of HPs in *B. mori* are studied through investigating their roles in nodule melanization. Which HPs are required for nodule melanization, and the way they are aggregated into nodules were confirmed

using antisera against BmHPs, first.

2.2 Materials and Methods

2.2.1. Identification of candidate HP orthologs of *B. mori*

B. mori orthologues of *M. sexta* HP1 (hemocyte protease 1, AF017663), HP3 (hemocyte protease 3, AF017665), HP5 (hemolymph proteinase 5, AAV91003), HP6 (hemolymph proteinase 6, AAV91004), HP8 (hemolymph proteinase 8, AAV91006), HP9 (hemolymph proteinase 9, AAV91007), HP10 (hemolymph proteinase 10, AAV91008), HP14 (pattern recognition serine proteinase, AY380790), HP17 (hemolymph proteinase 17, AAV91014), HP18 (hemolymph proteinase 18, AAV91016), HP19 (hemolymph proteinase 19, AAV91017), HP21 (hemolymph proteinase 21, AAV91019) which have been proved or predicted to participate in proPO-activating system or AMP-synthesizing system (Jiang et al., 2005) were identified using TBLASTN search systems of the KAIKObase (http://sgp.dna.affrc.go.jp/KAIKObase/) and DDBJ (DNA Data Bank of Japan, http://www.ddbj.nig.ac.jp/intro-e.html). Sequences with the highest identity to corresponding *M. sexta* HP (MsHP) were designated BmHP1 (AB436162), BmHP3 (BGIBMGA013013), BmHP5 (AK380629), BmHP6 (AK384444), BmHP8 (ABB58762), BmHP9 (DQ443346), BmHP10 (AK378029), BmHP14 (JQ954757), BmHP17 (BAB91156), BmHP18 (BGIBMGA010306), BmHP19 (AK386223), and BmHP21 (JF431073). Multiple sequence alignment between *B. mori* HPs and *M. sexta* HPs was conducted by ClustalW. Phylogenetic analysis was based on the neighbor-

joining method using Mega 6.06 software with 1000 bootstrap replicates and p-distance substitution model.

2.2.2. Preparation and specificity analysis of BmHPs antisera

Antisera against BmHPs orthologues including BmHP8 (ABB58762) and BmHP14 (JQ954757) were prepared by immunization of the mature peptides encoding regions. The cDNA fragments were amplified by PCR using specific primers in table 2.1 and inserted into the GST fusion protein expression vector pGEX-4T-3 (GE Healthcare, Little Chalfont, UK). Following sequence verification, the resulting plasmids were used for producing recombinant proteins in *Escherichia coli* BL21 competent cells (TaKaRa, Shiga, Japan) as mentioned in 1.2.3. Next, these recombinant proteins were injected to female mouse to raise antisera of BmHP8 and BmHP14. Moreover, anti-BmproPO1 and anti-BmHP21 antisera were raised as previously reported (Tokura et al., 2014). Specificities of all antisera were evaluated using normal *B. mori* plasma by Western blot. Plasma fraction, hemocytes pellets and nodules which were collected in section 1.2.1, were also used for the following experiments.

2.2.3. Microorganism-binding assay for the analysis of BmHPs binding property to microoganisms

Paraformaldehyde-fixed *E. coli*, *Saccharomyces cerevisiae* or *Micrococcus*

luteus cells which prepared as described in 1.2.2 (60 μl of precipitate) were mixed with 1 ml of cell free plasma diluted with IPS for 3 times or IPS alone, and incubated for 8 min with mild agitation. By another description in 1.2.4, the mixtures were separated by centrifugation at 2500 g for 3 min at 4 °C and pellets were washed with IPS twice. Proteins bound to microorganisms were treated with 120 μl of 2×SDS-sample buffer (125 mM Tris-HCl, pH 6.8, 4% SDS, 10% 2-mercaptoethanol, 0.05% bromophenol blue, 20% glycerol) at 98 °C for 5–30 sec. Eluted samples (12–25 μl) were separated by Laemmli-SDS-PAGE (Laemmli, 1970) and bound proteins were detected by immunoblot but using the antibodies described in Section 2.2.2.

2.2.4. Expression analysis of BmHPs by RT-PCR

Total RNA from fat bodies, hemocytes and nodules which were induced by *E. coli*, *M. luteus* or *S. cerevisiae* cells injection were prepared as previous description in 1.2.5. Double-stranded cDNA fragments of BmHPs were amplified by PCR using GoTaq DNA polymerase (TaKaRa, Shiga, Japan) for 35 cycles and the gene-specific primers for individual proteins indicated in table 2.2. The *B. mori β-actin* was used as an internal standard to normalize the cDNA pools. PCR products were separated by agarose gel electrophoresis and stained by ethidium bromide.

2.2.5. Immunofluorescent staining for the observation of BmHPs expression

and storage in hemocytes

Immunofluorescent staining of hemocytes were carried out as description in section 1.2.6, but now using mouse antiserum raised against BmproPO1, BmHP8, BmHP14, or BmHP21 in combination with 1000-fold diluted Alexa Fluor 488® conjugated goat anti-mouse IgG (Bio-Rad, Hercules, CA, USA). Antisera were diluted using 1% BSA solution containing 0.1% Triton X-100. The nuclei of hemocytes were counter stained with 4', 6-diamidine-2'- phenylindole dihydrochloride (DAPI; 1 µg/ml, Sigma Aldrich, Schnelldorf, Germany). Fluorescence was observed under a microscope, LSM710/LSM710 NLO (CARL ZEISS). Oenocytoids, granulocytes, spherulocytes, plasmatocytes and prohemocytes were identified by the differences which have been described in section 1.2.6.

2.2.6. Western blot analysis to confirm the concentration of BmHPs in the nodules

Western blot was performed as has been described in section 1.2.7. However, after blocking with 2% BSA, the transferred membrane was incubated with mouse antiserum against BmproPO1, BmHP8, BmHP14, or BmHP21 for 90 min following the appropriate dilution. After washing, the membrane was incubated with 30,000-fold diluted peroxidase-conjugated goat anti-mouse IgG (Bio-Rad, Hercules, CA, USA) for 45 min, and then stained using ECL™ prime Western blotting detection reagent (GE Healthcare, Little

Chalfont, UK).

2.2.7. Immunofluorescent staining for the confirmation of BmHPs in nodules

The immunofluorescent staining of nodules were carried out as description in section 1.2.8, but now using mouse antiserum raised against BmHP8, BmHP14, or BmHP21 in combination with 1000-fold diluted Alexa Fluor 488$^{®}$ conjugated goat anti-mouse IgG (Bio-Rad, Hercules, CA, USA).

Table 2.1. The specific primers for antisera production

Gene name	Forward primer (5´-3´)	Reverse primer (5´-3´)
BmHP8	CAACGGCGGATCCAACTGTATAC	GTGTAGACTCGAGGCCAGCCTT
BmHP14	ATGCACTCCAGGATCCGGCAGAGT	GTGTTTCGAGACTCGAGTGAATGTTGTG

Table 2.2. Primers for individual proteins used in RT-PCR

Gene name	Forward primer (5´-3´)	Reverse primer (5´-3´)
BmproPO1	GCCAGGATGCCAATAGT GAT	GAGGTCGCCGTAGTAG GGTC
BmHP1	TCTTCCTGCTACCGCTC CTA	CTTTCCGCCTTCAAGTC CA
BmHP3	ATGATTTGTGCTGGAGG TG	CCAAGGAAGTAGGGGA GAT
BmHP5	CCGAAGCCCGTTCCTAC TA	ACCTGCTACCACGCCAA AG
BmHP6	CGTGAATTCTCGGATAG AGCCCAGTT	GGAGTCGACAGGTAGT TTACGCCAAT
BmHP8	CAACGGCGGATCCAAC TGTATAC	GTGTAGACTCGAGGCC AGCCTT
BmHP9	GTGCAAACCGAATTCTC CAACAGT	GAGAGCACAGTCGACC CCGAATGA
BmHP10	TGTGTTTCTTGGATCCC CAAAATT	TAGTCATAGACTCGAGC GTATACAGC
BmHP14	ATGCACTCCAGGATCCG GCAGAGT	GTGTTTCGAGACTCGAG TGAATGTTGTG
BmHP17	AGCTGTCTGAATTCGCT CCAG TGC	ACAACCTTCTCTCGAGT CCAGGGAAC

Gene name	Forward primer (5´-3´)	Reverse primer (5´-3´)
BmHP18	CACTCATCCTGAATTCCAGGGATAGATC	TCAGCGTCGACCTCGCTCACTTCA
BmHP19	GGCTTTGTGACCGTTGTGCT	CCATTGTCGTCGTGGTGTTG
BmHP20	TAGCGATGTTGATGGAAGCG	CATTTGCGATATTTGAGGTGAG
BmHP21	CGAGGGTGAAGAATGTAA	GTCCTGTCTCCGTAGCA
β-actin	AACTGGGATGACATGGAGAAGATCTGGC	GAGATCCACATCTGCTGGAAGGTGGA

2.3 Results

2.3.1. BLAST search and phylogenetic analysis of *B. mori* orthologues based on *M. sexta* serine proteinases

More than 20 MsHPs have been identified in the hemolymph of *M. sexta*, a lepidopteran insect (An et al., 2009; Jiang et al., 2005). However, only a few are known about their partial functions in the proPO-activating system or AMP-synthesizing system. Moreover, in most of species of insect, such as *B. mori*, except for proPPAE, almost no physiological function of any other HPs has been known. On the other hand, based on results from the examinations on *B. mori*, it was suggested that nodule may be the preferential target for melanization, and its melanization mechanism should exist in the hemolymph (Sakamoto et al., 2011). To best understand the essence and mechanism of melanization, the roles of HPs in *B. mori* were studied through investigating their roles in nodule melanization. Based on the alignment with MsHPs, *B. mori* candidate orthologues of MsHPs were identified after obtaining amino acid sequences using a TBLASTN search of the KAIKObase (http://sgp.dna.affrc.go.jp/KAIKObase/) and DDBJ (DNA Data Bank of Japan, http://www.ddbj.nig.ac.jp/intro-e.html) databases. As shown in Fig. 2.1, 12 *B. mori* orthologue candidates were found. In the phylogenetic tree, each candidate and corresponding MsHP used for its TBLASTN search were located on the nearest branch in one subgroup, suggesting that all 12 *B. mori* candidates were orthologues of
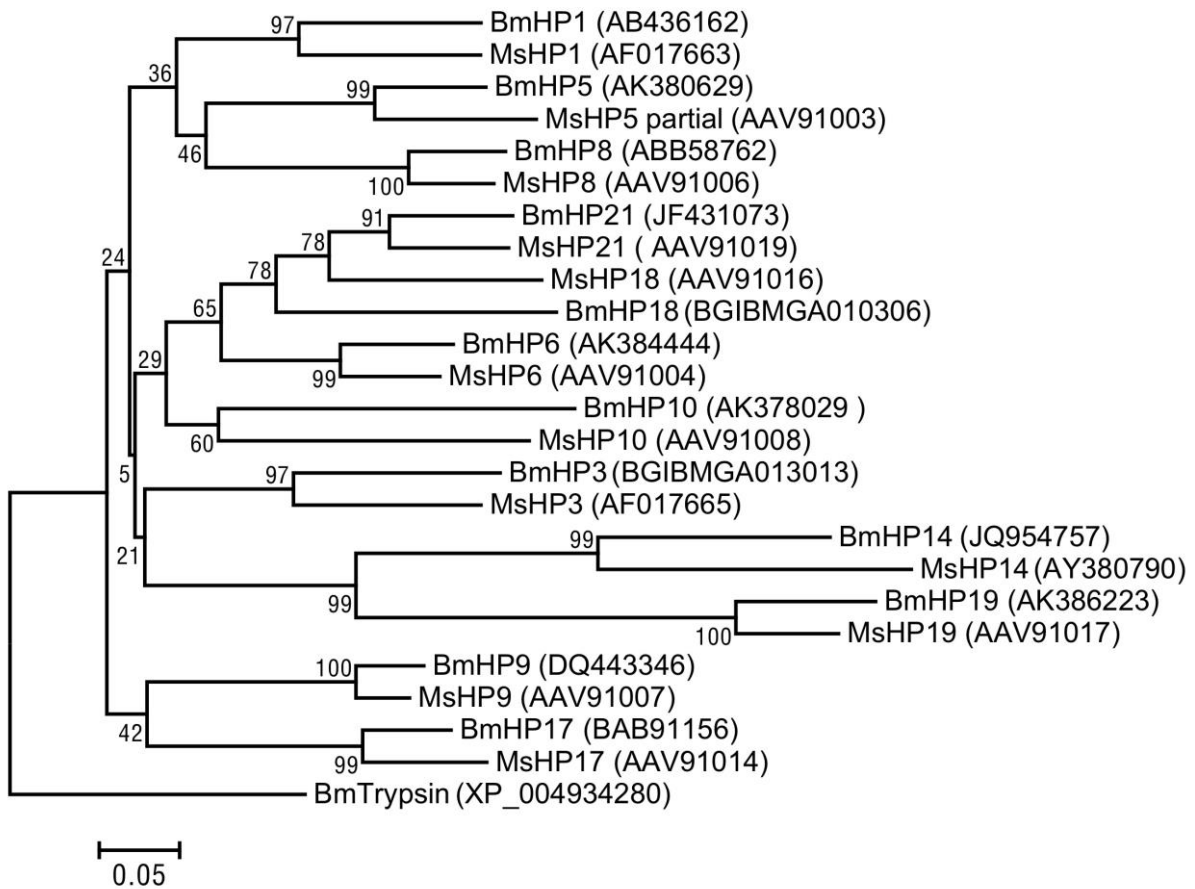
Fig. 2.1. Phylogenetic tree of candidate serine proteinase orthologs of *B. mori* and serine proteinases from *M. sexta*. Amino acid sequences of serine proteinase orthologs and serine proteinases were aligned using the neighbor-joining method integrated in ClustalW, in which *B. mori* trypsin (BmTrypsin) was used as an outgroup. Percent numbers at the nodes indicate bootstrap values (1000 trials). GenBank[TM] accession numbers are indicated in parentheses. MsHPs, *M. sexta* serine proteinases; BmHPs, *B. mori* serine proteinases, orthologue candidates.

corresponding MsHPs and had similar functions. The 12 *B. mori* orthologues of corresponding MsHPs were referred to as BmHP1, BmHP3, BmHP5, BmHP6, BmHP8, BmHP9, BmHP10, BmHP14, BmHP17, BmHP18, BmHP19, and BmHP21.

2.3.2. Specificity analysis of BmHPs antisera

To investigate the roles of the 12 BmHPs, mouse or rabbit polyclonal antisera specific to each of the 12 BmHPs were attempted to be prepared. However, only antisera against BmHP8, BmHP14, and BmHP21 were successfully prepared. The specificity of these antisera were verified using normal plasma from *B. mori* larvae as a control. Mouse anti-BmHP8 antiserum recognized a 41-kDa protein, which is close to the theoretical molecular mass of BmHP8 (Fig. 2.2). Mouse anti-BmHP14 antiserum recognized a 70-kDa protein (Fig. 2.2); however, two additional bands at 48 and 30 kDa were detected with longer exposure (as shown in Fig. 2.3). It is possible that BmHP14 was auto-activated in plasma under the experimental conditions because each band size is similar to a precursor or activated form of MsHP14 in *M. sexta* (Ji et al., 2004; Wang and Jiang, 2006, 2010). Mouse anti-BmHP21 antiserum recognized a single 45-kDa protein in normal plasma (Fig. 2.2), which corresponded well to previous report (Tokura et al., 2014). Besides, mouse antiserum against BmproPO1 were also prepared. This antiserum recognized single bands at 71 kDa in normal plasma. All of

results indicated that these prepared antisera were specific and could therefore be used in following experiments.
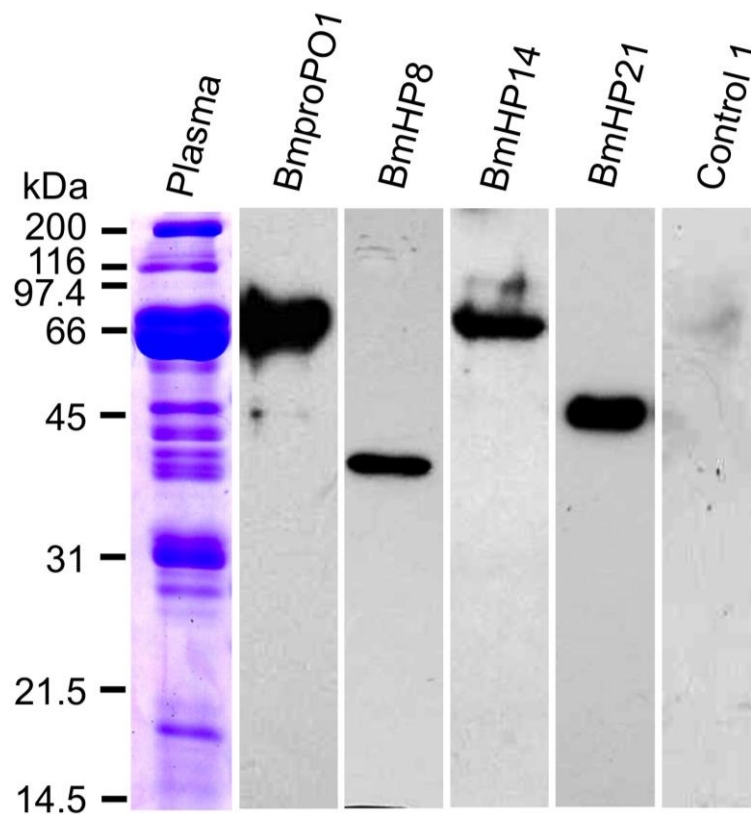

Fig. 2.2. Western blot analysis for confirmation of BmHPs antisera specificity. The specificity of mouse antisera against BmproPO1, BmHP8, BmHP14, and BmHP21 were confirmed using the plasma of *B. mori* larvae. Preimmune mouse (control 1) serum were used as primary antibody for negative control.

2.3.3. Microorganism-binding assay for detection of binding property of BmHPs

In previous studies, MsHP14 was indicated to trigger proPO-activation cascade through its auto-activation which is induced by interaction with molecules of *M. luteus* (Ji et al., 2004; Wang and Jiang, 2006). However, it remains unknown whether this interaction with microorganism is progressed directly by binding to microorganism or indirectly by PRRs, since in the case of fungi the process of proPO activation requires PRRs, βGRP1 and βGRP2 (Wang and Jiang, 2006, 2010), even in the case of *M. luteus* they are not needed (Ji et al., 2004; Wang and Jiang, 2006). To explore the role of BmHPs in nodule melanization, the interaction manner between them and microorganisms were first examined using microorganism-binding assay. As description in section 1.3.2, proteins that bound to *E. coli*, *S. cerevisiae*, and *M. luteus* cells were eluted, and detected by Western blot.

In the plasma, BmHP8 was activated during incubation with *S. cerevisiae* and *M. luteus*, and BmHP21 was activated during incubation with all three microorganisms, although both BmHP8 and BmHP21 were not detected on the surface of any of the microorganisms (Fig. 2.3A–C). In contrast, a significant quantity of BmHP14 was detected on the surface of *S. cerevisiae* as a 70-kDa proenzyme and as the 30-kDa activated form of BmHP14 (Fig. 2.3B). The binding property of BmHP14 was also indicated by its reduction in amount in the plasma after *S. cerevisiae* incubation.
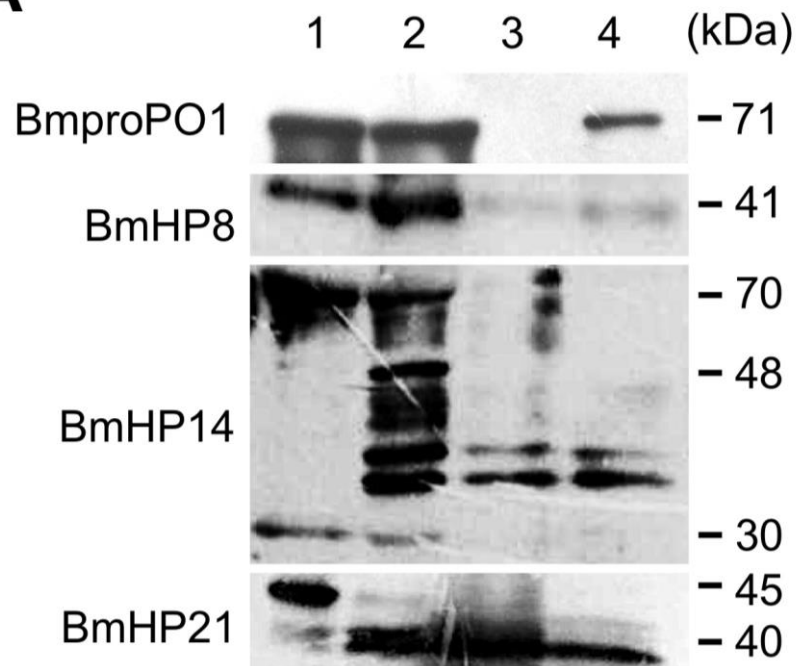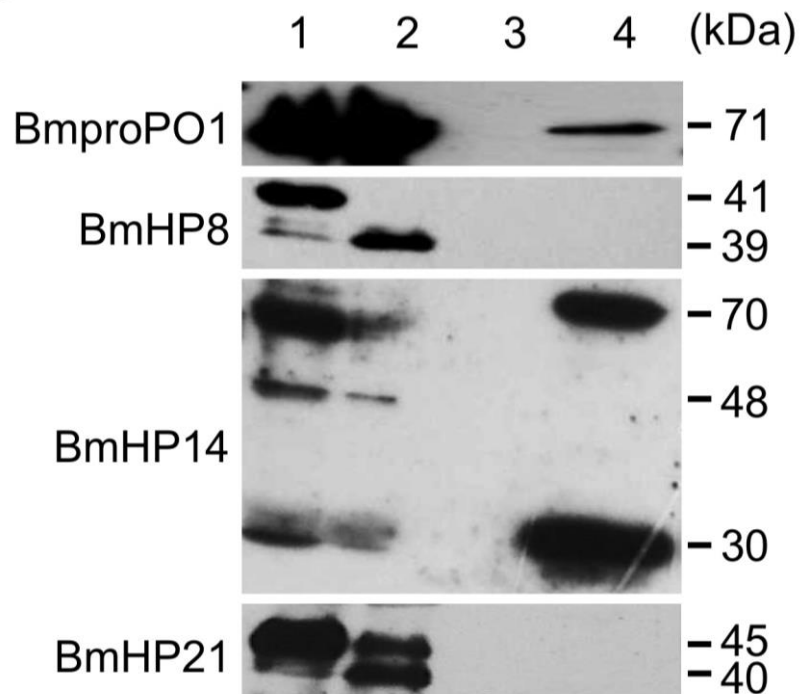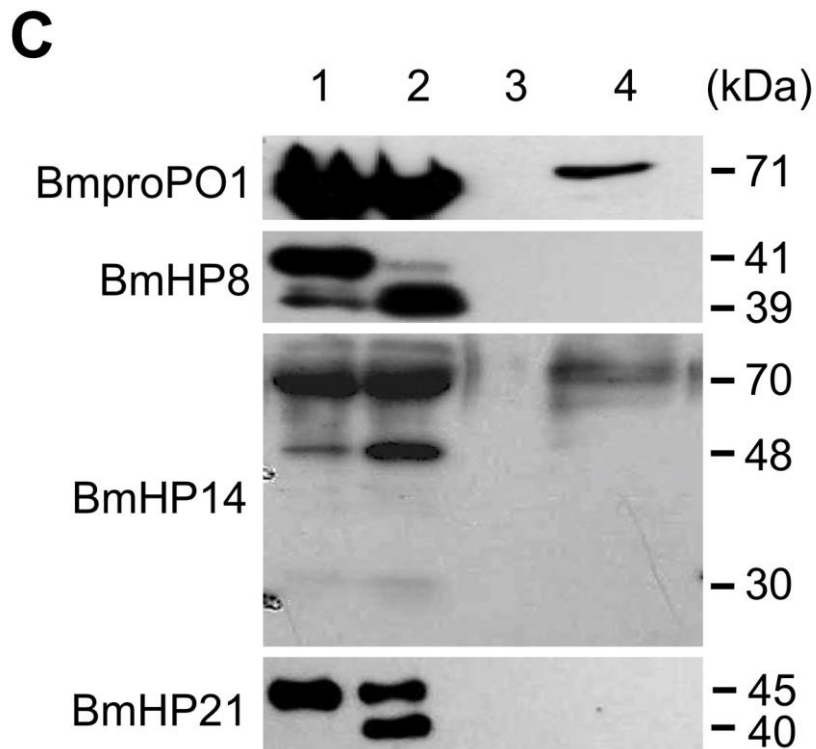
Fig. 2.3. Specific binding of BmHPs in plasma to microorganisms. The specific binding of BmproPO1, BmHP8, BmHP14, and BmHP21 to microorganisms were detected by immunoblot analyses after plasma (cell-free hemolymph) was incubated with paraformaldehyde-fixed *E. coli* (A), *S. cerevisiae* (B), and *M. luteus* (C) cells. Preimmune mouse serum was used as primary antibody for negative control and no signal was observed (data not shown). Lane 1, cell-free plasma; lane 2, cell-free plasma after absorption to microorganisms; lane 3, eluate from microorganisms reacted with IPS; lane 4, eluate from microorganisms reacted with cell-free plasma.

2.3.4. Tissue-specific expression of BmHPs

To consider the possibility that whether BmHP8, BmHP14 and BmHP21 are involved in nodule melanization in *B. mori* larvae, the expression patterns of the three genes encoding HPs, and gene encoding *BmproPO1* in fat bodies, hemocytes (the major nodule constituents), and nodules were first examined using RT-PCR. Nodule formation was induced by injecting with *E. coli* (EN), *S. cerevisiae* (SN), or *M. luteus* (MN). DNA sequencing was used to confirm the identity of PCR products. As shown in Fig. 2.4, cDNAs derived from mRNAs encoding *BmproPO1* and three HPs (*BmHP8*, *BmHP14*, and *BmHP21*) were found in fat bodies, hemocytes, and all three types of induced nodules (Fig. 2.4). using RT-PCR, the other ten *B. mori* genes encoding HPs were also examined. The results were as follows: mRNA of HPs members (*BmHP1*, *BmHP3*, *BmHP5*, *BmHP6*, *BmHP9*, *BmHP18*, *BmHP19*, *BmHP20*) were expressed in fat bodies, hemocytes and all three types of induced nodules (Fig. 2.4). These results suggested that these factors might involve in innate immunity system or nodule melanization. However, *BmHP10* was observed to express in hemocytes and all three types of nodules, whereas no expression was detected in fat bodies even though the experiments were repeated three times (Fig. 2.4). This observation suggested that BmHP10 may be a factor mainly relevant to cellular response. In addition, expression of *BmHP17* was found only in fat body (Fig. 2.4), suggesting that this protein may be involved in humoral responses.
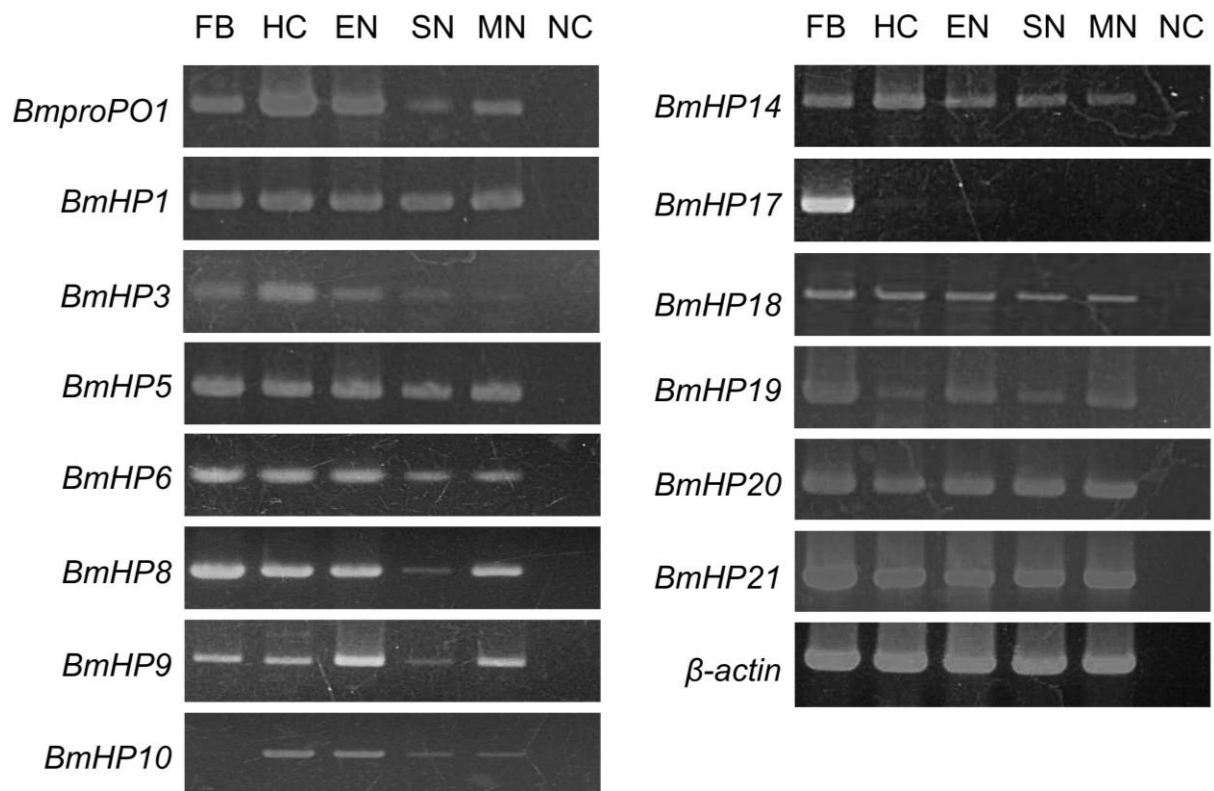
Fig. 2.4. RT-PCR analysis of genes encoding BmHPs. Gene expression was analyzed in normal fat bodies (FB), normal hemocytes (HC), and nodules induced by injection with *E. coli* (EN), *S. cerevisiae* (SN), or *M. luteus* cells (MN). *β-actin* was used as an internal standard to normalize the cDNA pools. For the negative controls (NC), cDNA was replaced by an equal amount of pure water.

2.3.5. Immunocytochemical localization of BmHPs in hemocytes

Tokura et al. (2014) showed that BmproPO1 was produced by granulocytes and oenocytoids (Tokura et al., 2014). In this study, RT-PCR showed that most of BmHPs genes were expressed in the hemocytes (Fig. 2.4). Thus, it is reasonable to speculate that some of the BmHPs proteins also can be expressed and stored in *B. mori* hemocytes. To confirm this speculation, immunofluorescent staining of smeared hemocytes using BmHPs antisera including anti-BmHP8, -BmHP14 and -BmHP21 were performed. It was observed the expression and localization of BmHPs in granulocytes, plasmatocytes, and oenocytoids. Granulocyte granules were weakly stained by anti-BmHP8, -BmHP14, and -BmHP21 antisera (Fig. 2.5B-D), whereas plasmatocyte granules were well stained. The cytoplasm of oenocytoids was weakly stained by anti-BmHP8 and -BmHP14 antisera (Fig. 2.5 B and C) and not at all by anti-BmHP21 antiserum (Fig. 2.5D). In addition, the oenocytoids and plasmatocytes were stained by anti-BmproPO1 antiserum (Fig. 2.5A) just as showed in Tokura et al. (2014). Percentage of oenocytoids in fifth-instar 3–4 days' larvae was around 3–5%. Almost 100% of oenocytoids was stained with anti-BmproPO1 antiserum.
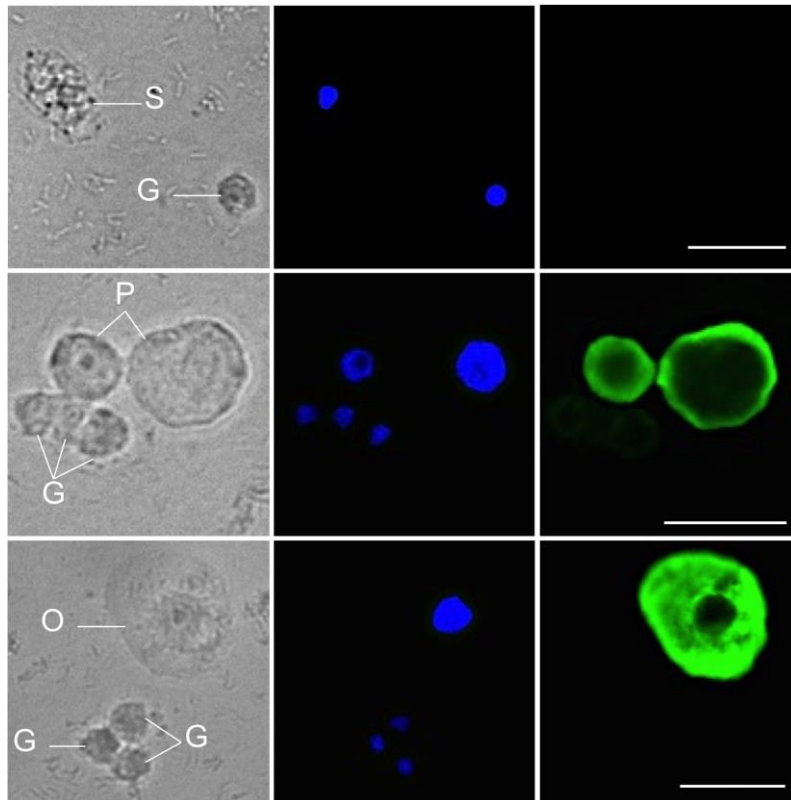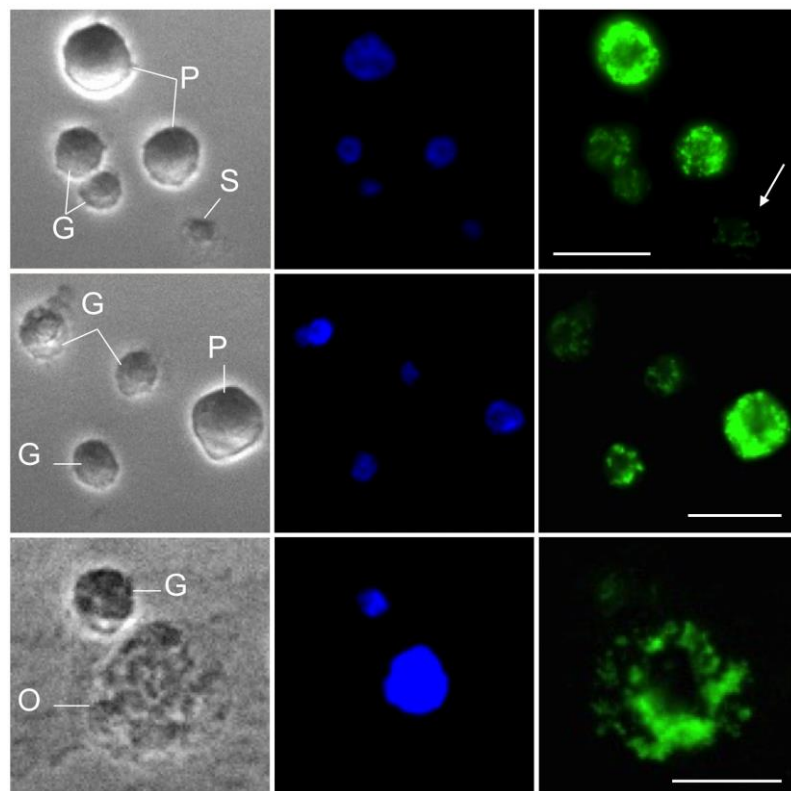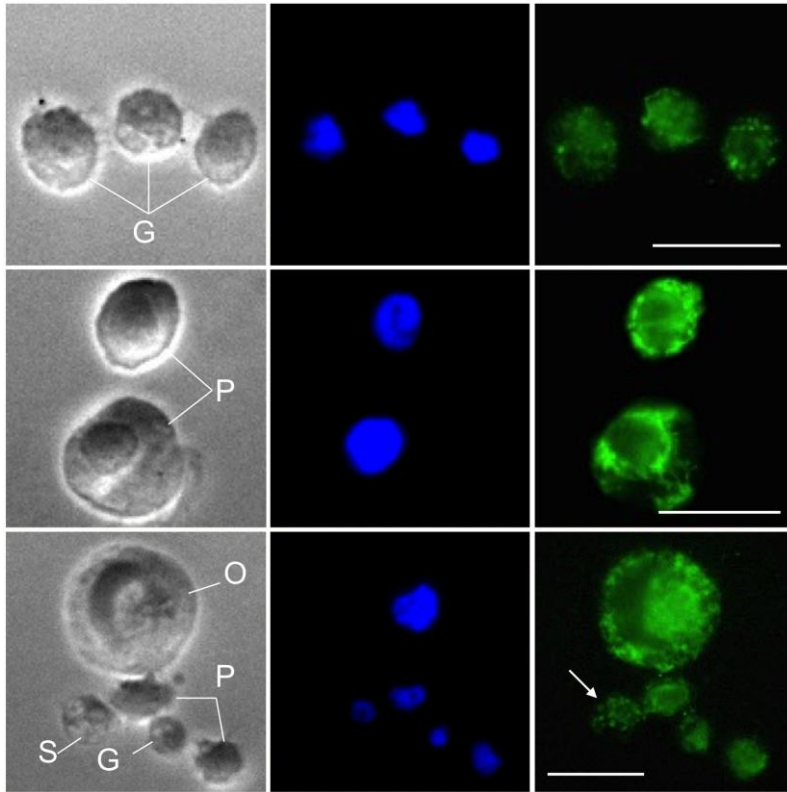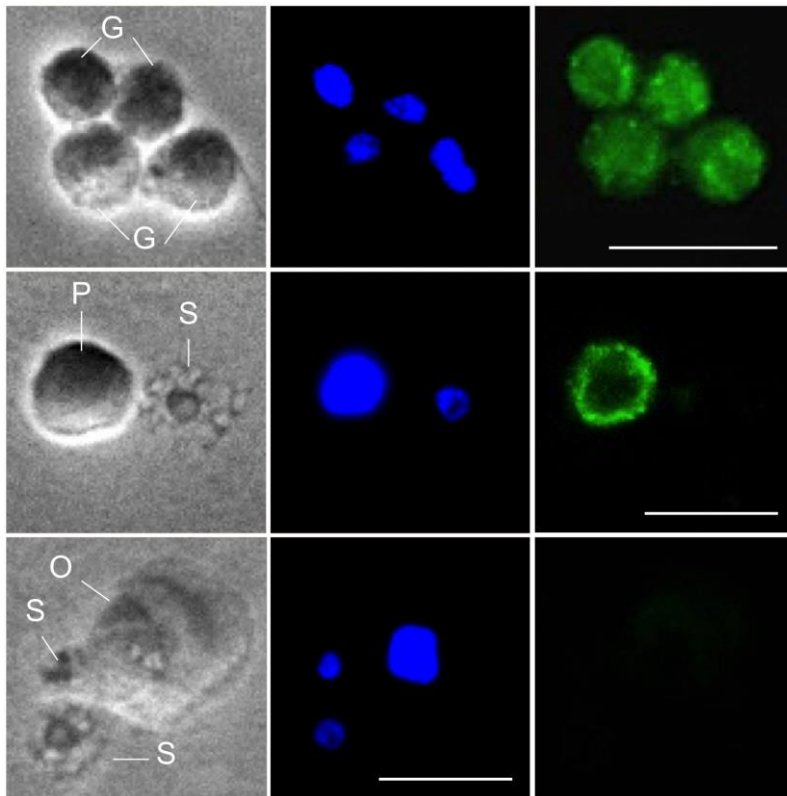
Fig. 2.5. Immunofluorescent detection of BmproPO1, BmHP8, BmHP14 and BmHP21 in smeared hemocytes from *B. mori* larvae. Left panels show transmitted-light pictures. Middle panels show DAPI-stained nuclei of hemocytes. Right panels show hemocytes stained with mouse anti-BmproPO1 (A), anti-BmHP8 (B), anti-BmHP14 (C) and anti-BmHP21 (D) in combination with anti-mouse IgG conjugated to Alexa Fluor 488®. P, plasmatocyte; G, granulocyte; O, oenocytoid; S, spherulocyte; Pr, prohemocyte. Arrows indicate weakly immunostained spherulocytes. Scale bars represent 10 μm.

2.3.6. Western blot analysis to deduce the origin of BmHPs and the way to transport them into the nodules

As mentioned above, BmHPs including BmHP8, BmHP14 and BmHP21 were not only detected in plasma, but also in hemocytes (Figs. 2.3 and 2.5). Moreover, all three of these proteins might be related to the antimicrobial activity of nodules by melanization or AMP production (Fig. 2.4). On the other hand, it was found that through binding to microorganisms, proteins in plasma such as BmPRRs could be transport into nodules for nodule-preferential melanization (chapter 1). In current study, it was also found that BmHP14 can bind specifically to *S. cerevisiae* cells, whereas BmHP8 and BmHP21 not bind to any of the three microorganisms (Fig. 2.3). To understand the origin and aggregation routes of these BmHPs proteins in nodule, Western blot analysis base on them are performed.

Both precursor and activated forms of BmHP8 and BmHP21 were more abundant in *E. coli-*, *S. cerevisiae-*, and *M. luteus*-induced nodules than in hemocytes, indicating that the BmHP8 and BmHP21 in these nodules originated from the plasma (Fig. 2.6), even though the mechanism by which these proteins accumulated in the plasma is unknown (Figs. 2 and 3). Although precursor and two activated forms of BmHP14 were detected in the plasma, only the 30-kDa activated form of BmHP14 was detected in the *S. cerevisiae*-induced nodules and not in the *M. luteus-* or *E. coli*-induced nodules (Fig. 2.6). Because almost no BmHP14 was detected in hemocytes,

it is likely that BmHP14 in *S. cerevisiae*-induced nodules originated from the plasma.

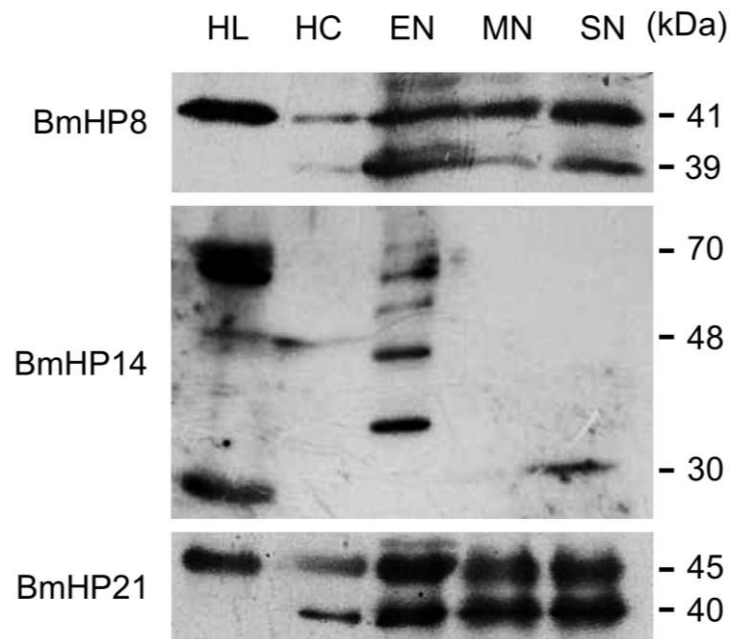**Fig. 2.6. Western blot analysis to deduce the aggregation route of BmHPs.** The protein samples come from hemolymph (HL), hemocytes (HC), and nodules induced by injection with *E. coli* (EN), *M. luteus* (MN), and *S. cerevisiae* cells (SN) respectively, were transferred onto a PVDF membrane. Western blot experiments were performed using antisera against BmHP8, BmHP14, and BmHP21 as the primary antibodies.

2.3.7. Immunocytochemical localization of BmHPs in nodules

The results of Western blot analysis confirmed that most of BmHP14 in *S. cerevisiae*-induced nodules come from plasma (Fig. 2.6) owing to its microorganism binding property (Fig. 2.3B). Therefore, BmHP14 should be on *S. cerevisiae* cells in nodule. Besides, even though both BmHP8 and BmHP21 did not bind to microorganisms (Fig. 2.3), these proteases in nodules looked to come from plasma (Fig. 2.6). To know the reason how BmHP8 and BmHP21 could congregate in nodules from plasma, the immunostaining was used to locate these proteins in nodule cryosections. As shown in Fig. 2.8, BmHP14 (green fluorescence) was only detected in nodule which was induced by *S. cerevisiae* cells, and at a higher magnification, green fluorescence was observed that mainly around the nuclei of *S. cerevisiae* cells and fit the shape and scale of *S. cerevisiae* cells (Fig. 2.8 C, arrowheads). BmHP8 and BmHP21 (green fluorescence) were detected in all three types of nodules as well as the hemocytes (arrows) aggregated in nodules (Figs. 2.7 and 2.9), which is consistent with the results of Western blot analysis (Fig. 2.6). Moreover, in *E. coli-* or *M. luteus*-induced nodule, at a higher magnification, green fluorescence was mostly observed that located in the area where could not be covered by the nuclei of hemocytes, and the shape and scale fit the *E. coli* and *M. luteus* cells (Figs. 2.7 A–B and 2.9 A–B, arrowheads). Additionally, in *S. cerevisiae*-induced nodules, at a higher magnification, green fluorescence was observed that fit

the shape and scale of *S. cerevisiae* cells (Figs. 2.7 C and 2.9 C, arrowheads). These results suggest that BmHP8 and BmHP21 may also bind to microorganisms in plasma, and then were aggregated in nodules with microorganisms. Whereas, this speculation cannot be explained by the results of binding assays, since, in the binding assays, BmHP8 and BmHP21 were not detected from any of microorganisms (Fig. 2.3).

A
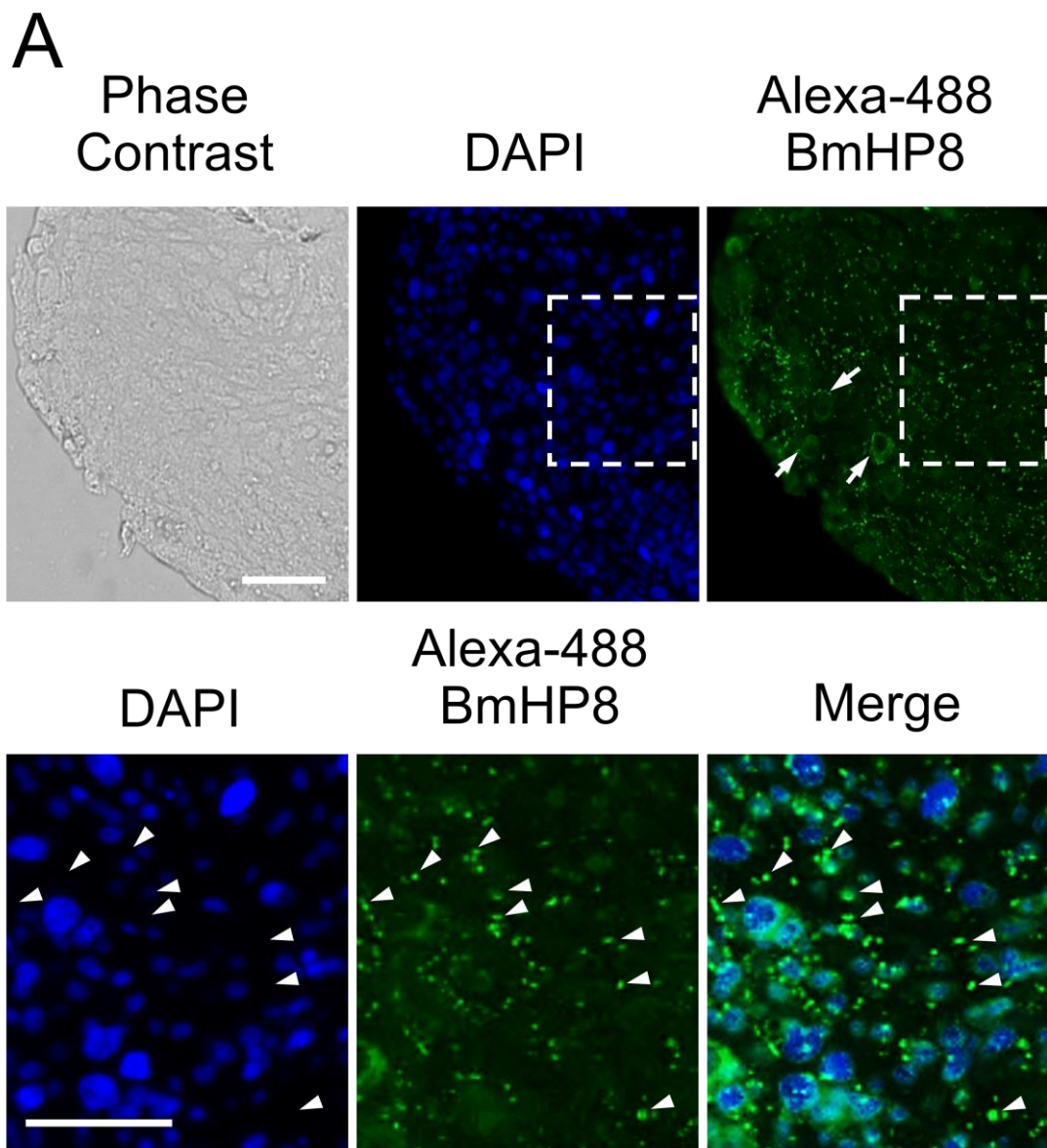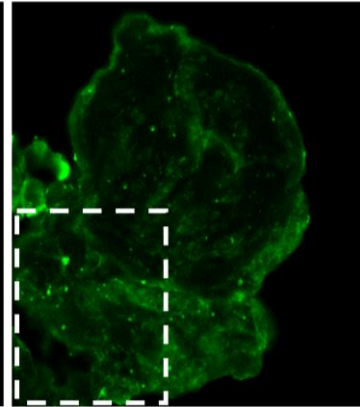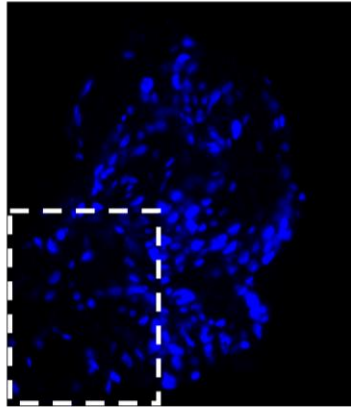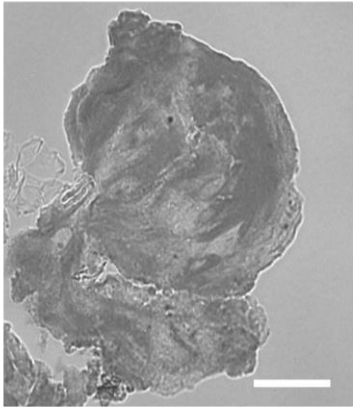
| Phase Contrast | DAPI | Alexa-488 BmHP8 |

| DAPI | Alexa-488 BmHP8 | Merge |
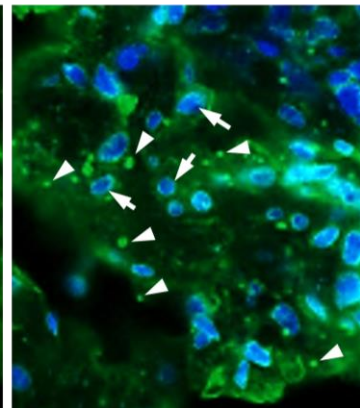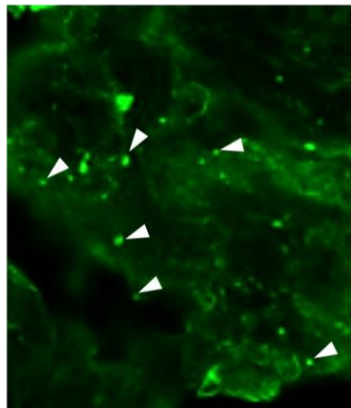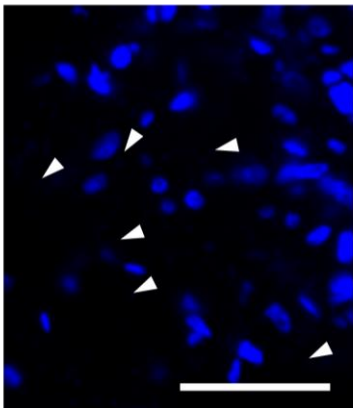
Fig. 2.7. Immunofluorescent detection of BmHP8 in cryosections of nodule. A, crysection from *E. coli*-induced nodule; B, crysection from *M. luteus*-induced nodule; C, crysection from *S. cerevisiae*-induced nodule. The nuclei of hemocytes in nodule crysections were densely stained by DAPI with blue fluorescence. BmHP8 was stained with mouse anti-BmHP8 antiserum in combination with anti-mouse IgG conjugated to Alexa Fluor

488®. Images indicated below in A, B and C are higher magnification of the area outlined in the dashed rectangle in the above images; green fluorescence which fit the shape and scale of *E. coli*, *M. luteus*, *S. cerevisiae* cells in nodules, and not merged by blue fluorescence (hemocytes nuclei), are indicated by arrowheads (the middle and right panels); the same regions in DAPI-stained images (left panel) are also indicated by arrowheads. Hemocytes which stained by BmHP8 in nodules are indicated by arrows. Scale bars represent 20 μm.

A

Phase Contrast | DAPI | Alexa-488 BmHP14

B

Phase Contrast | DAPI | Alexa-488 BmHP14
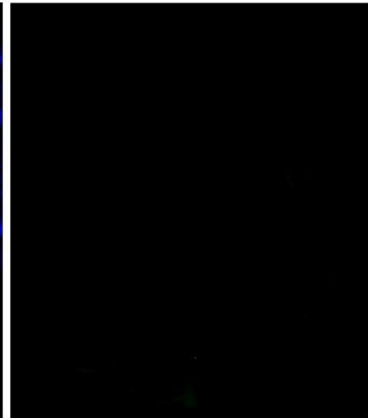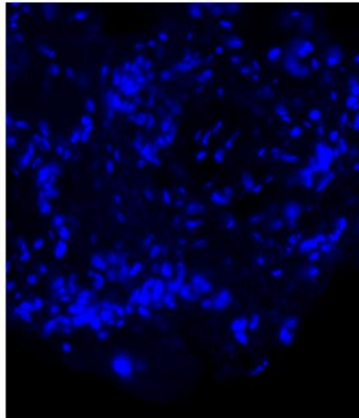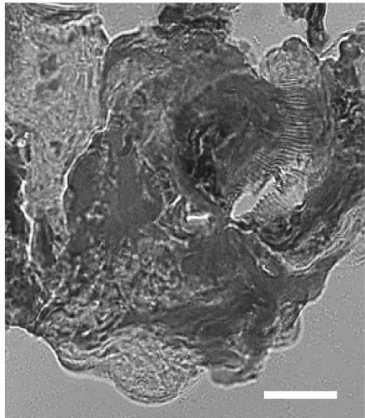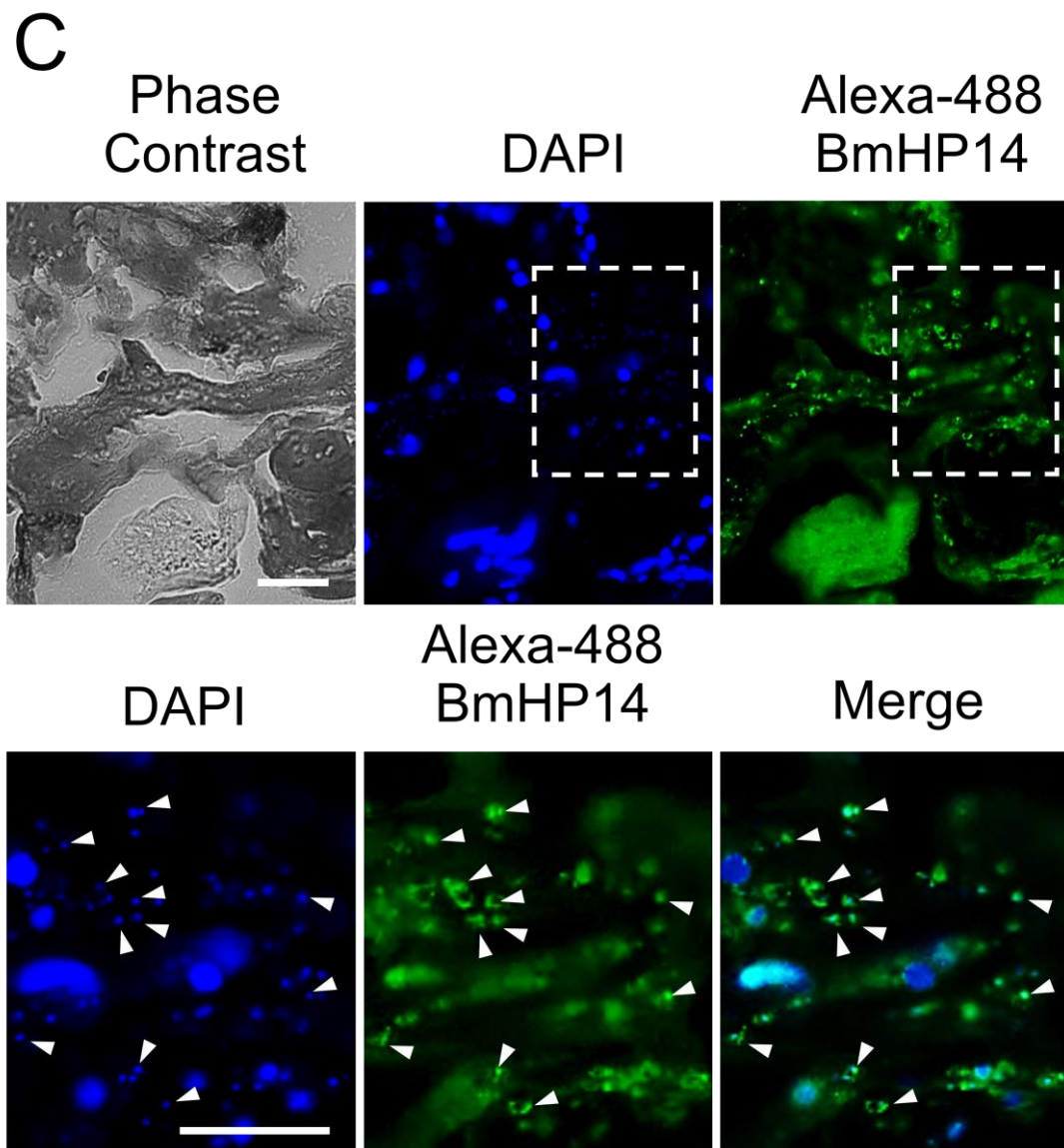
Fig. 2.8. Immunofluorescent detection of BmHP14 in cryosections of nodule. A, crysection from *E. coli*-induced nodule; B, crysection from *M. luteus*-induced nodule; C, crysection from *S. cerevisiae*-induced nodule. The nuclei of hemocytes in nodule crysections were densely stained by DAPI with blue fluorescence. BmHP14 was stained with mouse anti-BmHP14 antiserum in combination with anti-mouse IgG conjugated to Alexa Fluor 488®. Images indicated below in C are higher magnification of the area

outlined in the dashed rectangle in the above images, green fluorescence which fit the shape and scale of *S. cerevisiae* cells in nodule, and not merged by blue fluorescence (hemocytes nuclei), are indicated by arrowheads (the middle and right panels); the same regions in DAPI-stained image (left panel) are also indicated by arrowheads. Scale bars represent 20 μm.

A

Phase Contrast	DAPI	Alexa-488 BmHP21

DAPI	Alexa-488 BmHP21	Merge

B
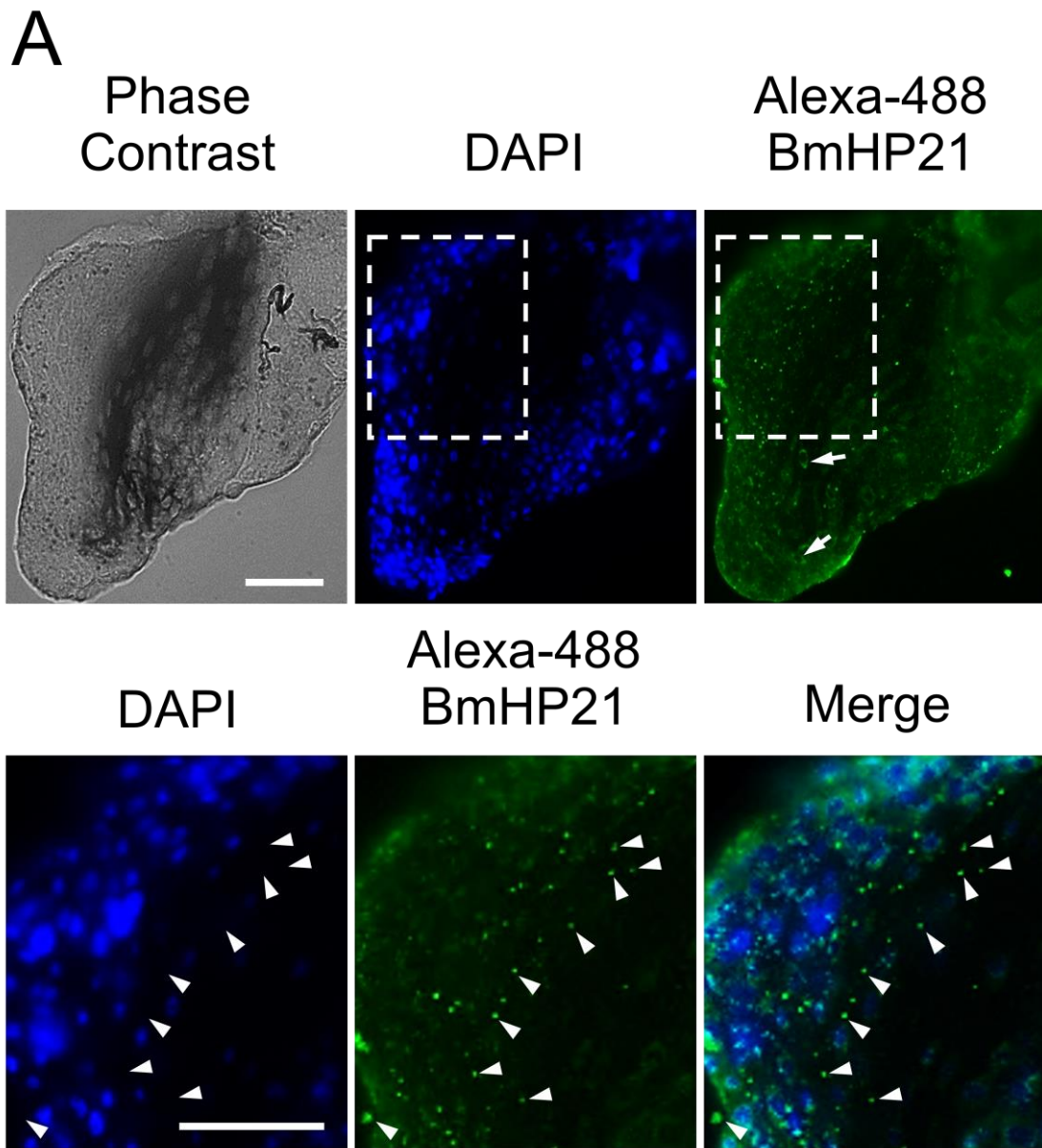
Phase Contrast	DAPI	Alexa-488 BmHP21
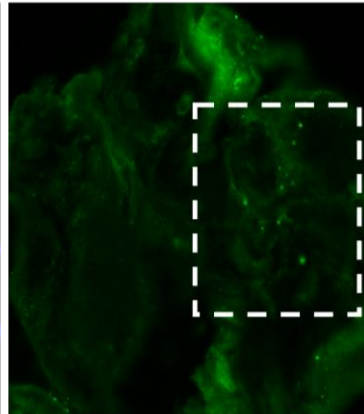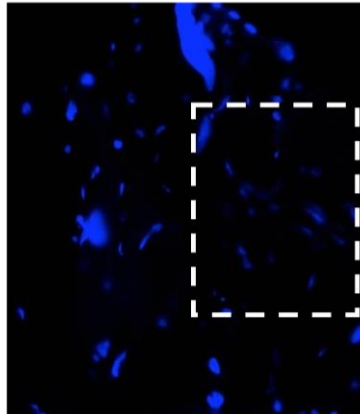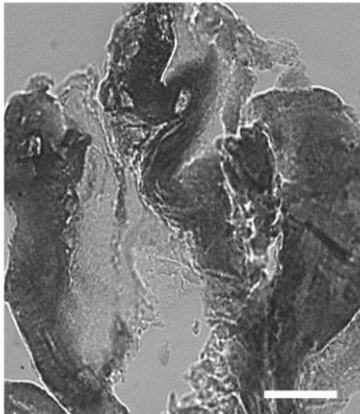
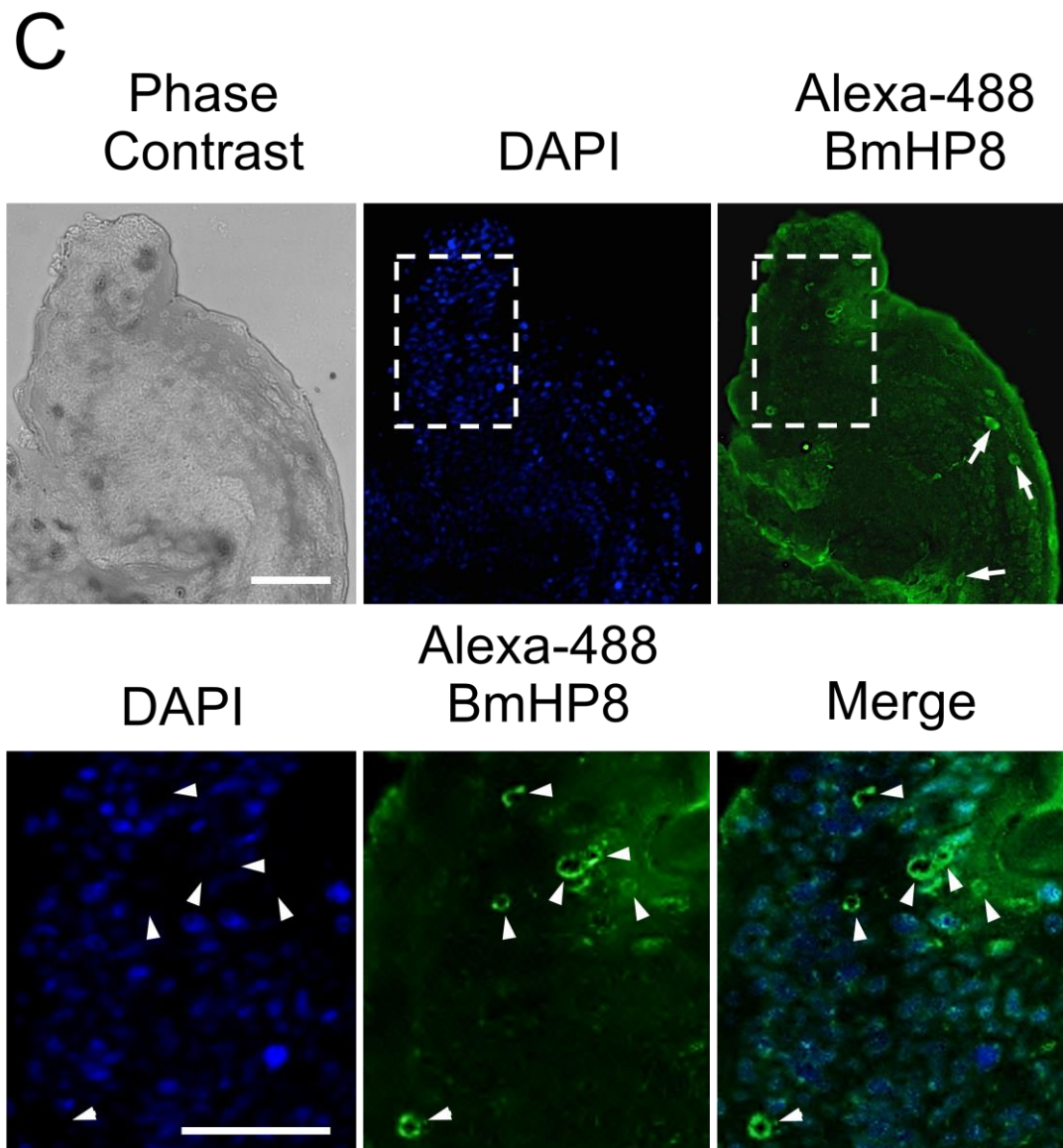| DAPI	Alexa-488 BmHP21	Merge
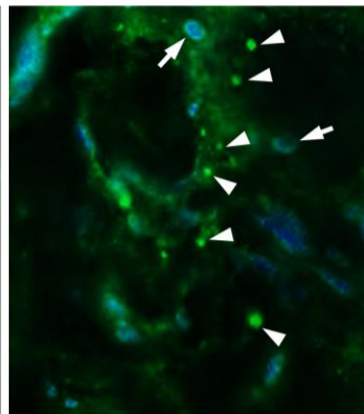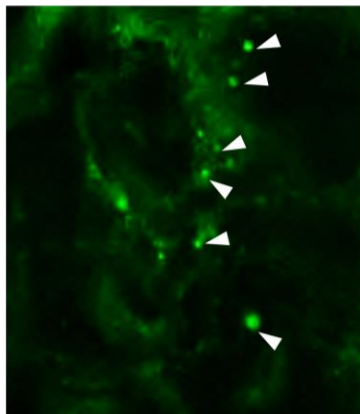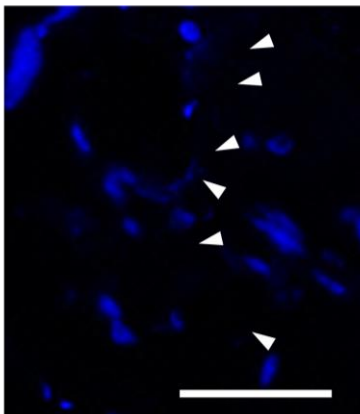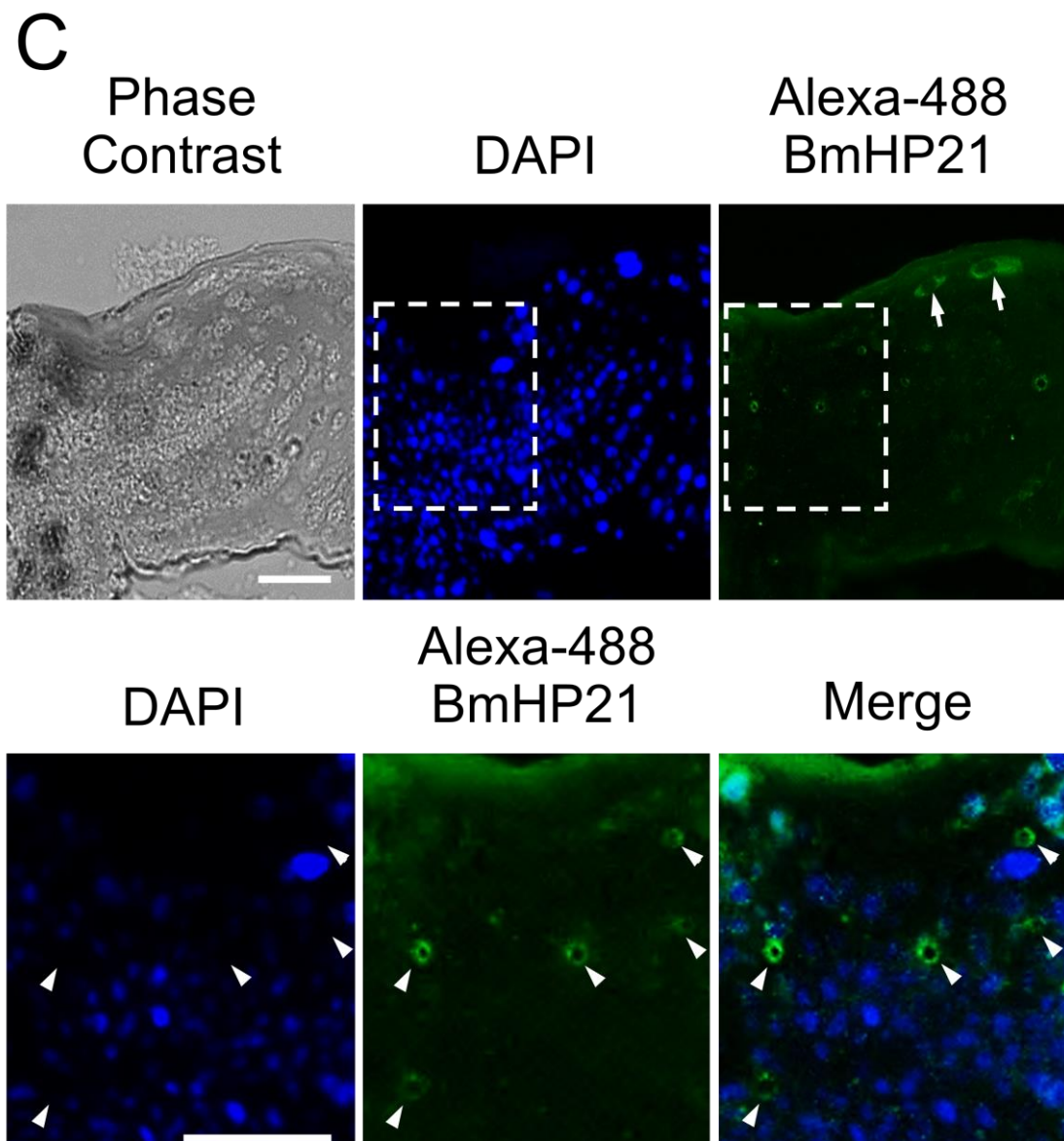
Fig. 2.9. Immunofluorescent detection of BmHP21 in cryosections of nodule. A, crysection from *E. coli*-induced nodule; B, crysection from *M. luteus*-induced nodule; C, crysection from *S. cerevisiae*-induced nodule. The nuclei of hemocytes in nodule crysections were densely stained by DAPI with blue fluorescence. BmHP21 was stained with mouse anti-BmHP21 antiserum in combination with anti-mouse IgG conjugated to Alexa Fluor
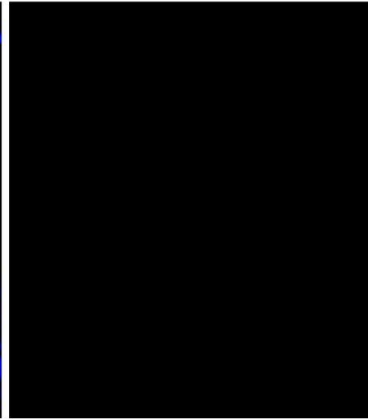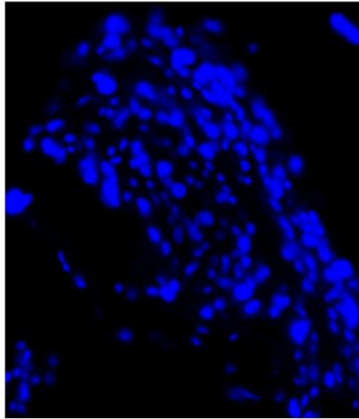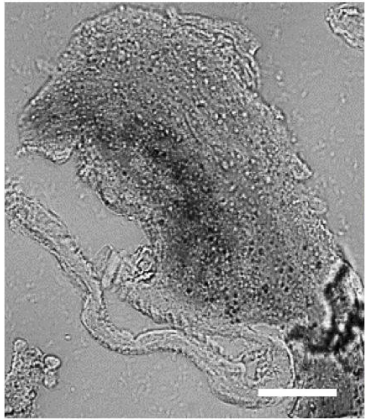
488®. Images indicated below in A, B and C are higher magnification of the area outlined in the dashed rectangle in the above images; green fluorescence which fit the shape and scale of *E. coli*, *M. luteus*, *S. cerevisiae* cells in nodules, and not merged by blue fluorescence (hemocytes nuclei), are indicated by arrowheads (the middle and right panels); the same regions in DAPI-stained images (left panel) are also indicated by arrowheads. Hemocytes which stained by BmHP21 in nodules are indicated by arrows. Scale bars represent 20 μm.

2.4 Discussion

M. sexta HP14 (MsHP14), which functions at the top of the proPO-activating cascade, was found to be auto-activated in the presence of Gram-positive bacteria. MsHP14 auto-activation led to the activation of a proteinase cascade downstream of the proPO-activating system in the hemolymph (Ji et al., 2004; Wang and Jiang, 2006). On the other hand, when fungi were used, cell wall components and their respective recognition proteins, such as MsβGRP1 and MsβGRP2, were needed for proteolysis of the MsHP14 precursor (Wang and Jiang, 2006, 2010). BmHP14 is a homologue of MsHP14 and, in this study, a 70-kDa BmHP14 precursor and a 30-kDa activated form of BmHP14 were able to bind directly to *S. cerevisiae* (Fig. 2.3B) but not to *M. luteus* or *E. coli* (Fig. 2.3A and C). Moreover, in Western blot analyses, the 30-kDa activated form of BmHP14 was detected only in nodules that were induced by *S. cerevisiae* but not *M. luteus* or *E. coli* (Fig. 2.6). These results suggest that, unlike MsHP14, BmHP14 is auto-activated on the cell surface of microorganisms and is activated only by immune responses induced by fungi, such as *S. cerevisiae*.

In this study, BmproPO1 weakly bound to *E. coli*, *S. cerevisiae*, and *M. luteus* (Fig. 2.3), supporting the idea that BmproPO1 has a sticky property as previously reported (Diao et al., 2012). However, it is still unclear whether this binding occurs in the hemolymph or nodule. It has been previously reported that BmHP21 and BmHP8 accelerate melanization and AMP

synthesis, respectively (An et al., 2009; Wang and Jiang, 2007). These proteins did not bind to *E. coli*, *S. cerevisiae*, or *M. luteus*, but their rapid activation was detected in the plasma (Fig. 2.3). Both precursor and activated forms of BmHP8 and BmHP21 were more abundant in induced nodules than in hemocytes (Fig. 2.6), indicating that the BmHP8 and BmHP21 in nodules were transferred from the plasma. Actually, on the surface of microorganisms in the nodules, not only BmHP14, which was observed to bind to *S. cerevisiae,* but also BmHP8 and BmHP21, which were not observed to bind to any microorganisms (Fig. 2.3), were observed (Figs. 2.7 and 2.9). It was suspected that the interaction between the two proteins and the microorganisms may be loose, so that they are easy to be washed-out before elution in the binding assay. Further examinations are needed to clarify the mechanism of congregation of activated BmHP8 and BmHP21 into nodules. On the other hand, if this hypothesis is true, it is very possible that BmHP members in the proPO cascade and AMP production-triggering system initiate by the recognition by different BmPRPs, but below BmHP8 and BmHP21 were the same at least regarding to bacteria. While, more examinations are needed to clarify this hypothesis.

By the way, it is plausible that hemocytes also contributed to the congregation of BmHP8 and BmHP21 in induced nodules (Fig. 2.5B and D, Figs. 2.6–2.7 and 2.9). Thus, in the proPO-activating cascade and AMP production-triggering system, most factors, including HP precursors and

their activated forms, seem to congregate in nodules or surround microorganisms in nodules by interacting with microorganisms directly or indirectly. At least, activation of BmHP8, BmHP14 and BmHP21 seems to be realized surrounding microorganisms, since the interaction with microorganisms could activate these HPs (Fig. 2.3). Microorganisms are captured by nodules. As a result, these may result in nodule-specific melanization and nodule-specific AMP production.

CHAPTER 3

The C-type lectin-dependent congregation routes of proPO-controlling factors, *B. mori* serine proteinase homologs, BmSPH1 and BmSPH2 to nodules

3.1 Introduction

In insect, proteolytic activation of prophenoloxidase (proPO) is an important physiological process against pathogen infection (González-Santoyo and Córdoba-Aguilar, 2012). This process has several controlling mechanisms including recognition of pathogen-associated molecular patterns (PAMPs) by a series of pattern recognition receptors (PRRs), activation of proPO by a cascade of serine proteinases (HPs), regulation of the proteolytic cascade by a range of serpins, and requirement of serine proteinase homologs (SPHs) sometimes for assisting proPO-activating proteinases (PAPs) to generate active phenoloxidase (PO) (An et al., 2009; An and Kanost, 2010; Cerenius and Söderhäll, 2004; González-Santoyo and Córdoba-Aguilar, 2012). Among them, there are somewhat controversial points in function of SPHs, and the detailed mechanism of them appear to be remain unclear (Andersson et al., 1989; Cerenius and Söderhäll, 2004; Felföldi et al., 2011; Finnerty et al., 1999; Gupta et al., 2005; Kim et al., 2002; Kwon et al., 2000; Lee et al., 2002; Satoh et al., 1999; Wang and Jiang, 2004). SPHs are similar in sequence to clip-domain serine proteinases (e.g. PAPs; proPO-activating factor, PPAF and proPO-activating enzyme, PPAE) but lack proteolytic activity, since their catalytic serine is replaced with glycine (An et al., 2009; Kan et al., 2008; Kim et al., 2002). Some species such as *Holotrichia diomphalia* and *Manduca sexta* require SPHs as a "PAP cofactor" for proPO activation (Gupta et al., 2005; Kim et al., 2002; Kwon et al., 2000; Lu and

Jiang, 2008; Wang and Jiang, 2004). In *H. diomphalia,* an active serine protease, PPAF-I was found to be able to cleave proPOs, but its proPOs-activating ability was restricted. However, in the presence of a SPH which was referred to as PPAF-II and previously activated by PPAF-III, the active PPAF-I could exert higher activity to generate active PO (Kim et al., 2002; Kwon et al., 2000). Also in *M. sexta*, serinproteases, PAPs themselves indicated limited activity to proteolysis proPO and generated only restricted PO activity, but in the presence of SPHs as a cofactor, the complete proteolysis of proPO and an increased PO activity were observed (Gupta et al., 2005; Lu and Jiang, 2008; Wang and Jiang, 2004). This process appears to be realized on the microbial surface by SPHs in combination with immulectin-2 (IML-2), a C-type lectin type PRR, since the IML-2 not only binds lipopolysaccharide (LPS) and mannan, but forms complex with SPHs in *M. sexta* plasma (Yu and Kanost, 2000; Yu et al., 2003). In addition, SPHs in the complex may function as mediators to recruit activated PAPs and PO to the site of infection (Gupta et al., 2005). In another species *Tenebrio molitor,* active Spätzle-processing enzyme (SPE) cleaves both proPO and SPH1, leading to formation of a stable melanization complex which induces local melanin synthesis on the surface of pathogens (An et al., 2009; Kan et al., 2008; Lee et al., 2002). However, in *Bombyx mori*, the mechanism of SPHs in proPO-activating system still remains unclear, since active PPAE was reported that it could yield active PO by itself, and no SPH was required

(Satoh et al., 1999). While, recently our laboratory suggested that BmSPH1 and BmSPH2 are possible to be involved in nodule melanization, by forming the protein-complex with *B. mori* Lipopolysaccharide binding protein (BmLBP) which is a member of PRRs and recognizes *E. coli* by binding to its surface (Sakamoto et al., 2011; Tokura et al., 2014). To know the possibility that BmSPH1 and BmSPH2 are involved in melanization in nodules which were induced by many kinds of microorganisms, the microorganism-binding assays and several examinations were performed. Furthermore, in order to understand the way that BmSPH1 and BmSPH2 are aggregated into nodules, the molecular associations among two BmSPHs, six BmPRRs and four BmHPs (including BmproPO) were investigated using pull-down assays.

3.2 Materials and Methods

3.2.1. Preparation and specificity analysis of BmSPHs antisera

Anti-BmSPH1 and anti-BmSPH2 antisera were raised as previously reported (Koizumi et al., 1997; Sakamoto et al., 2011; Tokura et al., 2014; Watanabe et al., 2006). Specificities of BmSPHs antisera were evaluated using normal *B. mori* plasma by Western blot. Plasma fraction, hemocytes pellets and nodules which were collected in section 1.2.1, were also used for the following experiments.

3.2.2. Microorganism-binding assay for the analysis of BmSPHs binding property to microoganisms

Gram-positive bacteria *Micrococcus luteus* (IAM1056), Gram-negative bacteria *Escherichia coli* (K-12W3110) and fungus *Saccharomyces cerevisiae* (IAM4125) were cultured and collected as described in section 1.2.2. Microorganism-binding assays were carried out as description in section 1.2.4. Bound proteins were detected by immunoblot using the antisera which have been prepared in section 3.2.1.

3.2.3. Pull-down assays to investigate the protein complexes in plasma

Rabbit anti-BmSPH1 IgG and anti-*B. mori* multibinding protein (BmMBP) IgG were immobilized to Protein A resin (APRO, Tokushima, Japan) with an overnight incubation at 4 °C. After centrifugation at 500 g for 2 min, the

resin was washed three times and finally resuspended in 400 µl wash buffer. To the resin, 0.5 mg disuccinimidyl suberate (DSS; Thermo, Rockford, USA) dissolved in 20 µl dimethyl sulfoxide (DMSO; Wako, Osaka, Japan) was added and gently mixed for 60 minutes at room temperature to cross-link the immobilised antibody to Protein A. Excess DSS and uncoupled antibody were washed 5 times with elution buffer (0.1 M Glycine-HCl, pH 3.0) and twice with wash buffer. Cell free plasma (500 µl) diluted with IPS was mixed with 1× conc. protease inhibitor and incubated with the resin bed for 1 h at 4 °C. After 5 times wash of the resin with 400 µl wash Buffer, the proteins remaining on the resin were eluted with the elution buffer. Plasma, proteins flowed through the resin, proteins contained in the fifth wash fraction, and eluates were separated by Laemmli-SDS-PAGE and analyzed by Western blot using antisera as already mentioned. For negative controls, antibodies against β-1, 3-glucan recognition proteins (βGRPs, including BmβGRP1, BmβGRP2 and BmβGRP3) and a peptidoglycan recognition protein BmPGRP-S1 were also cross-linked to Protein A resin and pull-down assays were conducted as described above.

3.2.4. Expression analysis of BmSPHs by RT-PCR

Fat bodies, hemocytes and nodules which were induced by *E. coli*, *M. luteus* or *S. cerevisiae* cells injection were collected, and total RNA from these tissues were extracted as previous description in section 1.3.5. Double-

stranded cDNA fragments of BmSPHs were amplified by PCR using GoTaq DNA polymerase (TaKaRa, Shiga, Japan) for 35 cycles and the gene-specific primers for individual proteins indicated in table 3.1. To normalize the cDNA pools, *B. mori β-actin* as an internal standard was used. All products of PCR were separated by agarose gel electrophoresis and stained by ethidium bromide for evaluation.

3.2.5. Immunofluorescent staining for the observation of BmSPHs in hemocytes

Immunofluorescent staining of hemocytes were carried out as description in section 1.2.6, but now using mouse antiserum raised against BmSPH1 or BmSHP2 in combination with 1000-fold diluted Alexa Fluor 488® conjugated goat anti-mouse IgG (Bio-Rad, Hercules, CA, USA). Antisera were diluted using 1% BSA solution containing 0.1% Triton X-100. The nuclei of hemocytes were counter stained with 4', 6-diamidine-2'-phenylindole dihydrochloride (DAPI; l µg/ml, Sigma Aldrich, Schnelldorf, Germany). Fluorescence was observed under a microscope, LSM710/ LSM710 NLO (CARL ZEISS). Oenocytoids, granulocytes, spherulocytes, plasmatocytes and prohemocytes were identified by the differences which have been described in section 1.2.6.

3.2.6. Western blot analysis to confirm the concentration of BmSPHs in the

nodules

Western blot was performed as has been described in section 1.2.7. However, after blocking with 2% BSA, the transferred membrane was incubated with mouse antiserum against BmSPH1 or BmSPH2 for 90 min following the appropriate dilution. After washing, the membrane was incubated with 30,000-fold diluted peroxidase-conjugated goat anti-mouse IgG (Bio-Rad, Hercules, CA, USA) for 45 min, and then stained using ECL^{TM} prime Western blotting detection reagent (GE Healthcare, Little Chalfont, UK).

3.2.7. Immunofluorescent staining for the confirmation of BmSPHs in nodules

The immunofluorescent staining of nodules were carried out as description in section 1.2.8, but now using mouse antiserum raised against BmSPH1 or BmSPH2 in combination with 1000-fold diluted Alexa Fluor 488$^®$ conjugated goat anti-mouse IgG (Bio-Rad, Hercules, CA, USA).

Table 3.1. Primers for individual proteins used in RT-PCR

Gene name	Forward primer (5´-3´)	Reverse primer (5´-3´)
BmSPH1	GTCGCTGACAGGGCTCCAT	TTCTGCGTGTCCCATTCG
BmSPH2	CGGTGCTGGTAACAGTCGG	CAAGTGTCCCTGCCCTCCT
β-actin	AACTGGGATGACATGGAGAAGATCTGGC	GAGATCCACATCTGCTGGAAGGTGGA

3.3 Results

3.3.1. Specificity analysis of BmSPHs antisera

The specificity of BmSPHs antisera were verified using normal plasma from *B. mori* larvae. Mouse antisera raised against BmSPH1 and BmSPH2 recognized single bands at 51 and 48 kDa, respectively, in normal plasma. These results corresponded well to previous reports (Sakamoto et al., 2011; Tokura et al., 2014), indicating that BmSPHs antisera were specific and could therefore be used in other experiments.

3.3.2. Microorganism-binding assay for detection of binding property of BmSPHs

To explore the role of BmSPHs by examining whether they could bind to microorganisms, microorganism-binding assay were conducted. cell-free plasma from *B. mori* larvae was incubated separately with three representative microorganisms, *E. coli*, *S. cerevisiae*, and *M. luteus*, respectively. Proteins that bound to these microorganisms were then detected by Western blot. BmSPH1 and BmSPH2 precursors (51 and 48 kDa, respectively) and activated forms (39 and 40 kDa, respectively) were detected form the surface of *E. coli*, *S. cerevisiae*, and *M. luteus* cells (Fig. 3.2A–C), suggesting that both BmSPH1 and BmSPH2 have mechanisms to bind these microorganisms.
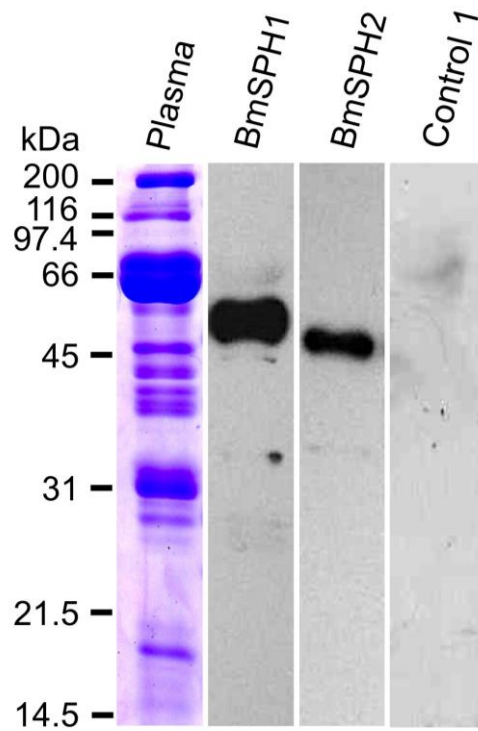
Fig. 3.1. Western blot analysis for confirmation of antisera specificity.
The specificity of mouse antisera against BmSPH1 and BmSPH2 were confirmed using the plasma of *B. mori* larvae. Preimmune mouse (control 1) serum was used as primary antibody for negative control.
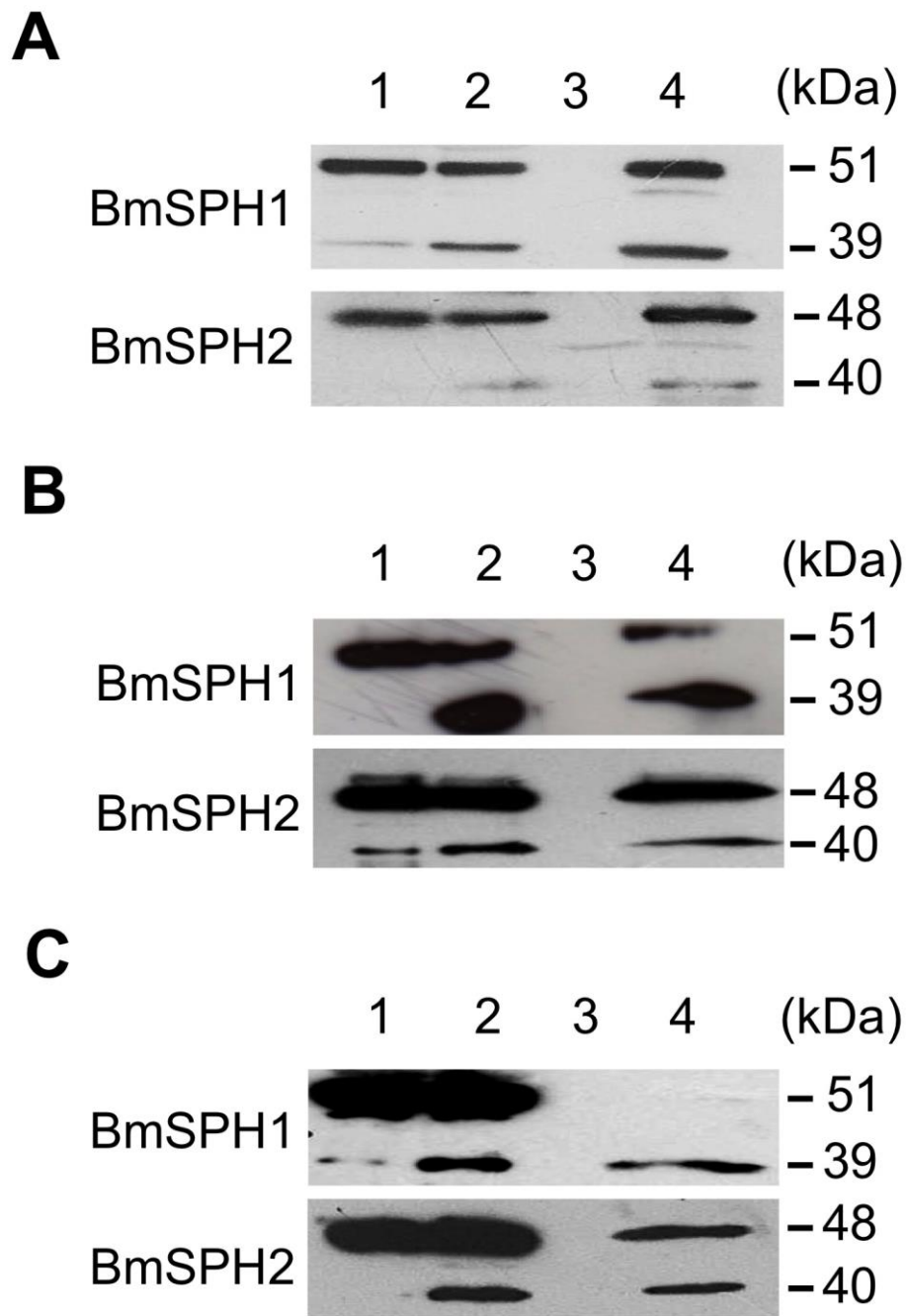
Fig. 3.2. Specific binding of *B. mori* plasma proteins to microorganisms.
The specific binding of BmSPH1 and BmSPH2 to microorganisms were detected by immunoblot analyses after plasma (cell-free hemolymph) was incubated with paraformaldehyde-fixed *E. coli* (A), *S. cerevisiae* (B), and *M.*

luteus (C) cells. Preimmune mouse and rabbit sera were used as primary antibodies for negative controls and no signals were observed (data not shown). Lane 1, cell-free plasma; lane 2, cell-free plasma after absorption to microorganisms; lane 3, eluate from microorganisms reacted with IPS; lane 4, eluate from microorganisms reacted with cell-free plasma.

3.3.3. Plasma protein complexes

A recent study showed that a PRR, BmLBP formed a protein complex with BmSPH1 and BmSPH2 in the *B. mori* larvae plasma (Tokura et al., 2014), suggesting that other BmPRRs may also form similar complexes with BmSPH1 and BmSPH2. To validate this, and further to investigate whether BmHPs make complexes with BmPRRs or not in the plasma, pull-down assays were performed first with *B. mori* larvae plasma using anti-BmSPH1 antibody-conjugated Protein A resin. BmMBP, BmLBP, BmSPH1, and BmSPH2 were co-eluted from the resin, but BmβGRP1, BmβGRP2, BmβGRP3, and BmPGRP-S1 were not (Fig. 3.3A). This indicated that only C-type lectins are able to form complexes with BmSPH1 and BmSPH2. To confirm this hypothesis, a reciprocal pull-down assay was performed using anti-BmMBP antibody-conjugated Protein A resin. BmSPH1 and BmSPH2 were co-eluted with BmMBP (Fig. 3.3B), but no any other proteins including BmHPs were eluted. Furthermore, antibodies against BmβGRP1, BmβGRP2, BmβGRP3, and BmPGRP-S1 were also conjugated to Protein A resin for pull-down assays, but none of these PRRs was able to pull down BmSPH1 or BmSPH2. These results suggested that among PRRs, C-type lectins were able to form complexes with BmSPH1 and BmSPH2 in the plasma but not with the HPs, BmHP8, BmHP14, and BmHP21, which were activated with microorganisms (Fig. 2.3).

A
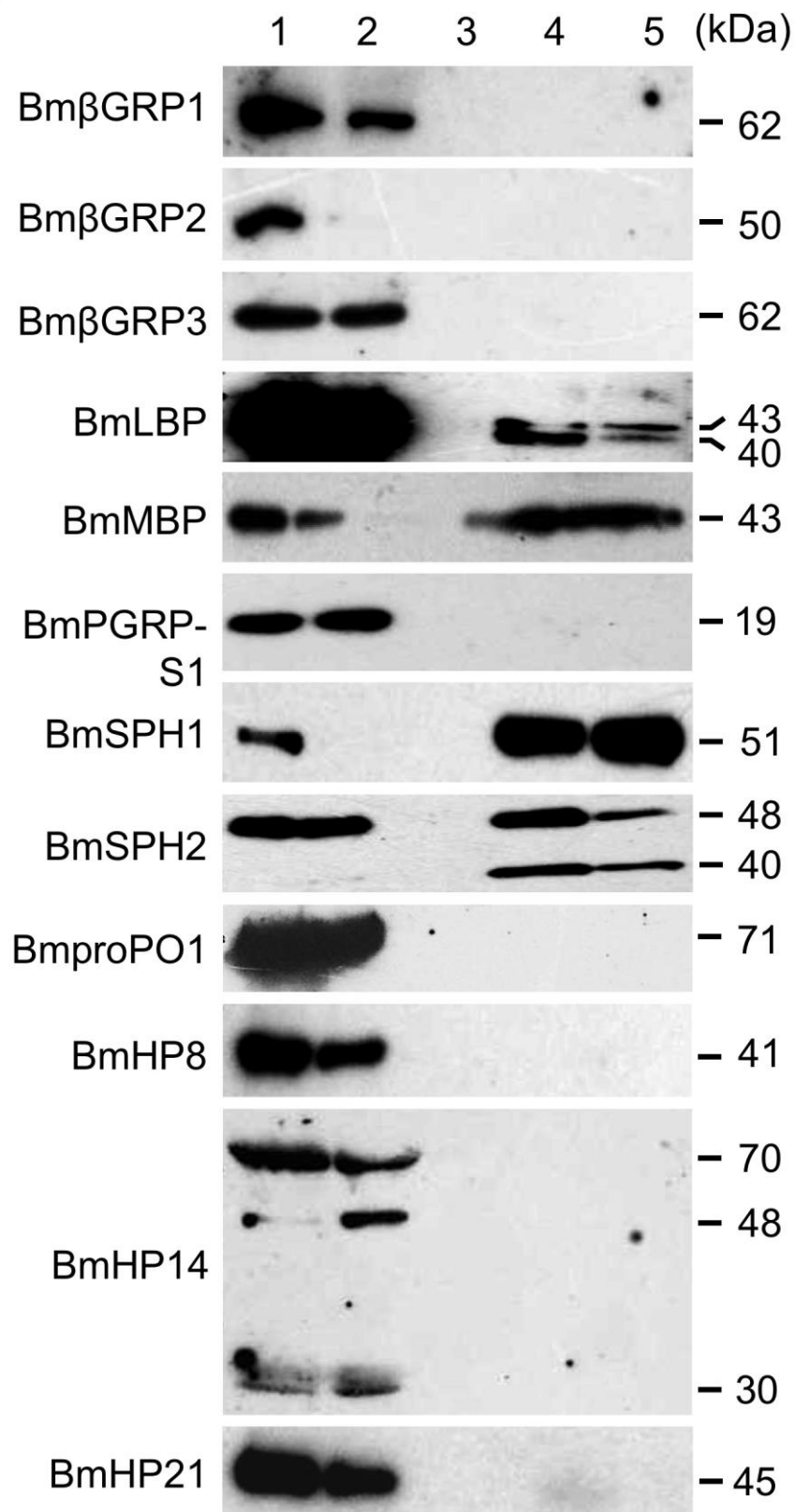
B
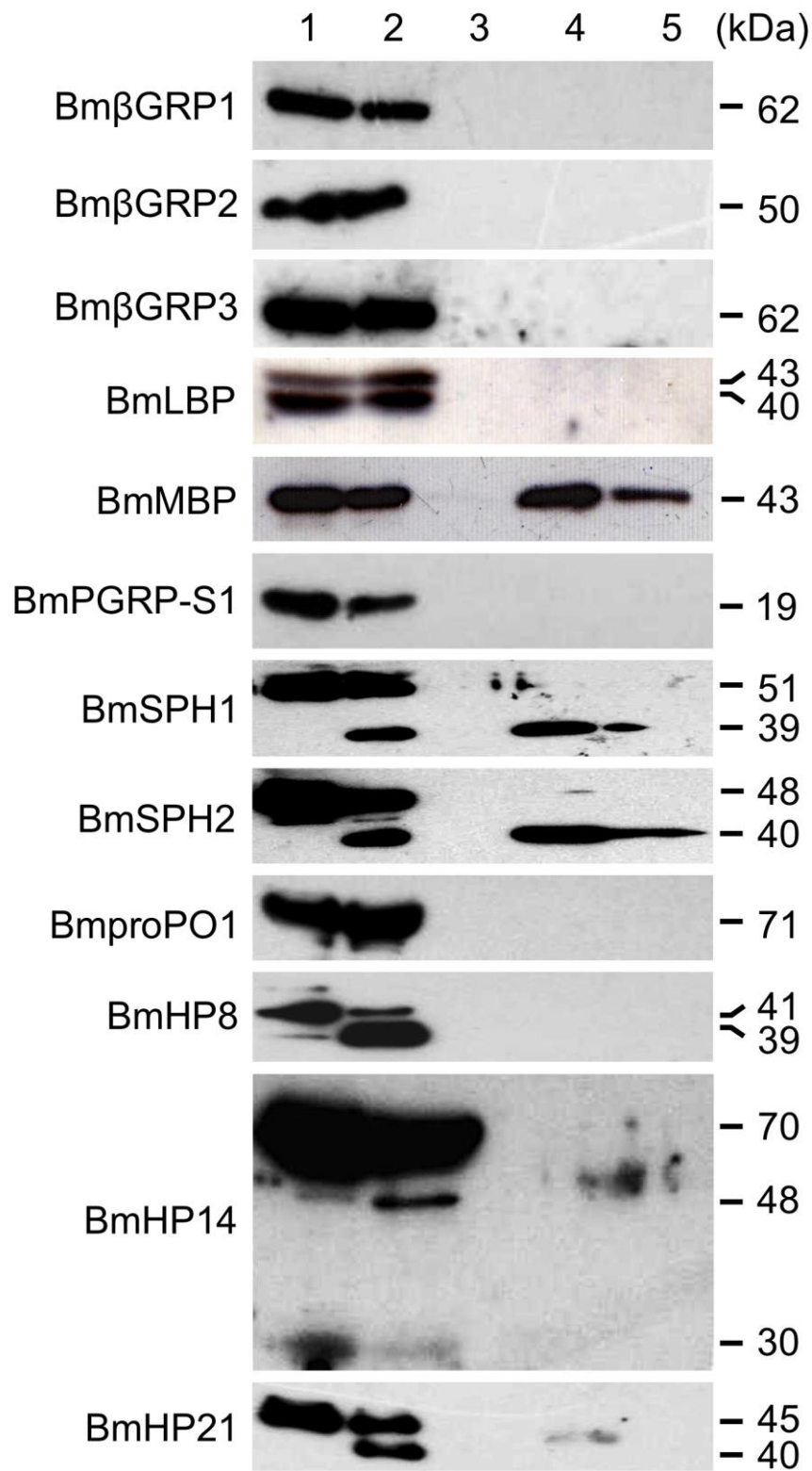
Fig. 3.3. Pull-down assay to identify plasma proteins that form a complex with BmSPH1 and BmMBP in cell-free plasma. Plasma was incubated with Protein A resin conjugated with rabbit anti-BmSPH1 (A) or anti-BmMBP (B) antibodies. After washing, the resin-bound proteins, flow-through, and fifth wash fraction were analyzed by SDS-PAGE on 12.5% gels. BmβGRP1, BmβGRP2, BmβGRP3, BmLBP, BmMBP, BmPGRP-S1, BmSPH1, BmSPH2, BmPO, BmHP8, BmHP14, and BmHP21 were detected by Western blot using mouse antisera raised against these proteins. Lane 1, cell-free plasma; lane 2, flow-through fraction of cell-free plasma; lane 3, wash fraction; lane 4, the first eluate from plasma-treated resin; lane 5, the second eluate from plasma-treated resin. For the negative controls, preimmune rabbit and mouse serum were bound to protein A resin, and the resin was then incubated with plasma. Western blot analysis of eluate from plasma-treated resin confirmed that no proteins were pulled down (data not shown).

3.3.4. Tissue-specific expression of BmSPHs

To investigate factors involved in nodule melanization in *B. mori* larvae, the expression patterns of BmSPHs in fat bodies, hemocytes (the major nodule constituents), and nodules were examined using RT-PCR. Nodule formation was induced by injecting with *E. coli* (EN), *S. cerevisiae* (SN), or *M. luteus* (MN). DNA sequencing was used to confirm the identity of PCR products. As shown in Fig. 3.4, cDNAs derived from mRNAs encoding *BmSPH1* and *BmSPH2* were found in fat bodies, hemocytes, and all three types of induced nodules (Fig. 3.4).

3.3.5. Immunocytochemical localization of BmSPHs in hemocytes

RT-PCR showed that *BmSPH1* and *BmSPH2* genes were produced by hemocytes (Fig. 3.4). Thus, immunofluorescent staining of smeared hemocytes was performed to examine the localization and accumulation of these two proteins. Plasmatocyte granules were stained well by anti-BmSPH1 and -BmSPH2 antisera (Fig. 3.5A and B), whereas granulocyte granules were stained weakly (Fig. 3.5A and B). Moreover, the cytoplasm of oenocytoids was stained weakly by anti-BmSPH1 and -BmSPH2 antisera (Fig. 3.5A and B). Prohemocytes were stained using only anti-BmSPH1 antiserum (Fig. 3.5A).
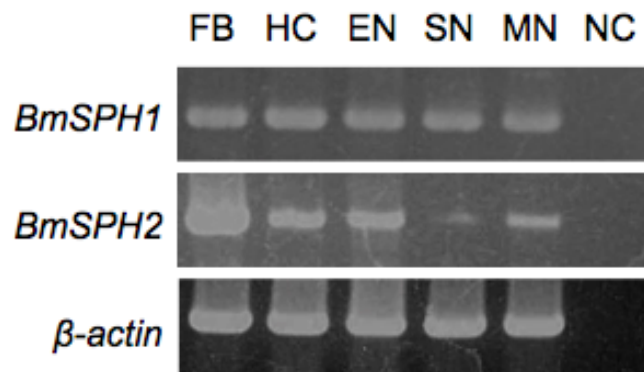
Fig. 3.4. RT-PCR analysis of genes encoding BmSPHs. Gene expression was analyzed in normal fat bodies (FB), normal hemocytes (HC), and nodules induced by injection with *E. coli* (EN), *S. cerevisiae* (SN), or *M. luteus* cells (MN). *β-actin* was used as an internal standard to normalize the cDNA pools. For the negative controls (NC), cDNA was replaced by an equal amount of pure water. Serine proteinase homologs (SPHs) included *BmSPH1* and *BmSPH2*.

A
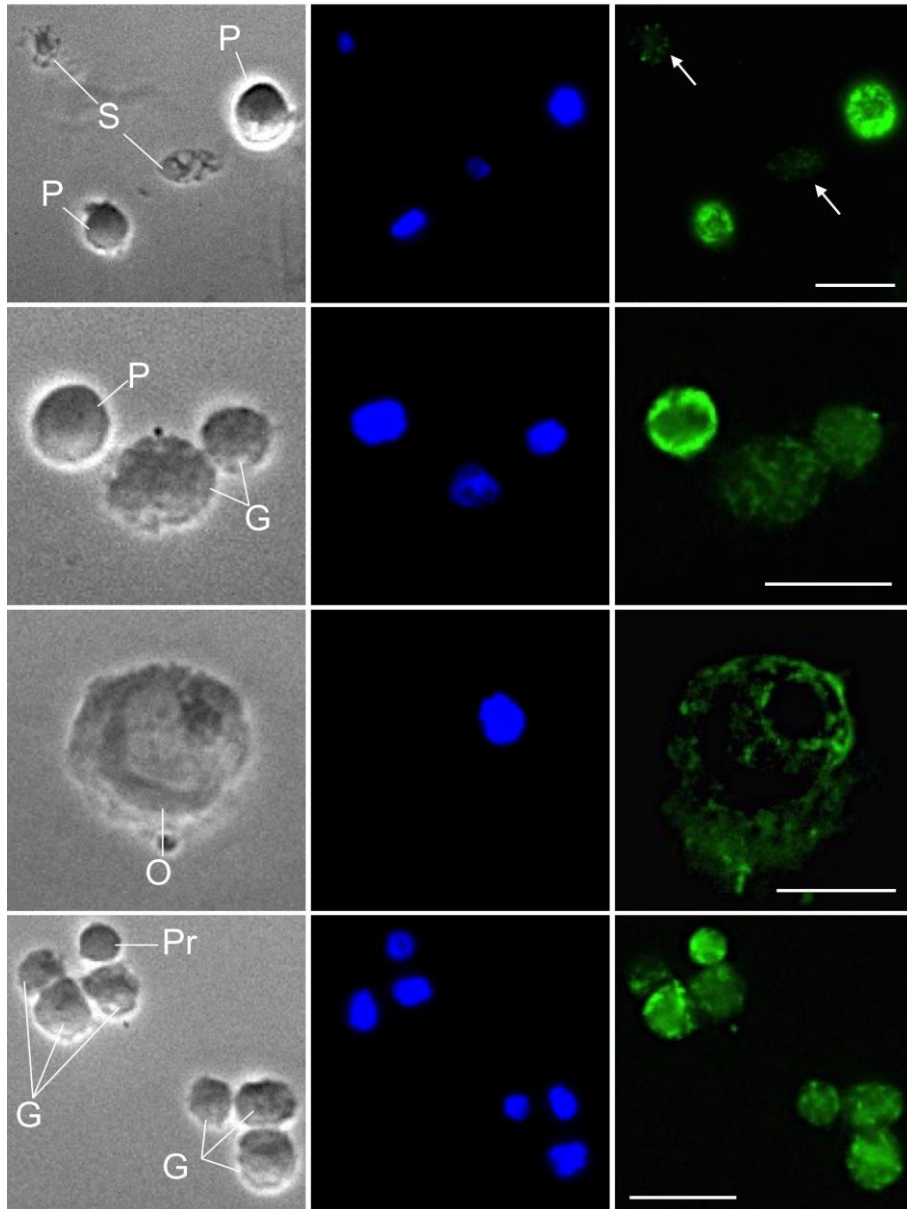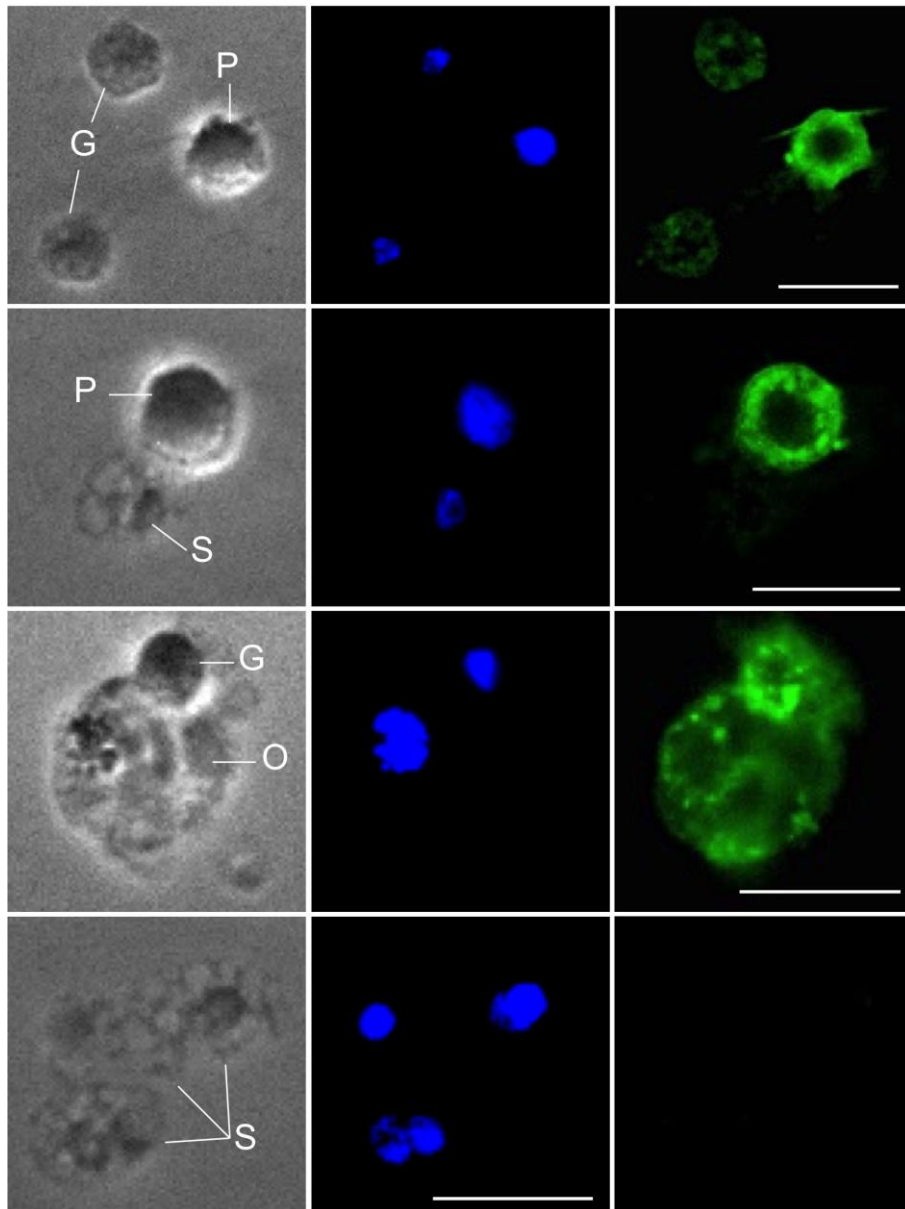
Fig. 3.5. Immunofluorescent detection of BmSPH1 and BmSPH2 in smeared hemocytes from *B. mori* larvae. Left panels show transmitted-light pictures. Middle panels show DAPI-stained nuclei of hemocytes. Right panels show hemocytes stained with mouse anti-BmSPH1(A) and anti-BmSPH2 (B) in combination with anti-mouse IgG conjugated to Alexa

Fluor 488®. P, plasmatocyte; G, granulocyte; O, oenocytoid; S, spherulocyte; Pr, prohemocyte. Arrows indicate weakly immunostained spherulocytes. Scale bars represent 10 µm.

3.3.6. Western blot analysis to deduce the origin of BmSPHs and the way to transport them into the nodules

In the RT-PCR and immunostaining, both BmSPH1 and BmSPH2 were detected in plasma, but also in hemocytes (Figs. 3.4 and 3.5). On the other hand, pull-down assays showed that BmSPH1 and BmSPH2 in hemolymph form complexes with C-type lectins, BmLBP and BmMBP (Fig. 3.3), which bind to microorganisms and was transport into nodules by ability of microorganisms gathering of nodules (chapter 1). These suggest that plasma may be the main source of BmSPHs in nodules, and hemocytes is the auxiliary source of these factors in nodules. To confirm this, Western blot analysis using cell-free plasma and, lysates of hemocytes and nodules was performed.

BmSPH1 and BmSPH2 were detected as precursor forms in the plasma, and as precursors and activated forms in hemocytes and nodules induced by *E. coli*, *M. luteus*, and *S. cerevisiae* (Fig. 3.6). It is unclear why the activated forms of BmSPH1 and BmSPH2 were detected in normal (non-sensitized) hemocytes, but it is possible they were artifacts that formed during the cell lysate preparation process. Both precursor and activated forms of BmSPH1 and BmSPH2 were more abundant in nodules induced by each of the three microorganisms than in hemocytes (Fig. 3.6). Therefore, it is likely that most of the BmSPH1 and BmSPH2 in nodules came from the plasma, although it is likely that some of these proteins were also transferred from hemocytes

(Fig. 3.6).

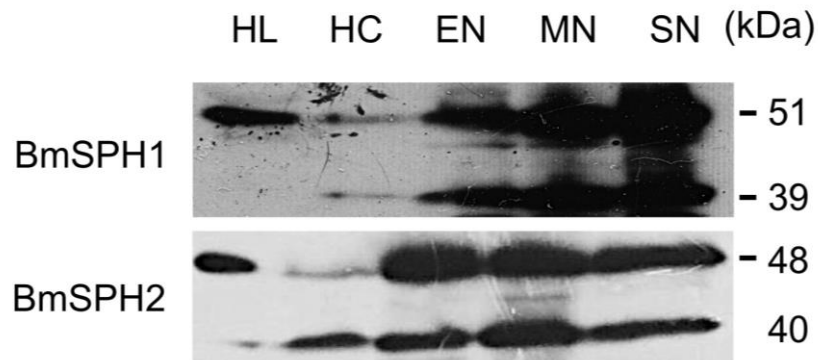**Fig. 3.6. Western blot analysis to deduce the aggregation route of BmSPHs.** The protein samples come from hemolymph (HL), hemocytes (HC), and nodules induced by injection with *E. coli* (EN), *M. luteus* (MN), and *S. cerevisiae* cells (SN) respectively, were transferred onto a PVDF membrane. Western blot experiments were performed using antisera against BmSPH1, and BmSPH2 as the primary antibodies.

3.3.7. Immunocytochemical localization of BmSPHs in nodules

The results of binding assay (Fig. 3.2), pull-down assay (Fig. 3.3) and Western blot (Fig. 3.6) have suggested that BmSPH1 and BmSPH2 in plasma are the main source of them in nodule; and by forming complex with C-type lectins, BmSPH1 and BmSPH2 in plasma were brought into nodules through interaction of C-type lectins and microorganisms. Therefore, it was thought that, just as observed in Figs. 1.9–1.14 as to BmPRRs in chapter 1, BmSPH1 and BmSPH2 should be also found mainly on the microorganisms in three kinds of nodules. To validate this hypothesis, immunostaining using BmSPH1 and BmSPH2 antisera of nodule cryosections was performed. As shown in Figs. 3.7 and 3.8, BmSPH1 and BmSPH2 (green fluorescence) were indeed observed in the all nodules induced by *E. coli*, *M. luteus*, and *S. cerevisiae* cells. At a higher magnification, as expected, green fluorescence was observed that mainly located in the area where could not be covered by the nuclei (blue fluorescence) of hemocytes in *E. coli- and M. luteus-* induced nodules; besides, the shape and scale also fit the *E. coli* and *M. luteus* cells (Figs. 3.7 and 3.8 A and B, arrowheads). In *S. cerevisiae*-induced nodule, at a higher magnification, green fluorescence which fit the shape and scale of *S. cerevisiae* cells was observed (Figs. 1.9–1.14 C, arrowheads). All of the results further conformed that BmSPH1 and BmSPH2 in plasma are brought into nodules by the help of plasma C-type lectins, BmLBP and BmMBP respectively.

A

Phase
Contrast

DAPI

Alexa-488
BmSPH1

DAPI

Alexa-488
BmSPH1

Merge

B
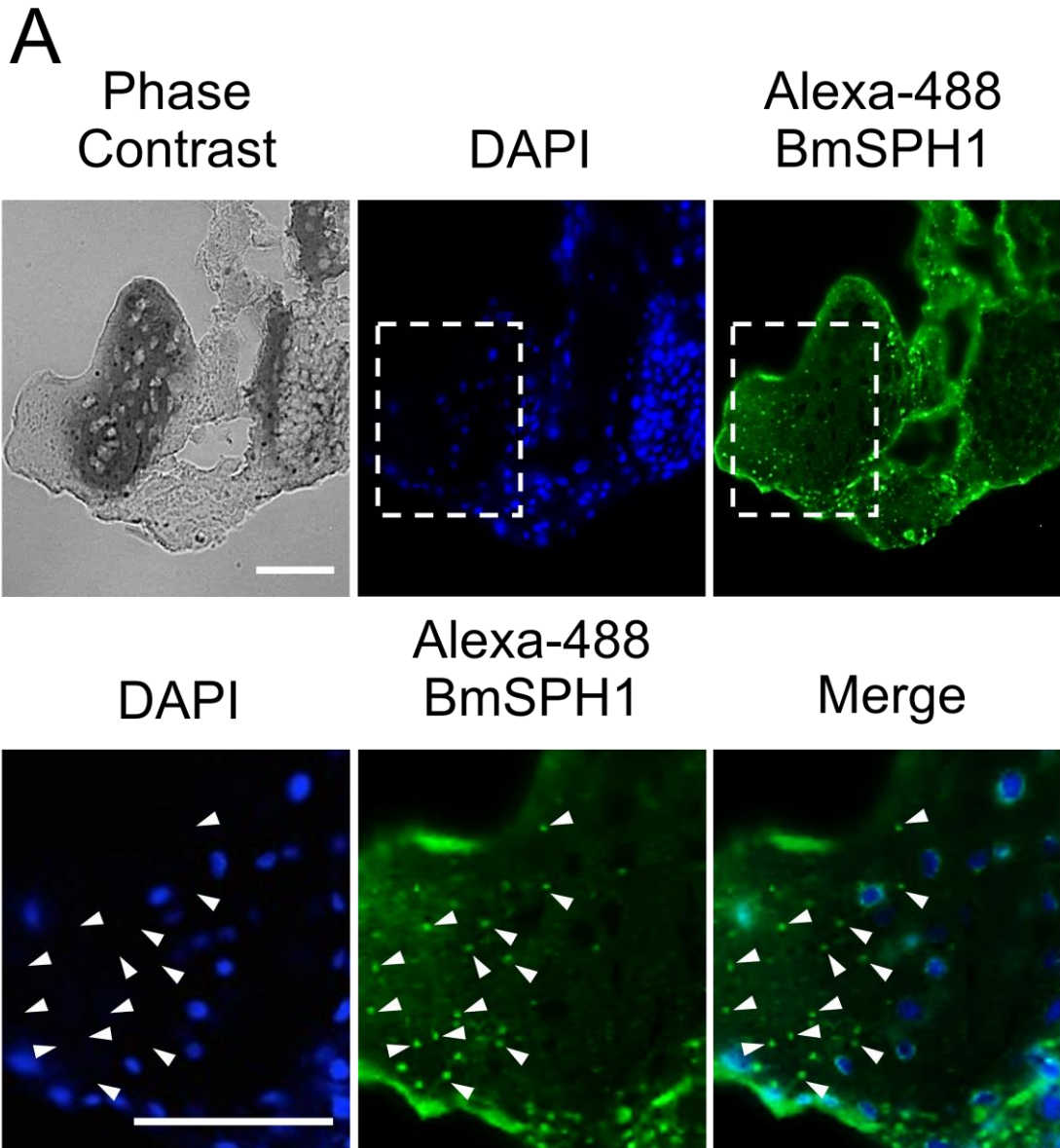
Phase
Contrast

DAPI
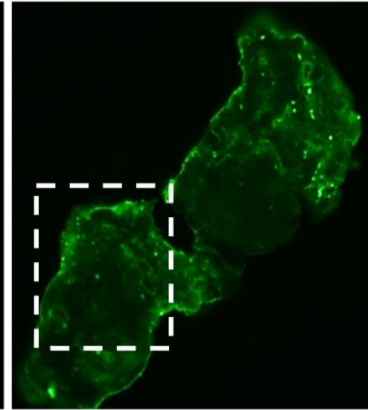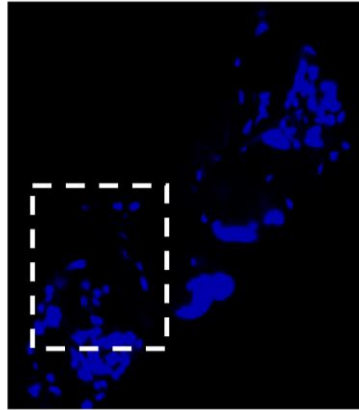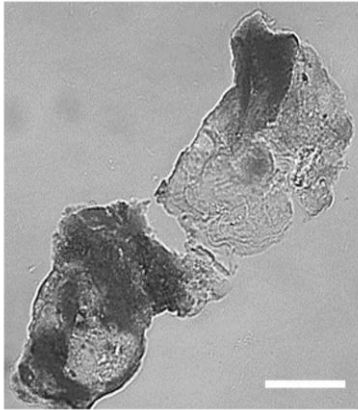
Alexa-488
BmSPH1

DAPI

Alexa-488
BmSPH1

Merge
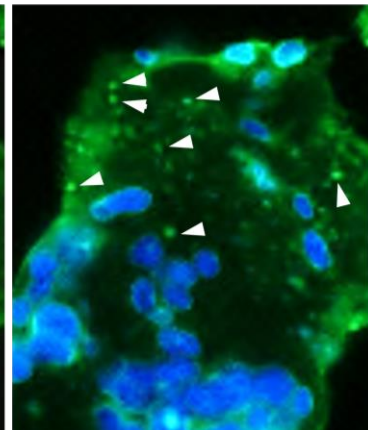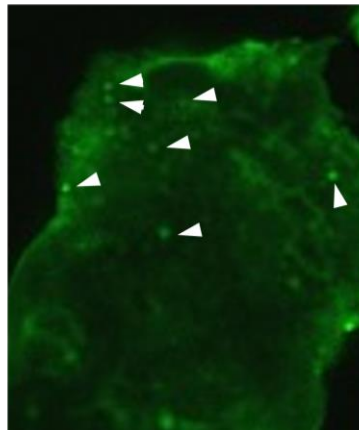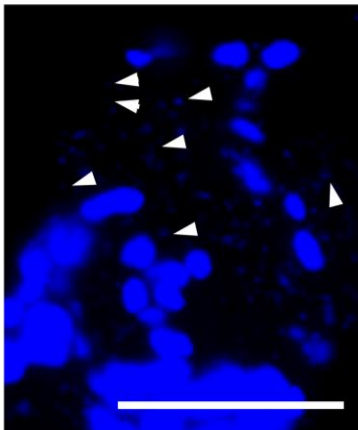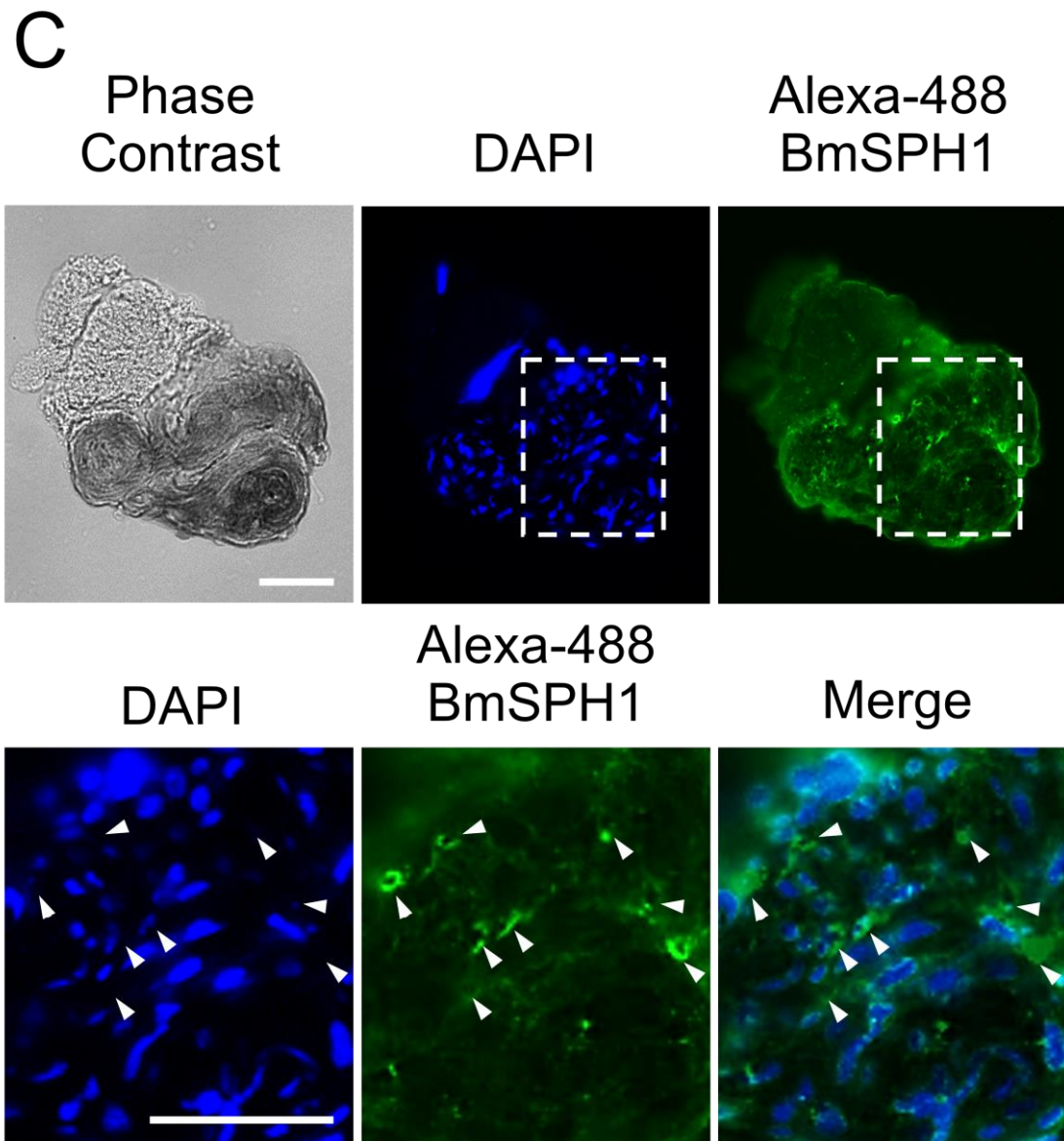
Fig. 3.7. Immunofluorescent detection of BmSPH1 in cryosections of nodule. A, crysection from *E. coli*-induced nodule; B, crysection from *M. luteus*-induced nodule; C, crysection from *S. cerevisiae*-induced nodule. The nuclei of hemocytes in nodule crysections were densely stained by DAPI with blue fluorescence. BmSPH1 was stained with mouse anti-BmSPH1 antiserum in combination with anti-mouse IgG conjugated to Alexa Fluor

488®. Images indicated below in A, B and C are higher magnification of the area outlined in the dashed rectangle in the above images; green fluorescence which fit the shape and scale of *E. coli*, *M. luteus*, *S. cerevisiae* cells in nodules, and not merged by blue fluorescence (hemocytes nuclei), are indicated by arrowheads (the middle and right panels); the same regions in DAPI-stained images (left panel) are also indicated by arrowheads. Scale bars represent 20 μm.

A

Phase
Contrast

DAPI

Alexa-488
BmSPH2

DAPI

Alexa-488
BmSPH2

Merge

B
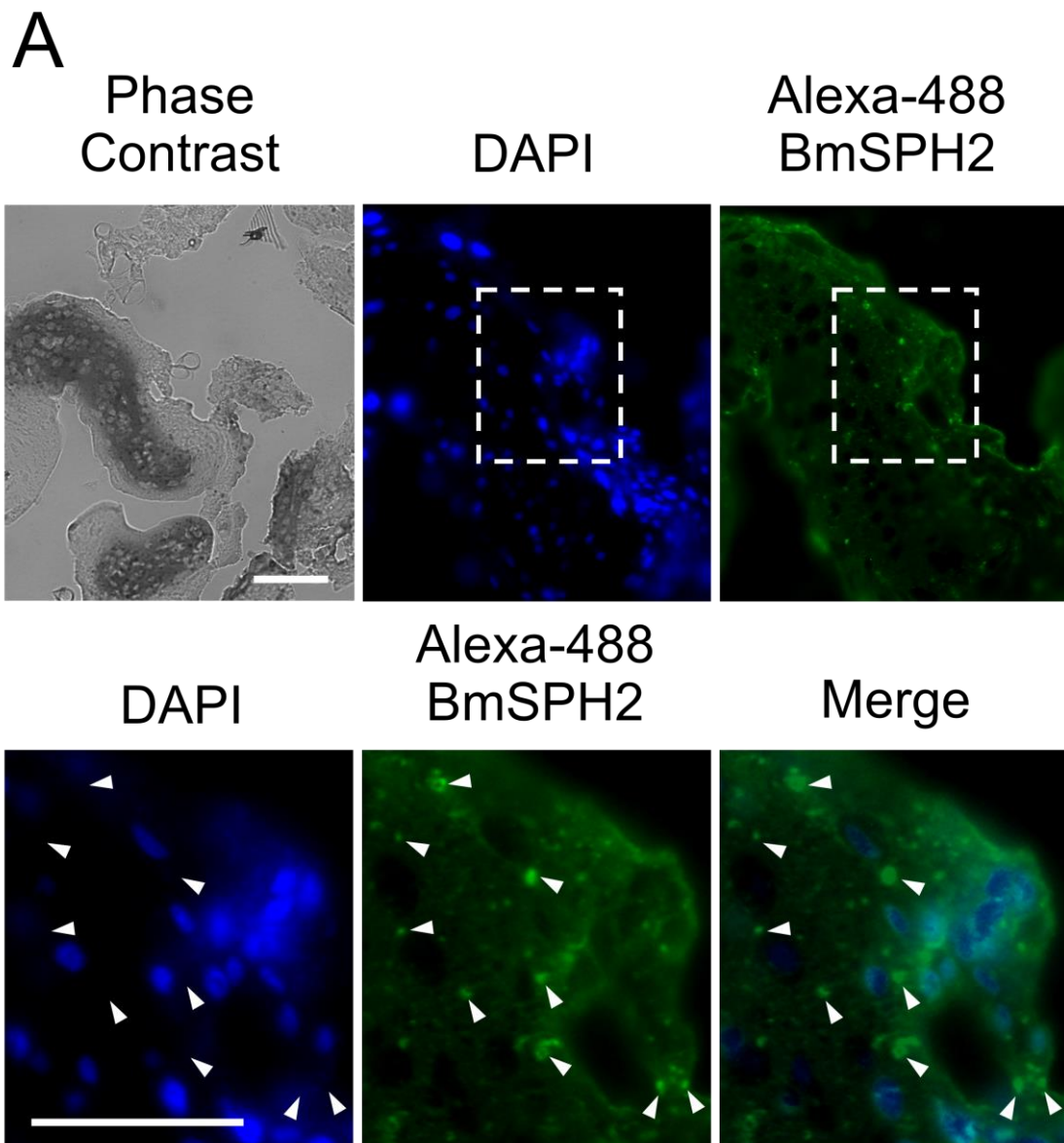
Phase Contrast | DAPI | Alexa-488 BmSPH2
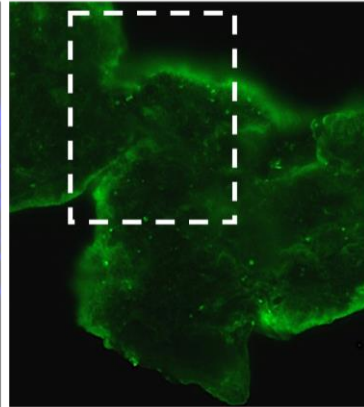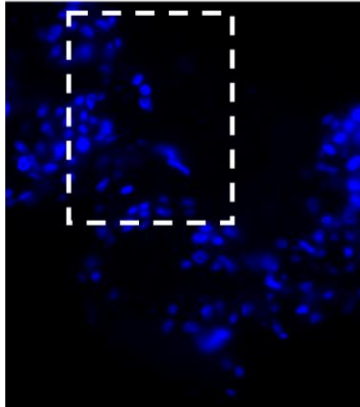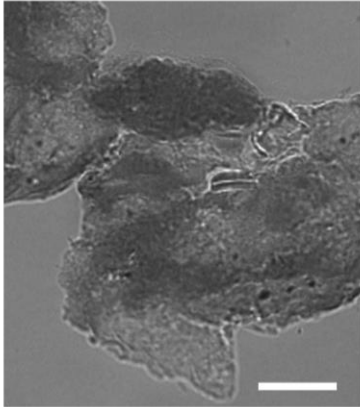
DAPI | Alexa-488 BmSPH2 | Merge
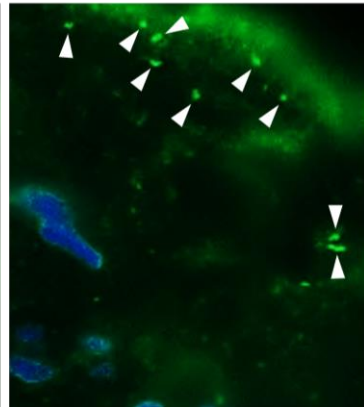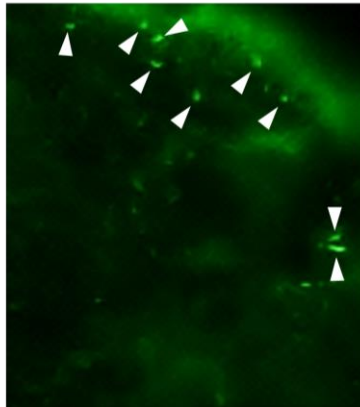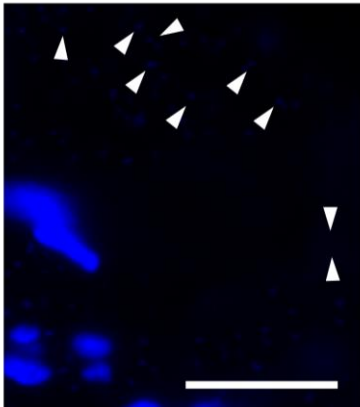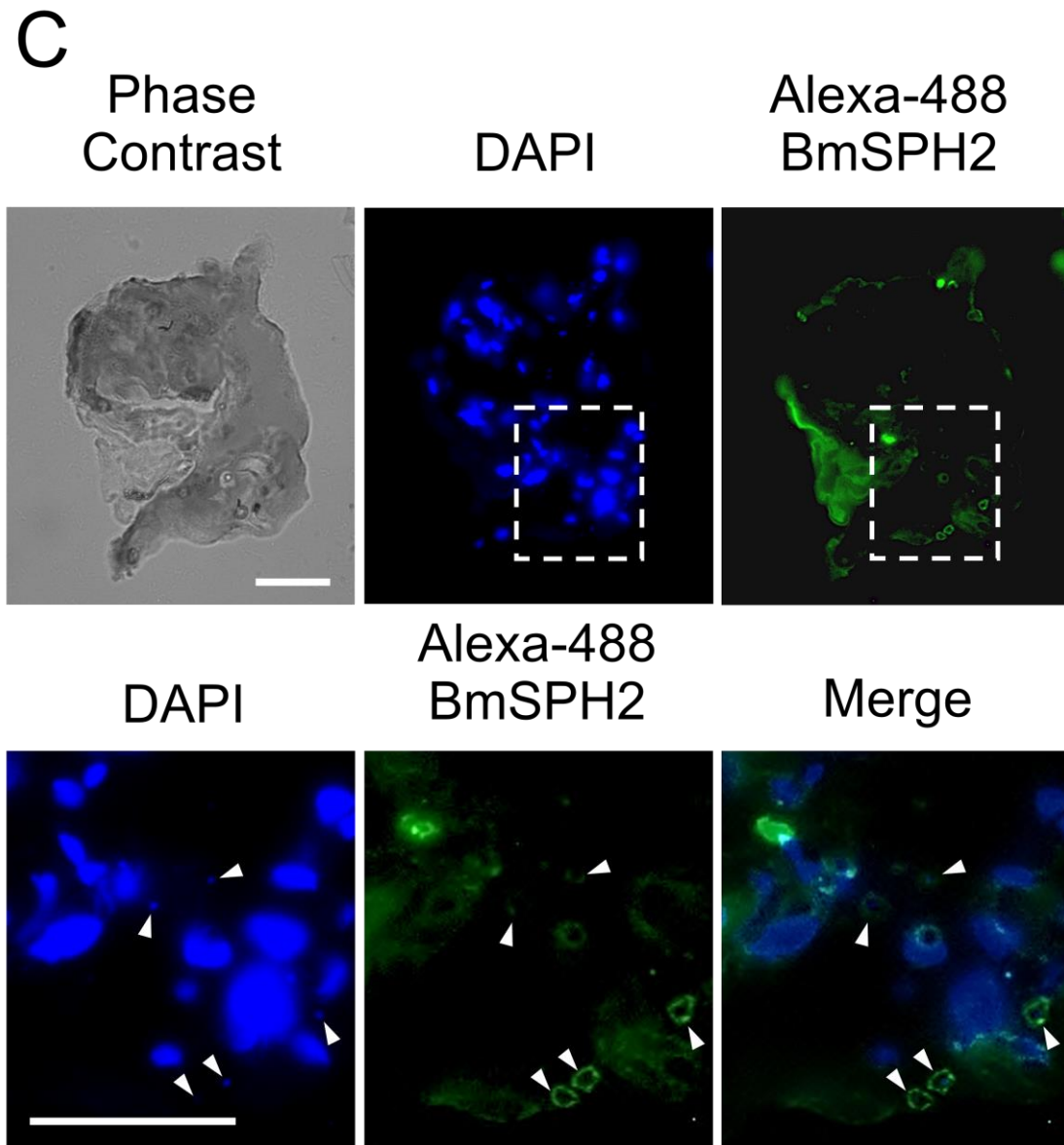
Fig. 3.8. Immunofluorescent detection of BmSPH2 in cryosections of nodule. A, crysection from *E. coli*-induced nodule; B, crysection from *M. luteus*-induced nodule; C, crysection from *S. cerevisiae*-induced nodule. The nuclei of hemocytes in nodule crysections were densely stained by DAPI with blue fluorescence. BmSPH2 was stained with mouse anti-BmSPH2 antiserum in combination with anti-mouse IgG conjugated to Alexa Fluor

488$^{®}$. Images indicated below in A, B and C are higher magnification of the area outlined in the dashed rectangle in the above images; green fluorescence which fit the shape and scale of *E. coli*, *M. luteus*, *S. cerevisiae* cells in nodules, and not merged by blue fluorescence (hemocytes nuclei), are indicated by arrowheads (the middle and right panels); the same regions in DAPI-stained images (left panel) are also indicated by arrowheads. Scale bars represent 20 μm.

3.4 Discussion

BmLBP and BmMBP are C-type lectins, and either of them was found to be co-localized in nodules with BmSPH1 and BmSPH2 (Tokura et al., 2014). In this and in a previous study (Tokura et al., 2014), together with the results of their pull-down assays, showed that BmMBP and BmLBP respectively could form a protein complex with BmSPH1 and BmSPH2 in the plasma (Fig. 3). However, four other PRRs (3 BmβGRPs and BmPGRP) were not detected in the protein complexes including BmSPH1 and BmSPH2 (Fig. 3A and B) and pull down assays using Protein A resins conjugated with antibodies against βGRPs and PGRP also indicated that they do not form complexes with BmSPH1 and BmSPH2. Western blot analyses revealed that BmLBP, BmMBP, BmSPH1, and BmSPH2 were primarily in the plasma and nodules and, to a lesser extent, in hemocytes (Fig. 8). Furthermore, granulocyte granules and the cytoplasm of oenocytoids were both only weakly stained by various anti-BmSPH antisera (Figs. 5 and 6). All these findings suggest that the plasma may be the main source of BmLBP, BmMBP, BmSPH1, and BmSPH2 in nodules and that BmSPHs in the plasma may have congregated into nodules by hemolymph C-type lectins through binding to microorganisms. This is supported by the fact that BmSPH1 and BmSPH2 were detected on the surface of microorganisms (Fig. 2). It was speculated that precursors of BmSPH1 and BmSPH2 form complex with C-type lectins in the plasma (Fig. 3) and they are activated by

the recognition of PAMPs by BmLBP and BmMBP, since apparent increase of the activated forms of BmSPH1 and BmSPH2 were observed after incubation with microorganisms (Fig. 2). These indicated that it is important for BmSPH1 and BmSPH2 to be on the surface of microorganisms in the nodule. A previous study on *M. sexta* reported that proPO proteolysis was mediated by the coexistence of MsSPHs and proPO-activating proteinases (MsPAPs) but not by MsSPHs alone (Gupta et al., 2005). On the other hand, active BmPPAE (also names PAP) was found that converts proPO to active PO by itself (Satoh et al., 1999). Whereas, Tokura et al. (2014) found that two new BmPAPs, BmPAP1 (AAX18636.1) and BmPAP3 (AAX18637.1) genes are expressed in *B. mori* hemocytes and nodules. Especially, the BmPAP1 has 75% similarity with MsPAP1 but only 41% similarity with BmPPAE in amino acid sequence, suggesting that BmPAP1 may have function close to MsPAP1 in proPO activation and, may need BmSPH1 and BmSPH2 coexistence to produce active PO. It is plausible that *B. mori* C-type lectins play important roles not only in the recognition of invading pathogens, but also in the initiation of proPO activation by means of BmSPH1 and BmSPH2. Clark and Strand (2013) reported that SPH1 and a kind of C-type lectin (C-type lectin 21) formed a complex with PO in *B. mori* (Clark and Strand, 2013). Thus, protein complexes consisting of BmSPH1, BmSPH2 and *B. mori* C-type lectins observed in our examination (Fig. 3) might be precursors of the PO-containing complex observed by

Clark and Strand (2013). It is possible that protein complexes consisting of BmSPH1, BmSPH2 and *B. mori* C-type lectins help PO to congregate around the surface of pathogens, resulting in the melanin deposition on the pathogens.

Complexes composed of BmLBP-BmSPHs and BmMBP-BmSPHs have similarities with factor C, a lipopolysaccharide-sensitive serine-protease zymogen from horseshoe crab; all have C-type lectin domains, two or one clip-domain, and serine proteinase-like domains or serine proteinase domain in the complexes or in the zymogen (Kawabata et al., 2009). Factor C can be activated auto-catalytically in the presence of bacterial LPS (Tokunaga et al., 1987, 1991). In the microorganism-binding assay, it was found that microorganisms could accelerate the activation of BmSPHs in plasma (Fig. 2); therefore, the complex formation might be indispensable for BmSPHs activation by an unknown reason, although auto-catalytic activation is not plausible, since BmSPHs does not have protease activity.

General Discussion

As described within this work, *Bombyx mori* larvae build an effective invading microorganism-surveillance network consisting of *B. mori* pattern recognition receptors (BmPRRs) in plasma to supervise and recognize different invading microorganisms (chapter 1). As inducted in Fig. GD1 and GD2, the network consists of at least six BmPRRs including two C-type lectins, three β-1, 3-glucan recognition proteins (βGRPs), and one peptidoglycan recognition proteins (PGRPs). In chapter 1, microorganism-binding assays suggested that BmPRRs which belong to the same PRR group can recognize different microorganisms. For instance, C-type lectins, *B. mori* lipopolysaccharide binding protein (BmLBP) and *B. mori* multibinding protein (BmMBP) recognize *Escherichia coli* or *Micrococcus luteus* and *Saccharomyces cerevisiae*, respectively (Fig. 1.2). On the other hand, BmPRRs which belong to different PRR groups can recognize the same microorganisms. For example, BmPGRP-S1 and βGRP2 which belong to PGRP and βGRP groups respectively can recognize *M. luteus* cells (Fig. 1.2 C). Finally, as the main congregation route, all BmPRRs in plasma can be aggregated and trapped into nodules with microorganisms, due to the microorganism-aggregating ability of nodules (Figs. 1.8-1.14).
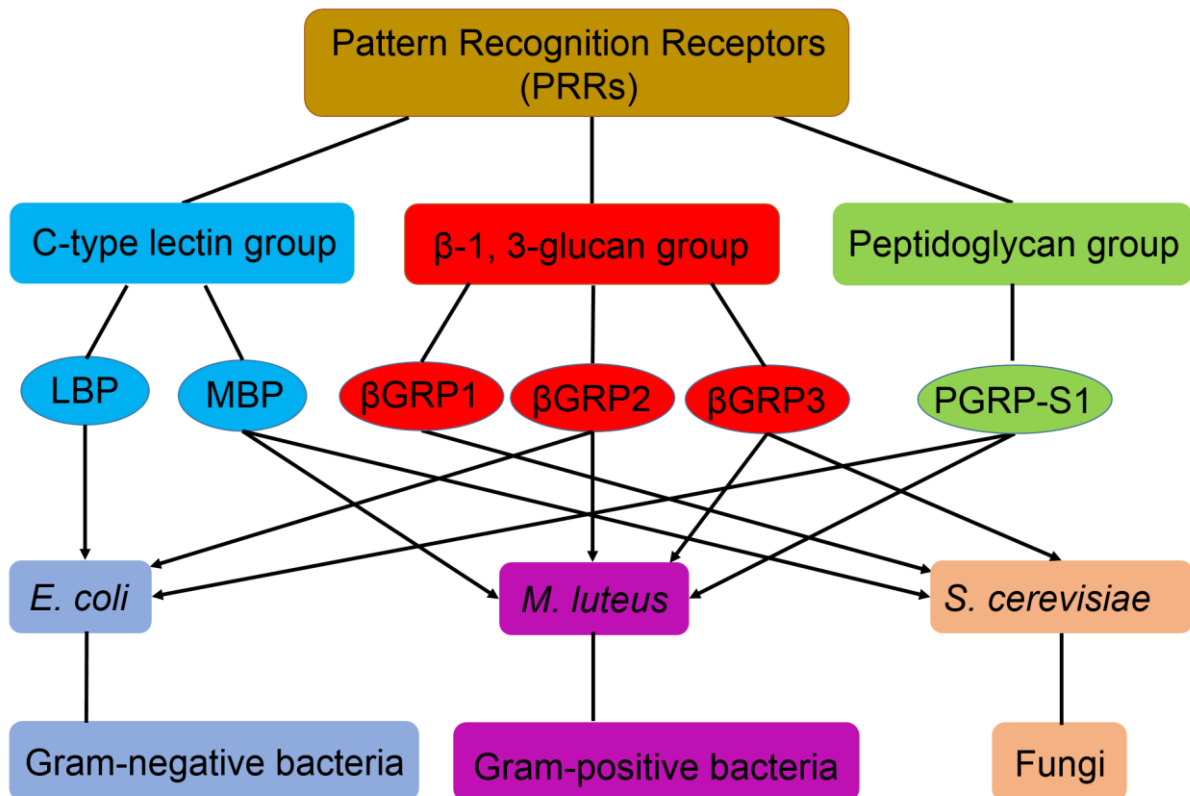
Fig. GD1. A model for the effective invading microorganism-surveillance network consisting of BmPRRs in *B. mori* larvae plasma. BmPRRs belonging to three different groups specially recognize and bind to surface of *E. col*, *M. luteus* or *S. cerevisiae* representing Gram-negative bacteria, Gram-positive bacteria and fungi, respectively.
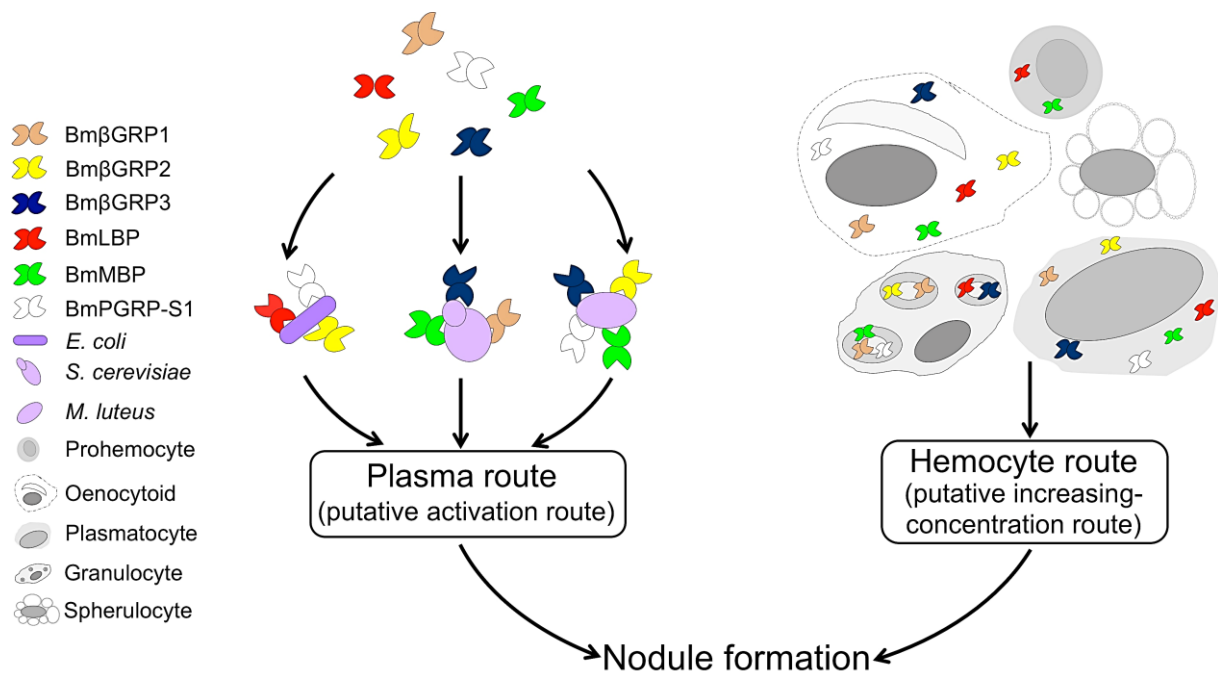
Fig. GD2 Predictive schematic model of the congregation mechanism of BmPRRs in nodules of *B. mori* larvae.

Previous studies on prophenoloxidase (proPO) activation suggested that recognition process of PRRs triggers the activation of the proPO cascade consisting of serine proteinases (HPs) and serine proteinase homologs (SPHs). However, it remains unclear that which BmHPs are required for proPO activation in each individual microorganism-group specific reaction cascade in *B. mori*. In current work, three BmHPs including BmHP8, BmHP14 and BmHP21 in plasma are found to aggregate in nodules by the interaction with microorganisms for nodule-preferential melanization (chapter 2). BmHP14 is found that specially binds to *S. cerevisiae* cells (Fig. 2.3C). BmHP8 and BmHP21 were not detected in the microorganism-binding assays (Fig. 2.3), however, were observed on the surface of microorganisms in the nodules (Figs. 2.7 and 2.9). The results suggest that BmHP8 and BmHP21 in plasma may loosely bind to microorganisms, and this loose binding may be removed by washing process before the elution in the binding assay. Further examinations are needed to clarify the mechanism of congregation of activated BmHP8 and BmHP21 into nodules. In addition, BmproPO1 in plasma is found that weakly binds to *E. coli*, *S. cerevisiae*, and *M. luteus* cells (Fig. 2.3). Altogether, proposed models for plasma BmHP8, BmHP14, BmHP21 and BmproPO1 aggregating in *E. coli*-, *S. cerevisiae*-, and *M. luteus*-induced nodules respectively, were given as Fig. GD3 and GD4. As discussed in chapter 2, plasma is the main congregation route of these four proteins, the binding to microorganisms of them leads to their

accumulation in nodules.
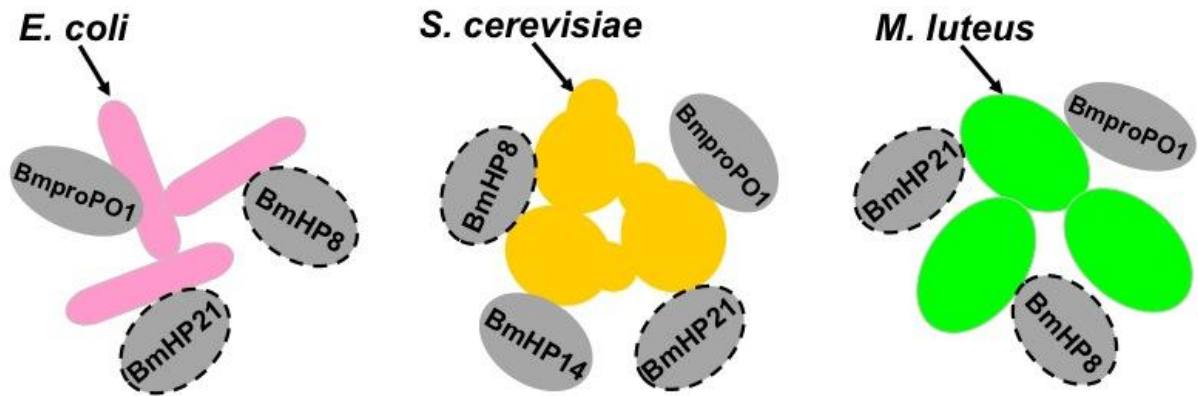
Fig. GD3. Proposed models for the way by which plasma BmHPs are aggregated into *B. mori* nodules. BmproPO1 in plasma weakly binds to *E. coli*, *S. cerevisiae*, and *M. luteus*. BmHP14 specially binds to *S. cerevisiae*. Even thogh BmHP8 and BmHP21 were not detected in microorganism-binding assays, the observation of them in the nodule cryosections suggest that the two proteins may loosely bind to microorganisms in the plasma and be removed before elution. These binding is considered to result in accumulation of HP8, 14 and 21 in the nodules, since they are made of aggregation of microorganism cells and hemocytes.
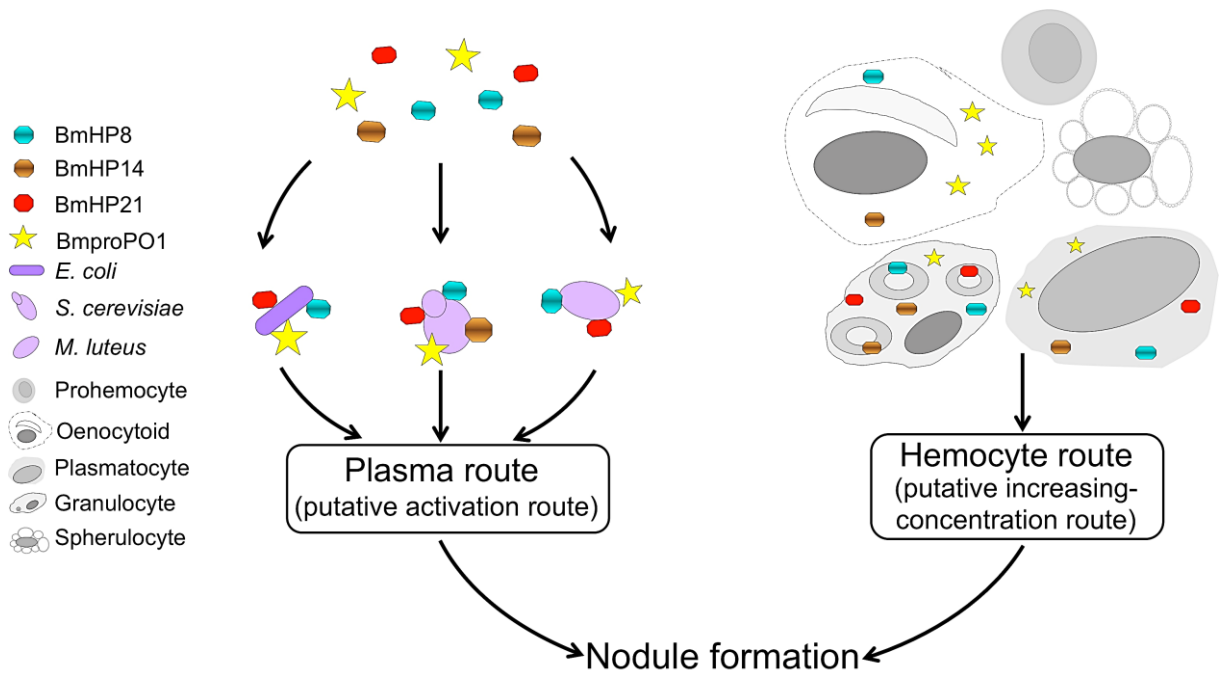
Fig. GD4 Predictive schematic model of the congregation mechanism of BmHPs in nodules of *B. mori* larvae.

As described in chapter 3, C-type lectins, BmLBP and BmMBP form protein complexes with BmSPH1 and BmSPH2 in the plasma, respectively (Fig. 3.3). However, the other four BmPRRs (3 BmβGRPs and BmPGRP) were not detected in the protein complexes including BmSPH1 and BmSPH2 in plasma of *B. mori* (Fig. 3.3). These results suggest that among BmPRRs, only C-type lectins are able to form complexes with BmSPH1 and BmSPH2 in the plasma. As inducted in Fig. GD5 and GD6, BmSPH1 and BmSPH2 are supposed to be brought into nodules induced by *E. coli*, *S. cerevisiae* and *M. luteus cells* by the help of BmLBP and BmMBP which specially bind to *E.coil*, *S. cerevisiae* or *M. luteus* cells in plasma, and the plasma is the main congregation route.

Immunofluorescent staining of hemocytes suggested that factors involved in melanization and antimicrobial peptides (AMPs) production are also expressed and stored in hemocytes of *B. mori* larvae (Figs. 1.5, 2.5 and 3.5). As inducted in Fig. GD7 with the models, six BmPRRs, three HPs and two SPHs are expressed and stored in plasmatocytes and granulocytes. These factors expressed in granulocytes were mainly located on the granules of granulocytes (Fig. 1.6). In addition, except for BmHP21, all of these factors are also expressed and stored in oenocytoids (Figs. 1.5, 2.5 and 3.5). In prohemocytes, only the expression of BmSPH1, BmLBP and BmMBP in prohemocytes are observed, maybe due to small number of prohemocytes in *B. mori* larvae plasma (Figs. 1.5, 2.5 and 3.5). However, in spherulocytes,

no expression of BmPRRs, HPs and SPHs were observed (Figs. 1.5, 2.5 and 3.5).

All results of RT-PCR, immunofluorescent staining and Western blot experiments showed that the 12 melanization-related factors or AMP production-related factors discussed above were present in the plasma, hemocytes, and nodules (Figs. 1.4–1.8, 2.4–2.6, 3.4–3.6). In addition, most of these factors were more abundant in the plasma and nodules than in the hemocytes (Figs. 1.8, 2.6, 3.6). Obviously, it is impossible to neglect the probability that nodule-constituting hemocytes release these factors in the nodule for example after their die with collapse of their cell membrane. Actually, Tokura et al. (2014) could not detect proPO-activating proteinases (PAPs) from the hemolymph by Western blotting, but they were detected by RT-PCR from the hemocytes and nodules. The presence of two routes (plasma route and hemocyte route) likely allows the nodule-specific melanization reaction to occur faster. However, for BmSPH1 and BmSPH2, and BmHP14, the plasma route seems to be more important in concentrating the activated forms of these factors in the nodule (Figs. 2.6 and 3.6). In addition, BmHP21 was activated when it was bound to microorganisms (Fig. 2.3), suggesting that the plasma route is also important for the activation of this factor.
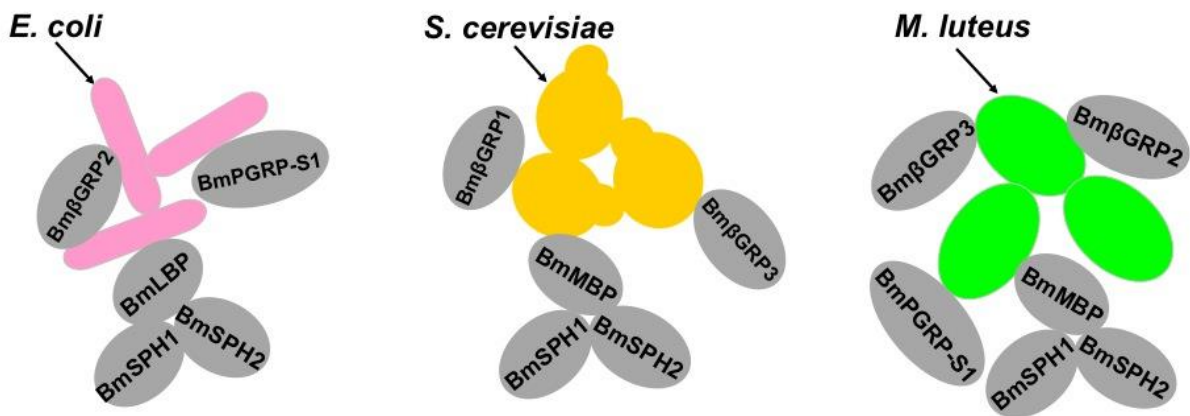
Fig. GD5. Models for the way of BmSPH1 and BmSPH2 in plasma are brought into *B. mori* nodules. In *B. mori* plasma, BmSPH1 and BmSPH2 form complexes with C-type lectin, BmLBP and BmMBP, respectively. By the special recognition process, BmLBP and BmMBP bind to *E. coli*, *S. cerevisiae* or *M. luteus* cells, leading to accumulation of proPO activation regulating factors, BmSPH1 and BmSPH2 in nodules due to the microorganism-aggregating ability of nodules.
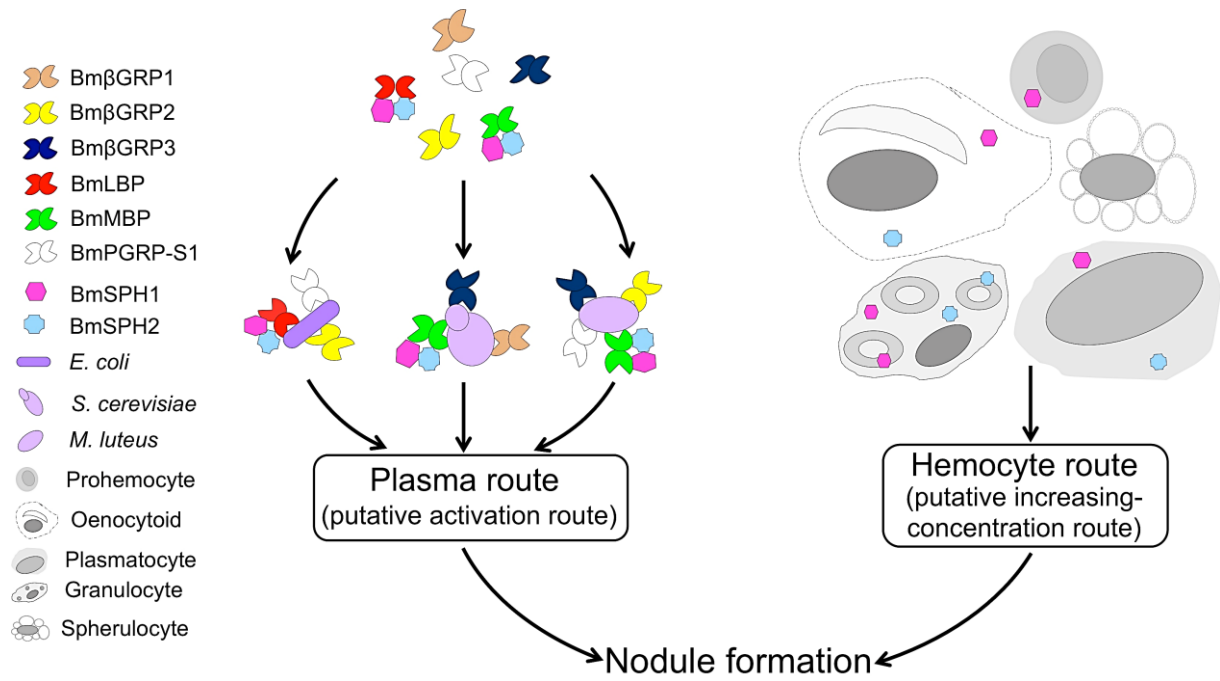
Fig. GD6 Predictive schematic model of the congregation mechanism of BmSPHs in nodules of *B. mori* larvae.
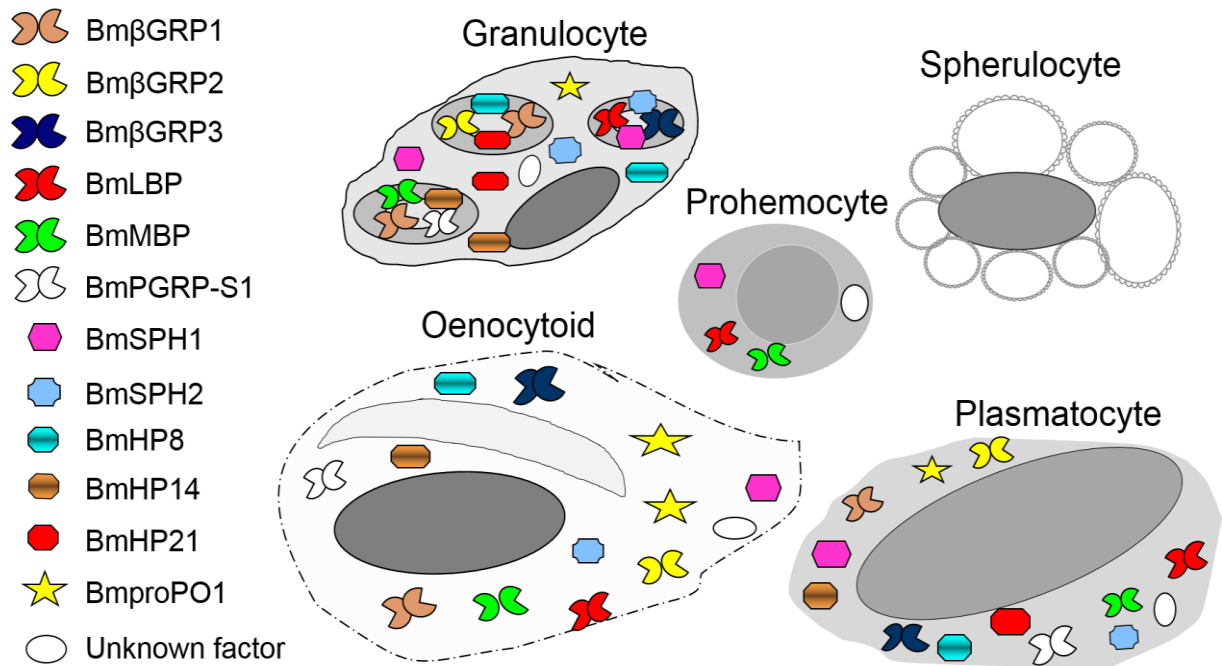
Fig. GD7. Models for melanization-related factors expressing and storing in hemocytes of *B. mori* larvae. Six BmPRRs, three HPs and two SPHs are expressed and stored in plasmatocytes and granulocytes. These factors expressed in granulocytes are mainly located on the granules of granulocytes. In oenocytoids, except for BmHP21, all of these factors are expressed and stored in oenocytoids. In prohemocytes, only BmSPH1, BmLBP and BmMBP were confirmed that are expressed and stored in prohemocytes, due to the little amount of prohemocytes in plasma. In spherulocytes, almost no fluorescence or very weak fluorescence was observed.

Based on all results, a model for the mechanism of assembly of melanization-related factors in the nodule in *B. mori* larval hemocoel was proposed (Fig. GD8). In plasma route, after infection, special BmPRRs in the hemolymph rapidly recognize the invading microorganisms (Figs. 1.2A–C, 1.3A–C). During this process, the recognition of microorganisms by *B. mori* C-type lectins makes it possible for BmSPHs to bind to microorganisms along with C-type lectins (Fig. 3.2A–C), because C-type lectins form complexes with BmSPHs in the hemolymph (Fig. 3.3A and B). BmHP14 can bind to fungi (Fig. 2.3C), resulting in its activation. When the invading microorganism is *S. cerevisiae*, the binding of activated BmHP14 to *S. cerevisiae* leads to its congregation in the nodule (Figs. 2.3C and 2.6). Moreover, BmHP21 and the AMP production-inducing factor BmHP8 may loosely bind to microorganisms (Figs. 2.7 and 2.9), and are activated on microorganisms (Fig. 2.3). At least, activation of BmHP8 and BmHP21 seems to be realized surrounding microorganisms (Fig. 2.3). BmproPO1 in plasma weakly binds to microorganism cells (Fig. 2.3). By binding to microorganisms in plasma, these proteins can be aggregated and trapped into nodules with microorganisms, due to the microorganism-aggregating ability of nodules (Figs. 1.8–1.14). On the other hand, melanization-related factors which are produced and stored in hemocytes might have an auxiliary role to help the concentration increase of these factors in the nodule (Figs. 1.5–1.8, 2.5–2.6, 3.5–3.6). Hemocytes can recognize invading microorganisms

directly using receptors that are located on the membrane of the hemocytes, or indirectly through the recognition of humoral factors which bind to invading microorganisms (Lavine and Strand, 2002; Ohta et al., 2006). These processes may stimulate degranulation of granulocytes and autolysis of oenocytoids. Because some granulocyte granules contain BmPRRs, BmSPHs, and BmHPs (Figs. 1.5–1.6, 2.5, 3.5), degranulation may cause an increase in the concentration of these factors around microorganisms. Other granules contain hemocytin, a putative aggregating factor of hemocytes and microorganisms (Arai et al., 2013). Induced degranulation from granulocytes causes nodule formation, which leads to the aggregation of hemocytes and microorganisms which bound with activated BmSPHs (Figs. 3.2 and 3.4). As a result, melanization-related factors come from plasma and hemocytes, are activated and congregated in nodules, resulting in contribution in nodule-specific melanization.
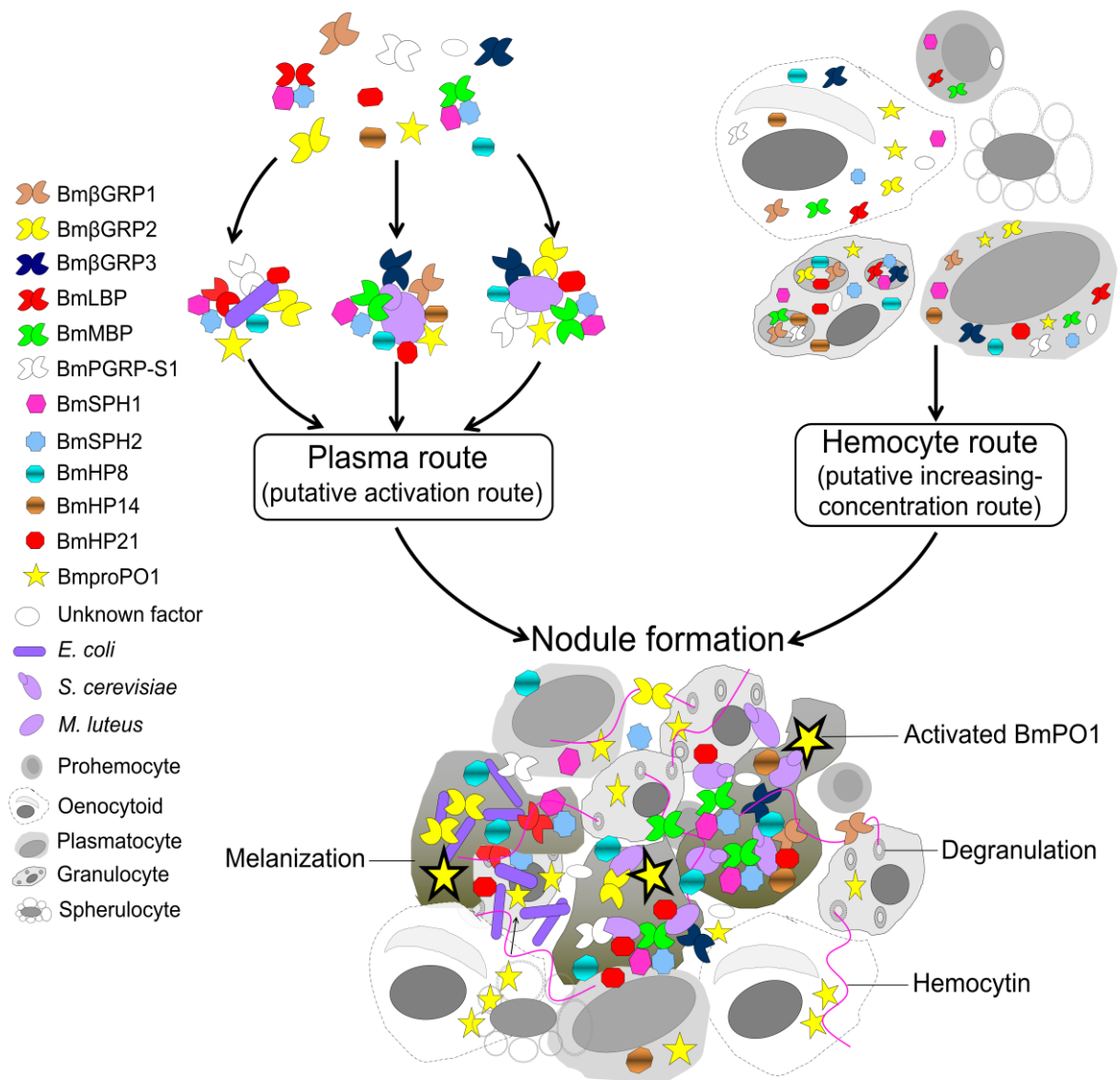
Fig. GD8. Predictive schematic model of the congregation mechanism of melanization-related factors in nodules of *B. mori* larvae.

Acknowledgements

First and foremost, I would like to express my special appreciation and thanks to my advisor Professor Ryoichi Sato, for supporting me during these past three years. I appreciate all his contributions of time, and funding to make my Ph.D. experience productive. I am also very grateful for his scientific advices and insightful discussions. He is my mainly resource for getting my science questions answered and was instrumental in helping me finish this thesis.

I would also like to thank the members of my Ph.D. committee, Professors Koki Toyoda, Shinya Kajita, Takeshi Suzuki, Hiroko Tabunoki for their numerous insights, guidance and above all, patience with me on this project.

In addition, I would like to thank all the former and present members of the Sato lab for being such helpful and friendly bunch of people! I really appreciate all the input I have received from you during the years, including technical advice and sharing of reagents.

I will forever be thankful to my former college and postgraduate research advisor, Professors Qinghuai Luo, Peilin Wang, Jiang Zhou and Zhaozhi Lv. They have been helpful in providing advice many times during my graduate school career. They were and remain my best role model for the scientist, mentor, and teacher. They were the reason why I

decided to go to pursue a career in research. Their enthusiasm and love for teaching is contagious.

I have to thank my family. Words cannot express how appreciative I am to my mother-in law, father-in- law, my mother, and my father for everything that you've made on my behalf. At the end I would like to express appreciation to my beloved husband Dingze Mang who spent sleepless nights and was always my support in the moments when I felt defeated, sad or lonely.

References

Akai, H., Sato, S., 1973. Ultrastructure of the larval hemocytes of the silkworm, *Bombyx mori* L. (Lepidoptera: Bombycidae). Int. J. Insect Morphol. Embryol. 2, 207–231.

An, C., Ishibashi, J., Ragan, E.J., Jiang, H., Kanost, M.R., 2009. Functions of *Manduca sexta* hemolymph proteinases HP6 and HP8 in two innate immune pathways. J. Biol. Chem. 284, 19716–19726.

An, C., Kanost, M.R., 2010. *Manduca sexta* serpin-5 regulates prophenoloxidase activation and the Toll signaling pathway by inhibiting hemolymph proteinase HP6. Insect Biochem. Mol. Biol. 40, 683–689.

Arai I., Ohta M., Suzuki A., Tanaka S., Yoshizawa Y., Sato R., 2013. Immunohistochemical analysis of the role of hemocytin in nodule formation in the larvae of the silkworm, *Bombyx mori*. J. Insect Sci. 13, 125.

Ashida, M., Brey, P., 1998. Recent advances on the research of the insect prophenoloxidase cascade, in: Brey, P.T., Hultmark, D. (Eds.), Molecular mechanisms of immune responses in insects. Chapman and Hall, London, pp. 135– 172.

Ashida, M., Dohke, K., Ohnishi, E., 1974. Activation of prephenoloxidase 111. Release of a peptide from prephenoloxidase by the activating enzyme. Biochem. Biophys. Res. Commun. 57, 1089–1095.

Ashida, M., Ohnishi, E., 1967. Activation of pre-phenol oxidase in hemolymph of the silkworm, *Bombyx mori*. Arch. Biochem. Biophys. 122, 411–416.

Au, C., Dean, P., Reynolds, S.E., Ffrench-Constant, R.H., 2004. Effect of the insect pathogenic bacterium Photorhabdus on insect phagocytes. Cell. Microbiol. 6, 89–95.

Cerenius, L., Lee, B.L., Söderhäll, K., 2008. The proPO-system: pros and cons for its role in invertebrate immunity. Trends Immunol. 29, 263–271.

Cerenius, L., Söderhäll, K., 2004. The prophenoloxidase-activating system in invertebrates. Immunol. Rev. 198, 116–126.

Clark, K.D., Strand, M.R., 2013. Hemolymph melanization in the silkmoth *Bombyx mori* involves formation of a high molecular mass complex that metabolizes tyrosine. J. Biol. Chem. 288, 14476–14487.

Diao, Y., Lu, A., Yang, B., Hu, W., Peng, Q., Ling, Q.Z., Beerntsen, B.T., Söderhäll, K., Ling, E., 2012. Existence of prophenoloxidase in wing discs: a source of plasma prophenoloxidase in the silkworm, *Bombyx mori*. PloS One 7, e41416.

Eleftherianos, I., Gökçen, F., Felföldi, G., Millichap, P.J., Trenczek, T.E., FfrenchConstant, R.H., Reynolds, S.E., 2007. The immunoglobulin family protein Hemolin mediates cellular immune responses to bacteria in the insect *Manduca sexta*. Cell. Microbiol. 9, 1137–1147.

Fauvarque, M.O., Williams, M.J., 2011. Drosophila cellular immunity: a story of migration and adhesion. J. Cell. Sci. 124, 1373–1382.

Felföldi, G., Eleftherianos, I., Venekei, I., 2011. A serine proteinase homologue, SPH-3, plays a central role in insect immunity. J. Immunol. 186, 4828–4834.

Finnerty, C.M., Granados, R.R., Karplus, P.A., 1999. The insect immune protein scolexin is a novel serine proteinase homolog. Protein Sci. 8, 242–248.

González-Santoyo, I., Córdoba-Aguilar, A., 2012. Phenoloxidase: a key component of the insect immune system. Entomol. Exp. Appl. 142, 1–16.

Gupta, S., Wang, Y., Jiang, H., 2005. *Manduca sexta* prophenoloxidase (proPO) activation requires proPO-activating proteinase (PAP) and serine proteinase homologs (SPHs) simultaneously. Insect Biochem. Mol. Biol. 35, 241–248.

Hultmark, D., 2003. Drosophila immunity: paths and patterns. Curr. Opin. Immunol. 15, 12–19.

Ji, C., Wang, Y., Guo, X., Hartson, S., Jiang, H., 2004. A pattern recognition serine proteinase triggers the prophenoloxidase activation cascade in the tobacco hornworm, *Manduca sexta*. J. Biol. Chem. 279, 34101–34106.

Jiang, H., Wang, Y., Gu, Y., Guo, X., Zou, Z., Scholz, F., Trenczekc, T.E., Kanost, M.R., 2005. Molecular identification of a bevy of serine proteinases in Manduca sexta hemolymph. Insect Biochem. Mol. Biol. 35, 931–943.

Johansson, M.W., Söderhäll, K., 1996. The prophenoloxidase activating system and associated proteins in invertebrates. Prog. Mol. Subcell. Biol. 15, 46–66.

Kan, H., Kim, C.H., Kwon, H.M., Park, J.W., Roh, K.B., Lee, H., Park, B.J., Zhang, R., Zhang, J., Soderhall, K., Ha, N.C., Lee, B.L., 2008. Molecular control of phenoloxidase-induced melanin synthesis in an insect. J. Biol. Chem. 283, 25316–25323.

Katsumi, Y., Kihara, H., Ochiai, M., Ashida, M., 1995. A serine protease zymogen

in insect plasma. Eur. J. Biochem. 228, 870–877.

Kawabata, S., Koshiba, T., Shibata, T., 2009. The lipopolysaccharide-activated innate immune response network of the horseshoe crab. Invert. Surviv. J. 6, 59–77.

Kim, M.S., Baek, M.J., Lee, M.H., Park, J.W., Lee, S.Y., Söderhäll, K., Lee, B.L., 2002. A new easter-type serine protease cleaves a masquerade-like protein during prophenoloxidase activation in *Holotrichia diomphalia* larvae. J. Biol. Chem. 277, 39999–40004.

Koizumi, N., Imai, Y., Morozumi, A., Imamura, M., Kadotani, T., Yaoi, K., Iwahana, H., Sato, R., 1999. Lipopolysaccharide-binding protein of *Bombyx mori* participates in a hemocyte-mediated defense reaction against gram-negative bacteria. J. Insect Physiol. 45, 853–859.

Koizumi, N., Morozumi, A., Imamura, M., Tanaka, E., Iwahana, H., Sato, R., 1997. Lipopolysaccharide-Binding Proteins and their Involvement in the Bacterial Clearance from the Hemolymph of the Silkworm *Bombyx Mori*. Eur. J. Biochem. 248, 217–224.

Krautz, R., Arefin, B., Theopold, U., 2014. Damage signals in the insect immune response. Front. Plant Sci. 5, 342.

Kurata, S., 2010. Extracellular and intracellular pathogen recognition by *Drosophila* PGRP-LE and PGRP-LC. Int. Immunol. 22, 143–148.

Kwon, T.H., Kim, M.S., Choi, H.W., Joo, C.H., Cho, M.Y., Lee, B.L., 2000. A masquerade-like serine proteinase homologue is necessary for phenoloxidase

activity in the coleopteran insect, *Holotrichia diomphalia* larvae. Eur. J. Biochem. 267, 6188– 6196.

Laemmli, U.K., 1970. Cleavage of structural proteins during the assembly of the head of bacteriophage T4. Nature 227, 680–685.

Lavine, M.D., Strand, M.R., 2002. Insect hemocytes and their role in immunity. Insect Biochem. Mol. Biol. 32, 1295–1309.

Lee, K.Y., Zhang, R., Kim, M.S., Park, J.W., Park, H.Y., Kawabata, S.I., Lee, B.L., 2002. A zymogen form of masquerade-like serine proteinase homologue is cleaved during pro-phenoloxidase activation by Ca2+ in coleopteran and *Tenebrio molitor* larvae. Eur. J. Biochem. 269, 4375–4383.

Lee, W.J., Lee, J.D., Kravchenko, V.V., Ulevitch, R.J., Brey, P.T., 1996. Purification and molecular cloning of an inducible gram-negative bacteria-binding protein from the silkworm, *Bombyx mori*. Proc. Natl. Acad. Sci. U. S. A. 93, 7888–7893.

Lu, Z., Jiang, H., 2008. Expression of *Manduca sexta* serine proteinase homolog precursors in insect cells and their proteolytic activation. Insect Biochem. Mol. Biol. 38, 89–98.

Ma, C., Kanost, M.R., 2000. A β1, 3-glucan recognition protein from an insect, *Manduca sexta*, agglutinates microorganisms and activates the phenoloxidase cascade. J. Biol. Chem. 275, 7505–7514.

Marmaras, V.J., Lampropoulou, M., 2009. Regulators and signalling in insect haemocyte immunity. Cell. Signal. 21, 186–195.

Medzhitov, R., Janeway, C.A., 2002. Decoding the patterns of self and nonself by the innate immune system. Science 296, 298–300.

Nappi, A.J., Vass, E., 1993. Melanogenesis and the generation of cytotoxic molecules during insect cellular immune reactions. Pigment Cell Res. 6, 117–126.

Ochiai, M., Ashida, M., 1988. Purification of a beta-1, 3-glucan recognition protein in the prophenoloxidase activating system from hemolymph of the silkworm, *Bombyx mori*. J. Biol. Chem. 263, 12056–12062.

Ochiai, M., Ashida, M., 2000. A pattern-recognition protein for β-1, 3-glucan the binding domain and the cDNA cloning of β-1, 3-glucan recognition protein from the silkworm, *Bombyx mori*. J. Biol. Chem. 275, 4995–5002.

Ochiai, M., Niki, T., Ashida, M., 1992. Immunocytochemical localization of β-1, 3- glucan recognition protein in the silkworm, *Bombyx mori*. Cell Tissue Res. 268, 431– 437.

Ohta, M., Watanabe, A., Mikami, T., Nakajima, Y., Kitami, M., Tabunoki, H., Ueda, K., Sato, R., 2006. Mechanism by which *Bombyx mori* hemocytes recognize microorganisms: direct and indirect recognition systems for PAMPs. Dev. Comp. Immunol. 30, 867–877.

Ribeiro, C., Brehélin, M., 2006. Insect haemocytes: what type of cell is that? J. Insect Physiol. 52, 417–429.

Richman, A., Kafatos, F.C., 1996. Immunity to eukaryotic parasites in vector insects. Curr. Opin. Immunol. 8, 14–19.

Sakamoto, M., Ohta, M., Suzuki, A., Takase, H., Yoshizawa, Y., Kitami, M., Sato,

R., 2011. Localization of the serine protease homolog BmSPH-1 in nodules of *E. coli*-injected *Bombyx mori* larvae and functional analysis of its role in nodule melanization. Dev. Comp. Immunol. 35, 611–619.

Satoh, D., Horii, A., Ochiai, M., Ashida, M., 1999. Prophenoloxidase-activating enzyme of the silkworm, *Bombyx mori*. Purification, characterization, and cDNA cloning. J. Biol. Chem. 274, 7441–7453.

Schmidt, O., Theopold, U., Strand, M., 2001. Innate immunity and its evasion and suppression by hymenopteran endoparasitoids. Bioessays 23, 344–351.

Strand, M.R., 2008. The insect cellular immune response. Insect Sci. 15, 1–14.

Sumathipala, N., Jiang, H., 2010. Involvement of *Manduca sexta* peptidoglycan recognition protein-1 in the recognition of bacteria and activation of prophenoloxidase system. Insect Biochem. Mol. Biol. 40, 487–495.

Suzuki, A., Yoshizawa, Y., Tanaka, S., Kitami, M., Sato, R., 2011. Extra- and intracellular signaling pathways regulating nodule formation by hemocytes of the silkworm, *Bombyx mori* (Lepidoptera: Bombicidae). J. Insect Biotechnol. Sericology 80, 49–56.

Tanaka, H., Ishibashi, J., Fujita, K., Nakajima, Y., Sagisaka, A., Tomimoto, K., Suzuki, N., Yoshiyama, M., Kaneko, Y., Iwasaki, T., Sunagawa, T., Yamaji, K., Asaoka, A., Mita, K., Yamakawa, M., 2008. A genome-wide analysis of genes and gene families involved in innate immunity of *Bombyx mori*. Insect Biochem. Mol. Biol. 38, 1087–1110.

Tokunaga, F., Miyata T., Nakamura, T., Morita, T., Kuma, K., Miyata, T., Iwanaga,

S., 1987. Lipopolysaccharide–sensitive serineprotease zymogen (Factor C) of horseshoe crab hemocytes: Identification and alignment of proteolytic fragment produced during the activation show that it is a novel type of serine protease. Eur. J. Biochem. 167, 412–416.

Tokunaga, F., Nakajima, H., Iwanaga, S., 1991. Further studies on lipopolysaccharide–sensitive serine protease zymogen (factor C): Its isolation from Limulus polyphemus hemocytes and identification as an intracellular zymogen activated by α–chymotrypsin, not by trypsin. J. Biochem. 109, 150–157.

Tokura, A., Fu, G.S., Sakamoto, M., Endo, H., Tanaka, S., Kikuta, S., Tabunoki H., Sato, R., 2014. Factors functioning in nodule melanization of insects and their mechanisms of accumulation in nodules. J. Insect Physiol. 60, 40–49.

Vilmos, P., Kurucz, E., 1998. Insect immunity: evolutionary roots of the mammalian innate immune system. Immunol. Lett. 62, 59–66.

Wang, Y., Jiang, H., 2004. Prophenoloxidase (proPO) activation in *Manduca sexta*: an analysis of molecular interactions among proPO, proPO-activating proteinase-3, and a cofactor. Insect Biochem. Mol. Biol. 34, 731–742.

Wang, Y., Jiang, H., 2006. Interaction of β-1, 3-glucan with its recognition protein activates hemolymph proteinase 14, an initiation enzyme of the prophenoloxidase activation system in *Manduca sexta*. J. Biol. Chem. 281, 9271–9278.

Wang, Y., Jiang, H., 2007. Reconstitution of a branch of the *Manduca sexta* prophenoloxidase activation cascade in vitro: Snake-like hemolymph proteinase 21 (HP21) cleaved by HP14 activates prophenoloxidase-activating proteinase-2

precursor. Insect Biochem. Mol. Biol. 37, 1015–1025.

Wang, Y., Jiang, H., 2010. Binding properties of the regulatory domains in *Manduca sexta* hemolymph proteinase-14, an initiation enzyme of the prophenoloxidase activation system. Dev. Comp. Immunol. 34, 316–322.

Wang, Y., Sumathipala, N., Rayaprolu, S., Jiang, H., 2011. Recognition of microbial molecular patterns and stimulation of prophenoloxidase activation by a β-1, 3- glucanase-related protein in *Manduca sexta* larval plasma. Insect Biochem. Mol. Biol. 41, 322–331.

Watanabe, A., Miyazawa, S., Kitami, M., Tabunoki, H., Ueda, K., Sato, R., 2006. Characterization of a novel C-type lectin, *Bombyx mori* multibinding protein, from the *B. mori* hemolymph: mechanism of wide-range microorganism recognition and role in immunity. J. Immunol. 177, 4594–4604.

Yoshida, H., Kinoshita, K., Ashida, M., 1996. Purification of a peptidoglycan recognition protein from hemolymph of the silkworm, *Bombyx mori*. J. Biol. Chem. 271, 13854–13860.

Yu, X.Q., Jiang, H., Wang, Y., Kanost, M.R., 2003. Nonproteolytic serine proteinase homologs are involved in prophenoloxidase activation in the tobacco hornworm, *Manduca sexta*. Insect Biochem. Mol. Biol. 33, 197–208.

Yu, X.Q., Kanost, M.R., 2000. Immulectin-2, a lipopolysaccharide-specific lectin from an insect, *Manduca sexta*, is induced in response to gram-negative bacteria. J. Biol. Chem. 275, 37373–37381.

Yu, X.Q., Kanost, M.R., 2002. Binding of hemolin to bacterial lipopolysaccharide

and lipoteichoic acid. Eur. J. Biochem. 269, 1827–1834.

Yu, X.Q., Zhu, Y.F., Ma, C., Fabrick, J.A., Kanost, M.R., 2002. Pattern recognition proteins in *Manduca sexta* plasma. Insect Biochem. Mol. Biol. 32, 1287–1293.